Elucidating the mechanism underlying Parkin's specificity towards Mitofusin-2

Yang Lu

Department of Pharmacology and Therapeutics

McGill University, Montreal

July, 2020

A thesis submitted to McGill university in partial fulfillment of the requirements of the degree of Master of Science

LISTS OF ABBREVIATIONS

Abbreviations and Notations

PD	Parkinson's Disease
PINK1	PTEN-induced putative kinase 1
SNpc	*Substantia nigra pars compacta*
ARJPD	Autosomal recessive juvenile Parkinsonism
Ub	Ubiquitin
Ubl	Ubiquitin-like
UBAs	Ubiquitin binding associated domains
polyUb	Polyubiquitin
CCCP	Carbonyl cyanide *m*-chlorophenyl hydrazine
OMM	Outer mitochondrial membrane
MDVs	Mitochondrial-derived vesicles
MTS	Mitochondrial targeting signal
TOM	Translocase of the outer mitochondrial membrane
TIM	Translocase of the inner mitochondrial membrane
MPP	Mitochondrial processing peptidase
PARL	Presenilin-associated rhomboid-like protein
pUb	Phospho-Ubiquitin
RBR	RING-in-Between-RING
VDAC	Voltage-dependent anion channel
Mfn2	Mitofusin-2

MEFs	Mouse embryonic fibroblasts
MAMs	Mitochondria-associated membranes
DUBs	Deubiquitinating enzymes
PLA	Proximity ligation assay
MHC	Major histocompatibility complex
ROS	Reactive oxygen species
MPPP	Desmethylprodine
MPTP	1-methyl-4-phenyl-1,2,3,6-tetrahydropyridine
DA	Dopamine
MQC	Mitochondrial quality control
TMD	Transmembrane domain
OA	Oligomycin A/antimycin A
CytC	Cytochrome c
LC3	Microtubule-associated protein 1A/1B-light chain 3
LIR	LC3-interacting region
Mfn1	Mitofusin-1

ABSTRACT

Parkin and PINK1 are two proteins involved in mitochondrial quality control pathways and their mutations cause an early onset autosomal recessive form of Parkinson's Disease (PD). Upon mitochondrial damage, PINK1 accumulates on the outer mitochondrial membrane (OMM) where it phosphorylates ubiquitin (Ub) to generate phospho-Ub (pUb), which in turn recruits Parkin to the site of damage. Parkin, an E3 ubiquitin ligase, catalyzes the transfer of Ub onto lysines of target substrates. The buildup of Ub chains serves as a target signal for proteasomal degradation, formation of mitochondria-derived vesicles, or autophagy. Numerous Parkin substrates are located on the OMM, but at low physiological concentrations, Parkin primarily ubiquitinates Mitofusin-2 (Mfn2). In the current literature, several groups have reported Mfn2 as a preferred substrate of Parkin, but the molecular mechanism underlying substrates' recognition and specificity for Mfn2 are still unknown. Our overall objective is to determine the mechanism underlying Parkin's substrate selectivity towards Mfn2. We have confirmed, in our *in vitro* assays, that Parkin primarily ubiquitinates Mfn2 over other well-characterized OMM substrates. We further demonstrated that Mfn2 is located into close proximity to PINK1 in cells, thereby explaining its substrate specificity from Parkin. More importantly, we report that other Parkin's OMM substrates, such as the voltage-dependent anion channel (VDAC), Mfn1 and Miro are not located in close proximity to PINK1. Furthermore, our data revealed that pUb moieties are made in Parkin-null HeLa cells, therefore suggesting that other E3 ubiquitin ligases must catalyze the addition of pre-existing Ub chains onto OMM substrates such as Mfn2. We have identified three mitochondrial E3 ligases that have been reported to ubiquitinate Mfn2, and we further aim to determine the structural basis for Mfn2 recognition by those priming E3 ubiquitin ligases.

FRENCH ABSTRACT

Parkin et PINK1 sont deux protéines impliquées dans la voie de contrôle de la qualité mitochondriale et leurs mutations provoquent la Maladie de Parkinson (MP) autosomique récessive à début hâtif. Lors des dommages mitochondriaux, PINK1 s'accumule sur la membrane mitochondriale externe (MME) où il phosphoryle l'ubiquitine (Ub) pour générer du phospho-Ub (pUb), qui à son tour recrute Parkin. Parkin, une ligase d'ubiquitine E3, catalyse le transfert d'Ub sur les lysines des substrats cibles. L'accumulation des chaînes Ub devient un signal pour la dégradation des substrats par le protéasome, la formation des vésicules dérivées des mitochondries ou par l'autophagie. De nombreux substrats de Parkin sont situés sur la MME, mais à des concentrations physiologiques, Parkin ubiquitine principalement Mitofusin 2 (Mfn2). Plusieurs groupes ont rapporté Mfn2 comme un substrat préféré de Parkin, mais le mécanisme moléculaire expliquant cette spécificité est toujours inconnu. Notre objectif est de déterminer le mécanisme qui explique la sélectivité du substrat de Parkin envers Mfn2. Les essais de *in vitro* ont confirmé que Parkin ubiquitine principalement Mfn2 plutôt que d'autres substrats localisés sur la MME. Nous avons aussi prouvé que Mfn2 est situé à proximité immédiate de PINK1 dans les cellules, expliquant ainsi sa spécificité de substrat provenant de Parkin. D'autres substrats de Parkin, tels que le canal anionique dépendant du voltage (VDAC), Mfn1 et Miro ne sont pas situés à proximité de PINK1. Nos données ont révélé que des fragments pUb sont produits dans des cellules HeLa privées de Parkin, suggérant que d'autres ligases d'ubiquitine E3 doivent catalyser l'ajout des chaînes d'Ub préexistantes sur Mfn2. Trois ligases mitochondriales E3 aptes à ubiquitiner Mfn2 ont été rapportés dans la littérature. Nous envisageons, dans le futur, de déterminer la base structurelle de la reconnaissance de Mfn2 par ces ligases d'ubiquitine E3.

ACKNOWLEDGEMENTS

I would like to first express my sincere gratitude to my supervisor Dr. Jean-François Trempe for his constant guidance, expertise and kindness throughout my entire journey as a master student. I would like to thank Andrew Bayne, who trained me as an inexperienced undergraduate student and has continuously supported me throughout the past three years. I would also like to thank Nathalie Croteau for her kindness and her words of motivation on a daily basis. Additionally, I would like to thank all lab members of the Trempe lab: Dr. Simon Veyron, Shafqat Rasool, Anthony Duchesne, Tara Shomali, Jerry Dong, Dr. Marta Vranas (former), Nimra Khan (former), Luc Truong (former) and Dylan Pelletier (former) for making my journey in the lab a unique and unforgettable experience.

I would like to thank my committee members, Dr. Dusica Maysinger, Dr. Terry Hebert and Dr. Siegfried Hekimi for providing their invaluable feedback during the completion of this thesis. I would also like to thank Dr. Nicolas Audet for his assistance with the imaging and molecular biology platform and Dr. Mark Hancock for his help with the operation of the mass spectrometer.

I would like to thank FRQS for awarding me the GEPROM Summer Studentship in 2017 and in 2018; the McGill Department of Pharmacology and Therapeutics for awarding me the Grad Excellence Award in 2018; and *Centre de Recherche en Biologie Structurale* for awarding me the CRBS Studentship Award in 2019. Furthermore, I would to thank NSERC, CIHR, Parkinson Society Canada, and the Michael J. Fox Foundation for funding the present project.

Last but not least, a special thanks to all the people who along the way believed in me. I am extremely grateful for all the friends I met during my graduate studies, who everyday continue

to inspire me to become a better version of myself. Finally, I would like to thank my parents for their emotional support and motivation throughout this journey. Thank you both for being by my side and believing in me, I would not be who I am without your love.

CONTRIBUTION OF AUTHORS

I performed all the experiments presented in the following thesis, with the exception of the *in organello* assays performed by Dr. Jean-François Trempe (figure 9 in Results and figure 1 in Appendix).

All experiments were conceptualized and planned by with Dr. Jean-François Trempe and myself.

INTRODUCTION

Parkinson's Disease and Mitochondrial Dysfunction

Parkinson's disease (PD) is the second most common neurodegenerative disease and it is characterized by a loss of dopaminergic neurons in the *Substantia nigra pars compacta* (SNpc), which causes the characteristic motor impairments. First described by James Parkinson in 1817, apparent symptoms of PD include resting tremor, instability, rigidity and bradykinesia (Parkinson, 2002; Gibb and Lees, 1988). Additionally, PD is often associated with a number of non-motor symptoms such as loss of olfaction, mental health issues, sleep disorders and autonomic dysfunctions (Kalia and Lang, 2015). With age being the main risk factor, the number of predicted PD patients worldwide is estimated to reach over 9 million in the next decade (Dorsey et al. 2007). Existing treatments such as dopamine replacement therapies are available only for symptomatic relief, but there is currently no disease modifying treatments. Extensive research over the years has focused to reveal the underlying molecular events that lead to such neurodegeneration and henceforth, a causal relationship between mitochondrial dysfunction and the pathogenesis of PD has been established.

The first observation linking PD and mitochondrial damage was in the late 1970s when drug addicts developed Parkinsonian symptoms overnight after consuming 1-methyl-4-phenyl-1,2,3,6-tetrahydropyridine (MPTP), a chemical by-product of clandestine synthesis of a recreational drug Desmethylprodine (MPPP) (Langston et al. 1983). MPTP inhibits mitochondrial respiration by blocking complex I activity and this in turns resulted in the selective loss of SNc DA neurons. Similarly, administrating other complex I inhibitors such as rotenone and paraquat in rodents also resulted in a selective and local degradation of dopaminergic neurons (Heikkila et

al. 1985). Furthermore, a significant reduction of mitochondrial complex I activity was found in PD patients and an extensive damage to mitochondrial DNA (mtDNA) resulted in loss of complex I function (Schapira et al. 1989). These evidences all hinted towards the implication of mitochondrial damage of selective SNc DA neurons in the pathogenesis of PD.

Dopaminergic neurons are found in many areas in the brain. They are, however, not equally affected in PD. For instance, dopaminergic neurons in the ventral tegmental area (VTA) are not affected in patients with PD. Hence, research has unraveled the difference between DA neurons regarding their susceptibility to damage. The vulnerability of SNc DA neurons can be explained by a selective vulnerability hypothesis put forward by James Surmeier. In this proposed model, SNc DA neurons are autonomous pacemakers that have large dendritic fields and broad action potential spikes, rendering them particularly reliant to proper mitochondrial function. Indeed, SNc DA neurons express high levels of voltage-gated $Ca_v1.3$ Ca^{2+} channels, which are responsible for large calcium influx into the neurons, while only expressing low levels of calbindin, a calcium buffering protein. This results in SNc neurons experiencing a higher level of basal oxidative stress thus rendering them extremely sensitive to any further mitochondrial damages (Surmeier et al. 2010). Furthermore, SNc DA neurons have elevated bioenergetic requirements with a higher rate of oxidative phosphorylation and ROS production compared to other neurons. Indeed, SNc DA neurons display a larger axonal arborization, which is associated with a higher basal energy demands and mitochondrial activity, which altogether contribute to neuronal vulnerability (Pacelli et al. 2015, Pissadaki et al. 2013).

The majority of PD cases are idiopathic and are believed to be caused by a combination of exposure to environmental toxins and/or genetics factors. In fact, although reduction of complex I activities and damage to mtDNA were evidences found in post-mortem PD patients' brain tissues, it was however evident that not all PD patients were self-administering complex I inhibitors (Schapira et al. 1989; Bender et al. 2006). Research over the past decades have pinpointed genetics to be the molecular link between synucleinopathy and mitochondrial damage, which altogether improved our understanding of the pathogenesis of PD.

Genome-wide association studies (GWAS) of single-nucleotide polymorphisms (SNPs) and locus mapping have identified risk loci and several genes whose mutations lead to the development of PD (Chang et al. 2017; Martin et al. 2011). Mutations on those genes lead to the development of autosomal dominant or recessive forms of PD that have highly variable symptoms and age of onset. For instance, missense mutations and gene duplication in Leucine-Rich Repeat Kinase 2 (LRRK2) and SNCA (encoding for α-synuclein) cause the autosomal dominant forms of PD, which is late-onset and has similar Lewy bodies pathology to the sporadic forms of PD (Singleton et al. 2003; Khan et al. 2005). On the other hand, the early-onset autosomal recessive forms of PD are caused by loss-of-function mutations of Parkin, PINK1 and DJ-1 (Kitada et al. 1998). Onset of motor symptoms are typically displayed as early as 18 years old (Bonifati et al. 2012). The monogenic PD types accounts for 1-2% of all PD cases, but they represent the most of early-onset cases (Kalinderi et al. 2016).

Since its discovery, Parkin has been shown to be implicated in many biological processes including, but not limited to, mitochondrial quality control (MQC), synaptic excitability, lipid

uptake, inflammation and immunity. Among those processes, the implication of Parkin in MQC has been extensively studied in the last decade (Green et al. 2003; Narendra et al. 2008; Narendra et al. 2012; Vincow et al. 2013; Winklhofer et al. 2014; Ashrafi et al. 2014). Parkin plays an essential role in maintaining mitochondrial health and orchestrating the degradation of damaged mitochondria in conjunction with PINK1 (Matsuda et al. 2010). Parkin was first shown to be implicated in MQC using drosophila models where Parkin mutant drosophila exhibit locomotor defects, reduced lifespan and mitochondrial pathology in their flight muscles (Green et al. 2003). Interestingly enough, the same pathological phenotype can also be observed in PINK1 mutant drosophila, which was rescued when Parkin was overexpressed (Park et al. 2006). Additionally, a systemic loss of Parkin synergizing with mtDNA damage, caused by a deficiency in mtDNA polymerase, resulted in nigrostriatal dopaminergic neurons death in mouse model (Pickrell et al. 2015). Taken together, these observations suggest that Parkin and PINK1 are implicated in maintaining proper mitochondrial function and that mitochondrial dysfunction lies at the root of the pathogenesis of PD.

Parkin and PINK1 Regulate Mitophagy

The molecular pathway in which Parkin and PINK1 are implicated is now well-established. At the onset of mitochondrial damage, PINK1 accumulates on the outer mitochondrial membranes (OMM) where it uses its kinase activity to phosphorylates nearby ubiquitin (Ub) to generate phospho-ubiquitin (pUb), which in turn recruits Parkin to the sites of damage (Koyano et al. 2014). Parkin, an E3 Ub ligase, will catalyzes the addition of Ub chain onto OMM substrates including, but not limited to, Mfn2, Mitofusin-1 (Mfn1), voltage-dependent anion channel

(VDAC), hexokinase 1 and Miro. Parkin-dependent ubiquitination leads to proteasomal degradation of OMM substrates, the formation of mitochondrial-derived vesicles (MDVs) (McLelland et al. 2014) and ultimately, a selective degradation of damaged mitochondria termed mitophagy (Pickrell and Youle, 2015). It is unquestionable that Parkin operates downstream to PINK1 and that they work in a meticulous fashion to ensure proper mitochondrial function. The remaining sections of this introduction will enlighten in detail the molecular and the structural mechanisms underlying Parkin and PINK1 function.

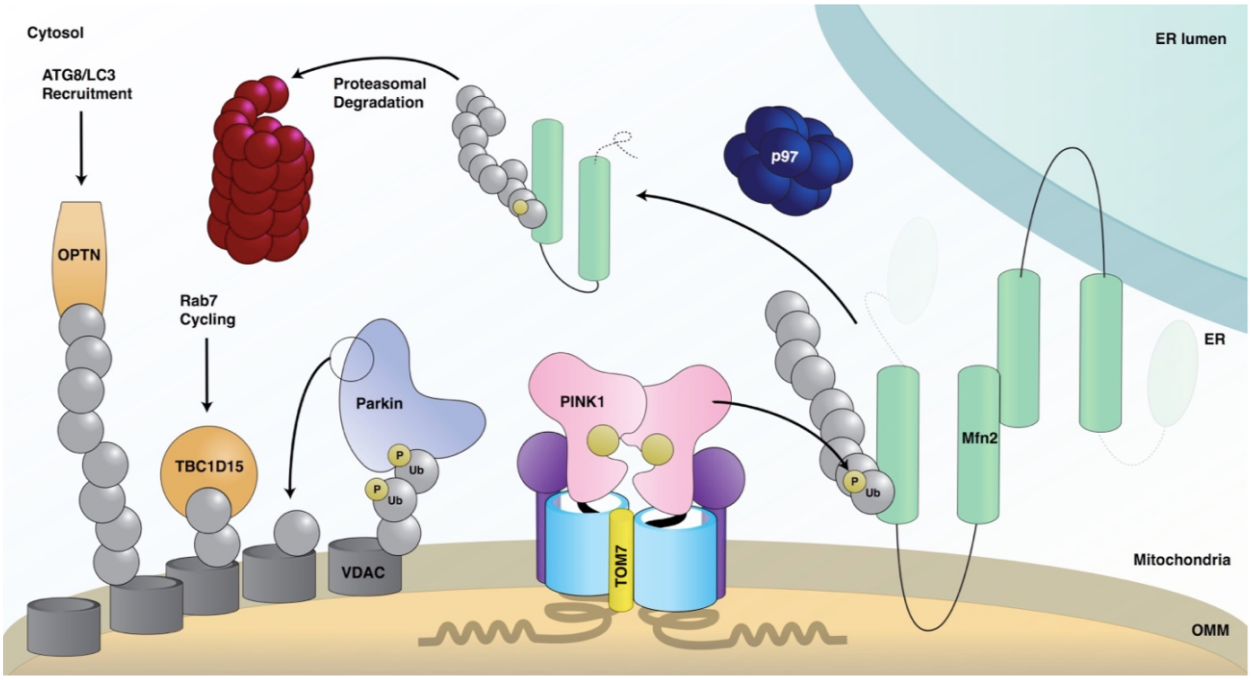

Figure 1: Overview of the mitochondrial quality control pathways governed by Parkin and PINK1 at the onset of mitochondrial damage (Bayne and Trempe, 2019). Proteins involved in the pathway are annotated, Ub is represented by the gray spheres and phosphorylation events are represented by golden spheres.

PINK1 Is A Sensor of Mitochondrial Damage and A Unique Ubiquitin Kinase

Even though mitochondria possess their own genome and translational machinery, the majority of mitochondrial proteins are encoded by the nuclear genome and are synthesized in the cytosol. These cytosolic precursors contain a N-terminal presequence often referred to as the mitochondrial target sequence (MTS). These MTS guide the precursor proteins through the translocases of the outer and inner membranes (TOM and TIM, respectively). The TOM complex consists of surface receptors (TOM70, TOM22 and TOM20), the pore (TOM40) and small accessary subunits (TOM7, TOM6 and TOM5). Precursor proteins' MTS are recognized by the surface receptors, guided through the translocation pore (Lazarou et al. 2012) and then transferred to the TIM complex in the IMM. After passing through the TIM complex, MTS domain reaches the matrix before being cleaved off by the mitochondrial processing peptidase (MPP) located in the mitochondrial matrix (Vogtle et al. 2009). Distal regions to the MTS are further removed by other mitochondrial proteases, allowing for proper protein folding and maturation to their respective mitochondrial compartments (Quiros et al. 2016).

PINK1 is a serine/threonine kinase and a unique substrate whose proper import and processing are critical to fulfill its health sensing function. Critical features of its primary sequence reveal the regulation and the functionality of PINK1: its N-terminus (amino acids residues 1-94) contains the MTS spanning from residues 1-34 and residues from 74-94 represents the outer mitochondrial membrane localization signal (OMS) (Okatsu et al. 2015). Its transmembrane domain (TMD) is spanning from amino acids residues 94 to 110 and it is connected to the kinase domain via a linker (residues 110-156). The kinase domain, spanning from residues 156-509, harbours three inserts (insert 1, 2 and 3) and an important autophosphorylation site at serine 228 in human. The

remaining C-terminus from residues 509-581 is termed as the C-terminal extension (CTE) (Woodroof et al. 2011).

Like all mitochondrial proteins imported from the cytosol, PINK1 has an MTS in its N-terminus. In a first proteolytic step, MPP in the matrix first removes the MTS of PINK1 at an unknown site (Greene et al. 2012) and Presenilin-associated rhomboid-like protein (PARL) in the IMM further cleaves PINK1 within its transmembrane domain, yielding the 52 kDa form of PINK1. The second cleavage by PARL exposes an N-terminal phenylalanine residue (Phe104), which is a N-degron signal for degradation by the proteasome via the work of E3 ligase enzymes UBR1, UBR2 and UBR4 (Yamano et al. 2013). Upon mitochondrial damage, accumulation of misfolded proteins or a loss of membrane potential caused by a chemical uncoupler carbonyl cyanide *m*-chlorophenyl hydrazine (CCCP)-induced depolarization (Sekine et al. 2018), PINK1 fails to reach the TIM complex due to a lack of membrane potential to drive its import, and does not get cleaved. Therefore, full length PINK1 accumulates on the OMM and forms a high molecular weight complex (720 kDa) with the TOM complex. This OMM-localized full length PINK1 has shown to be the recruitment signal for cytosolic Parkin to the damaged mitochondria, therefore acting as the gateway for the initiation of mitophagy, further discussed in later sections (Matsuda et al. 2010; Narendra et al. 2008). Therefore, PINK1 is considered as a damage sensor given its ability to localize to all mitochondria but only accumulate on the damaged ones and triggering the downstream clearance machinery. In healthy mitochondria, PINK1 is constitutively imported, cleaved, and degraded in an apparent futile cycle, and its underpinning biological function will only become evident when mitochondria are damaged.

It has become evident with decades of research that PINK1's kinase activity is indispensable for its biological function and regulation. The kinase domain of PINK1 harbours many PD-linked mutations and their loss-of-function mutations will result in the development of autosomal recessive form of PD. It was first shown that pathogenic mutations of PINK1 causing its catalytic inactivation would, though still localize to the mitochondria, block Parkin's recruitment to the damaged sites (Narendra et al. 2010; Matsuda et al. 2010). PINK1 was later found to be the only so far known ubiquitin kinase given its ability to phosphorylate Ub and the ubiquitin-like domain (Ubl) of Parkin (Kondapalli et al. 2012; Koyano et al. 2014; Kane et al. 2014). These pioneering studies allowed the field to gain more insight into the biochemical basis of PINK1 function and regulation, while more recent crystallographic studies revealed the more precise structural changes that take place for PINK1 activation and substrate binding.

PINK1 activation by autophosphorylation occurs following its accumulation on the OMM (Okatsu et al. 2012). This critical step occurs at Serine 228 in human PINK1 was first reported in 2012 (Matsuda et al. 2012). The insect orthologs from *Tribolium castaneum* (i.e. TcPINK1) and from *Pediculus humanus corporis* (i.e. PhPINK1) were later found to be phosphorylated at the conserved residue Serine 205 and Serine 202, respectively (Woodroof et al. 2011; Schubert et al. 2017). Phosphorylation at Ser228 in human PINK1 (or its equivalent Ser205 in TcPINK1 and Ser202 in PhPINK1) enables it to undergo conformational changes, allowing it to bind and phosphorylates Ub and Parkin Ubl. Mutations to that specific serine residue yielded the inability of PINK1 to phosphorylate Ub or Parkin Ubl *in vitro*. Similarly, TcPINK1 loses the ability to bind Ub and Parkin Ubl without its autophosphorylation at Ser205 (Rasool et al. 2018). Previous

studies have established that PINK1 dimerizes and autophosphorylates as it accumulates on the OMM (Okatsu et al. 2012). Our group have shown, in 2018, that PINK1 molecules undergo intermolecular autophosphorylation (i.e. phosphorylation occurring in *trans*). This established that at least two molecules of PINK1 must first interact to trigger autophosphorylation at Ser228 and to enable downstream Ub phosphorylation. Similarly, mutation at Ser228 can still localize to the mitochondria, but is unable to generate pUb and downstream Parkin recruitment (Rasool et al. 2018).

Autophosphorylation and Ub binding will cause PINK1 to undergo noticeable structural conformational changes, which were recapitulated in three X-ray crystallographic structures showing the *apo* unbound TcPINK1, TcPINK1 bound to a unhydrolyzable ATP analogue AMP-PNP, and a structure of PhPINK1 bound to Ub (Kumar et al. 2017; Okatsu et al. 2018; Schubert et al. 2017, respectively). In the structure of the unbound apo TcPINK1 and TcPINK1 bound to AMP-PNP, the insert 3 is either deleted or disordered. This is in contrast to the PhPINK1 structure bound to Ub, in which the phosphate group on Ser202 is stabilizing the insert 3, priming it to make interactions with Ub. Indeed, the side-chain of Ser65 on Ub is in close conjunction and ready to be phosphorylated by PINK1 (Schubert et al. 2017). PINK1 activation and Ub phosphorylation represent the trigger of mitophagy and the activation of MQC pathway, and undeniably the critical step that precedes Parkin recruitment.

PINK1-Dependent Parkin Activation

Parkin and PINK1 orchestrate the degradation of damaged mitochondria in a well-coordinated stepwise manner. The current model regarding PINK1-dependent Parkin recruitment is the

following: upon mitochondrial damage, PINK1 builds up on the OMM where it phosphorylates Ub chains on OMM proteins. Parkin is an E3 ubiquitin ligase that catalyzes the transfer of Ub onto substrate proteins (Shimura et al. 2000). But how exactly is PINK1-dependent Parkin activation achieved?

Parkin is a RING-in-Between-RING (RBR) ligase that catalyzes the transfer of Ub moieties from E2 ubiquitin-conjugating enzymes onto protein substrates (Shimura et al. 2000). Parkin harbours a E2 enzyme-binding domain called RING1; an In-Between-RING (IBR); a catalytic RING2 which contains the catalytic Cysteine 431 (Cys431) serving as the acceptor site for Ub; a ubiquitin-like (Ubl) domain; an additional RING domain called RING0; and finally, a small helix that binds to RING1 termed the Repressor Element of Parkin (REP) (Trempe et al. 2013) (figure 2, inactive Parkin). The active site Cys431 located on RING2 is crucial to ensure proper Parkin's ligase activity and its mutation will cause autosomal recessive juvenile Parkinsonism (ARJPD) (Maruyama et al. 2000). Structural studies performed by our group and others have demonstrated that Parkin is basally auto-inhibited (Trempe et al. 2013; Wauer and Komander, 2013; Riley et al. 2013). First, the Repressor Element of Parkin (REP) binds to RING1 and blocks any E2 from binding (Figure 2, inactive Parkin). In support of this model, mutation of Trp403, which anchors the REP to RING, will dislodge the REP domain thereby allowing Parkin to gain catalytic activity (Trempe et al. 2013). Second, the Ubl domain of Parkin is bound to RING1 in a manner that occludes its phosphorylation by PINK1 (Figure 2). Third, the RING0 domain of Parkin is positioned to block the active Cys431 located on RING2. In fact, Parkin can be activated when key residues (Phe146) located in between the RING0:RING2 interface are mutated (Tang et al. 2017).

PINK1 activates Parkin at the sites of damage in a stepwise fashion. The production of pUb by PINK1 will act as a recruitment signal and a receptor for Parkin, which binds to pUb (but not Ub) with high affinity (Kd ~ 100-400 nM). Crystal structures of Parkin bound to pUb showed that it binds to RING1 while engaging in important interactions with RING0 and the IBR domains (Kumar et al. 2017; Wauer et al. 2015; Sauvé et al. 2015). The binding of pUb induces the dissociation and the release of Ubl domain away from RING1. Critical steps following Ubl release occur to achieve Parkin activation: Ubl, precisely its hydrophobic patch involving Ile44, binds to Parkin-RING1 the same fashion it would to PINK1. Therefore, its dissociation allows for its Ser65 phosphorylation. Ubl phosphorylation increases drastically Parkin's E3 ligase activity (Sauvé et al. 2015). Phosphorylated Ubl (pUbl) moves and binds to RING0 at a site that overlaps with the RING2 binding site, therefore triggering RING2 to be displaced and exposing its catalytic Cys431 (figure 2, Parkin phosphorylated). Additionally, the dissociation of the RING2 causes the REP domain to be displaced, simultaneously freeing the E2 binding site (Sauvé et al. 2018, Figure 2, active complex). It is noteworthy that the occurrence of pUb binding to Parkin is key to initiate the cascade of Parkin activation, this current model thus implies that pUb chains must be present prior to Parkin recruitment and activation. In fact, total pUb level can be detected in a Parkin-null HeLa cells upon treatment with CCCP (Fiesel et al. 2015). Furthermore, our group has shown that a mutant of Parkin that cannot bind to pUb cannot be phosphorylated on the Ubl, implying that binding to pUb is the primordial first step (Tang et al 2017). Similarly, a TOM70-Ub-PINK1 chimera can recruit Parkin C431S to mitochondria even in the absence of CCCP treatment (Zheng et al. 2013). The implication of pre-existing pUb prior to Parkin recruitment will be explored in later sections.

In sum, pUb recruits Parkin to the damaged mitochondria and its binding dislodges Ubl on Parkin, allowing for its phosphorylation. Sequential Parkin's domains rearrangement, notably the freeing of E2 binding site on RING1 and RING2's catalytic Cys431, altogether renders Parkin catalytically active and ready to ubiquitinate substrate proteins.

Figure 2: Schematic for the stepwise activation of Parkin. All domains of Parkin are illustrated and annotated. Figure reproduced from Sauvé et al (2018).

Parkin Catalyzes the Transfer of Ubiquitin onto OMM Substrates

The cascade of protein substrates ubiquitination is generally achieved via three steps: 1) Ub must first be activated by the E1 ubiquitin-activating enzymes (E1). This step requires ATP hydrolysis, and results in the formation of a thioester between the carboxyl group on the C-terminus of Ub and the E1's catalytic cysteine. The human genome only encodes two E1 enzymes for ubiquitin, namely UBA1 and UBA6; 2) Ub is transferred from the E1 enzyme onto a cysteine acceptor on an E2 ubiquitin-conjugating enzyme (E2). There exists a larger variety of E2 enzymes compared to E1 enzymes, such that eukaryotes possess up to 35 E2 enzymes; 3) E3 ubiquitin ligases catalyze the final step of ubiquitination of substrates by transferring the Ub from the E2 enzyme onto the substrate lysine ε-amino group. The large variety of E3 enzymes, over 500 in human, confers to dictating substrate specificity of the ubiquitination cascade. E3 ubiquitin ligases are generally

categorized based on their biochemical mechanisms: 1) Really Interesting New Gene (RING) ligases catalyze the transfer of Ub directly from an E2 enzyme onto the substrate whereas; 2) HECT type ligases contain a cysteine acceptor site that allows for the Ub to be first transferred onto the ligase itself and in a sequential step, onto the substrate; 3) RBR E3 ligases such as Parkin function through a hybrid mechanism between the RING and HECT. RBR ligases bind E2 on one domain (RING1) and possess a separate domain containing the catalytic cysteine on which Ub is transferred (RING2) (Wenzel et al. 2011). These two domains are linked by an IBR domain, which coordinates the thioester transfer reaction and plays additional roles.

Parkin thus catalyzes the transfer of Ub from E2 enzymes onto the targeted substrates' lysine residues in two distinct steps: 1) Ub is first transferred from an E2 enzyme onto the acceptor cysteine 431 (Cys431) in Parkin, in a step called transthiolation, and 2) an acyl transfer to the target substrates to form a lysine-Ub isopeptide bond (Wenzel et al. 2011; Figure 3). Given that the amino groups of lysine's side chain are typically protonated at neutral pH, they are intrinsically poor nucleophiles that will require a deprotonation step in order to carry out the formation of the lysine-Ub isopeptide bond. Interestingly, structural analysis of Parkin's RING2 domain revealed the presence of a histidine 433 (His433) in close proximity to the catalytic Cys431 (Figure 4). His433 is thought to act as a base to deprotonate any substrates' lysine side chain in order to facilitate the acyl transfer step. Its mutation diminishes Parkin's activity, thereby damping down downstream substrates ubiquitination (Trempe, 2013).

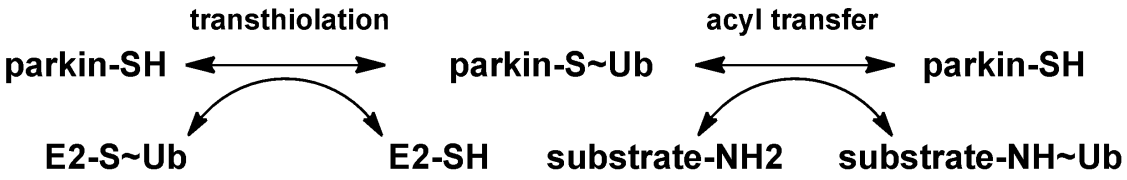

Figure 3: Schematic representing the stepwise Parkin-catalyzed ubiquitination. Ub is first transferred from an E2 ubiquitin-conjugating enzyme onto the catalytic cysteine (Cys431) of Parkin via a transthiolation step. The subsequent acyl transfer step enables the transfer of Ub from Parkin onto a substrate's lysine.

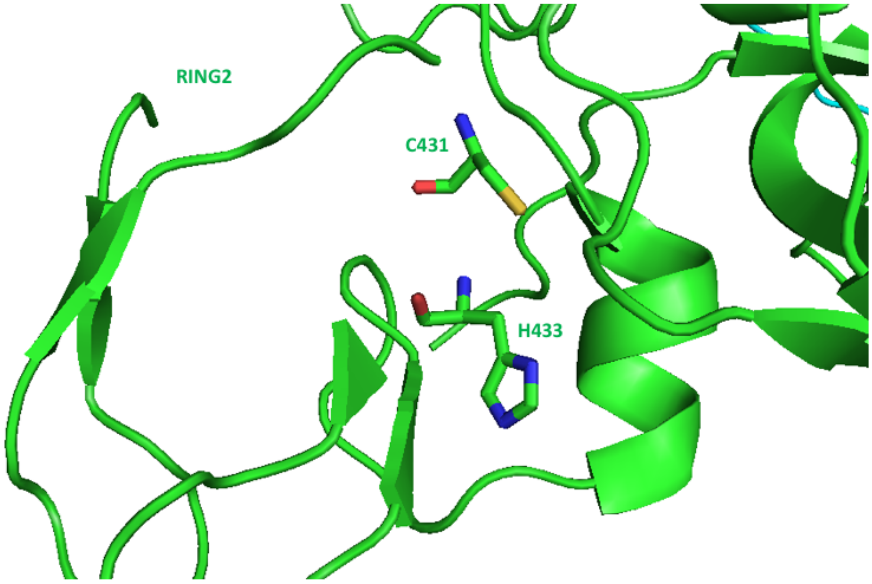

Figure 4: Parkin's RING2 domain contains the catalytic Cys431 and a nearby histidine (His433). Both residues are essential for successful Ub transfer on substrates' lysines (PDB: 4k7d).

Substrates Ubiquitination and Downstream Degradation

Upon activation, Parkin ubiquitinates substrates that are localized at the sites of damage. Unlike many other E3 ubiquitin ligases that have strict substrates specificity, Parkin rather ubiquitinates a variety of substrates located on the OMM. Parkin does not recognize a specific motif within a substrate for ubiquitination to occur, it will rather ubiquitinate any lysine in its proximity after

activation. In fact, proteomics studies have successfully identified a large number of Parkin substrates, which do not share a specific sequence or structural recognition motif (Sarraf et al. 2013). In 2010, voltage-dependent anion channel 1 (VDAC1) was identified to be a substrate of Parkin. VDAC is an abundant mitochondrial OMM ion channel that allows exchange of small ions and mitochondrial metabolites between the cytosol and the intermembrane space (IMS). VDAC was shown to be ubiquitinated in a Parkin-dependent manner after CCCP treatment (Geisler et al. 2010).

In 2010, Mitofusin 1/2 (Mfn1/2) was also identified as substrates of Parkin (Tanaka et al. 2010). Mitofusins are large transmembrane guanosine triphosphatases (GTPase) that control the topology of OMM by acting as membrane fusion proteins. The conserved domains of Mfn1/2 consist of a GTP binding domain, followed by a coiled-coil domain (heptad repeat HR1), a bipartite transmembrane domain and a second coiled-coil domain (heptad repeat HR2). The HR2 domain is involved in the tethering between two adjacent mitochondria by forming either homotypic or heterotypic dimers (Chen et al. 2003; Koshiba et al. 2004). Further studies showed that both the GTPase and the HR2 domains are indispensable for Mfn1/2's proper function. Mutations in these domains disrupt the GTPase activity required for fusion to occur and disorder the coiled-coil structures needed for membrane tethering (Qi et al. 2016). In regard to its regulation, the steady state levels of mitofusins are controlled by their degradation by the ubiquitin-proteasome system. In fact, Mfn1/2 ubiquitination leads to their extraction from the OMM by the AAA+ ATPase P97 and downstream degradation by the proteasome (Tanaka et al. 2010; Kim et al. 2013). The loss of Mfn1/2 following mitochondrial insult leads to mitochondrial

fragmentation. The loss of fusion activity induces mitochondrial fission controlled by dynamin-related protein 1 (Drp1). One hypothesis is that mitochondrial fragmentation mitigates the spread of the damage by separating and preventing the refusion of healthy and damaged mitochondria (Knott et al. 2008; Tanaka et al. 2010; Yang and Yang, 2013). The dynamics between mitochondrial fusion and fission result into different morphological outcomes, ranging from tubular mitochondrial network to fragmented mitochondrial projections. This plasticity allows mitochondria to be highly dynamic organelles and permits for proper mitochondrial function in response to cellular stress (Liesa and Shirihai, 2013). Dimerized Mfn2, but not Mfn1, also acts as a tether between the endoplasmic reticulum (ER) and the mitochondria in a juxtaposition termed the mitochondria-associated ER membranes (MAMs) (de Brito et al. 2008). These appositions are critical sites in which several processes take place such as mitochondrial dynamics, lipids biosynthesis and calcium (Ca^{2+}) transfer (Pinton, 2018). Conversely, silencing Mfn2 in HeLa cells is enough to disrupt the ER morphology and to loosen the ER-mitochondria contact sites (de Brito et al. 2008). More recent studies have shown that AAA+ ATPase P97-dependent Mfn2 extraction from the ER-mitochondria interfaces and its downstream degradation by the proteasome facilitates mitophagy (McLelland et al. 2018). However, recent studies have shown that proteasomal degradation of Mfn2 might be an artefact of Parkin overexpression (Ordureau et al 2018). But regardless of whether it is degraded or not, Mfn2 is ubiquitinated by Parkin.

Recent work from the Edward Fon lab further highlights the importance of Mfn2 regulation and ubiquitination in relationship to mitophagy: Mfn2 is shown to be a negative regulator of mitophagy and exerts its antagonistic effect by tethering the ER to mitochondria (McLelland et

al. 2018). In their studies, mitophagy was monitored and quantified using the mitochondrially-targeted mKeima (mtKeima), a pH sensitive fluorescent protein that is targeted to the mitochondria and shifts its fluorescence excitation when acidified by the lysosome. Lysosomal positive mtKeima are detected upon mitochondrial depolarization with CCCP (Katayama et al. 2011). McLelland et al. employed mtKeima to demonstrate that Mfn2 degradation promotes the induction of mitophagy and allows for a rapid recruitment of Parkin to the sites of damage (McLelland et al. 2018). More precisely, the degradation of Mfn2 shortly following mitochondrial damage causes the dissociation of the ER-mitochondria apposition, which in turn increases the rate of bulk mitophagy (McLelland et al. 2018). Consistently, Parkin resistant mutations in Mfn2's HR1 domain, including K406R, K416R and K420R, all failed to induce mitophagy. All those lines of evidence suggest that Mfn2 acts as a gateway for the initiation of mitophagy once Parkin is recruited and activated at the damaged OMM.

Other well-established substrates of Parkin identified via the quantitative proteomics approach include subunits of the TOM complex, CISD1/2 (an iron-sulfur containing protein that plays a role in mitochondrial bioenergetics), Hexokinase 1 (HK1; an enzyme catalyzing the first step of glycolysis) and mitochondrial Rho GTPase 1 (Miro1; a GTPase involved in mitochondrial transport on microtubules along the axons by associating with Milton and motor proteins such as kinesin and dynein) (Wang et al. 2011; Ordureau et al. 2018; Sharraf et al. 2013). Miro was also reported to be implicated in mitochondrial fusion dynamics along with Mfn2. In fact, degradation of Miro1 by Parkin/PINK1 causes mitochondrial arrest, thereby preventing the fusion of healthy and

damaged mitochondria, and allowing for repair or clearance (Escobar-Henriques and Langer, 2014).

Although Parkin indeed ubiquitinates many OMM substrates following mitochondrial damage, it certainly does not ubiquitinate all the substrates at the same rate. For instance, there exists a substrate hierarchy that is governed by Parkin ubiquitination. Studies have shown that Mfn2 is rapidly ubiquitinated by Parkin at the onset of mitochondrial damage (Tanaka et al. 2010). Recent quantitative proteomics studies by Ordureau et al. used heavy isotope labeled peptides derived from a panoply of Parkin substrates to quantify the kinetics of substrates ubiquitination. In this study, Mfn2 ubiquitination rapidly reaches a plateau thirty minutes post the induction of mitochondrial damage using oligomycin A/antimycin A (OA) (figure 5, highlighted in purple). Given its low protein abundance in comparison to other OMM proteins such as VDAC1, Mfn2 is by far the most ubiquitinated substrate, more specifically at its Lys416 (K416) (Ordureau et al. 2018). One remaining question is the following: given that Parkin does not have a substrate recognition motif, then how does it selectively and rapidly ubiquitinate Mfn2 at physiological concentrations over other OMM substrates? This topic is further exploited throughout this thesis in later sections.

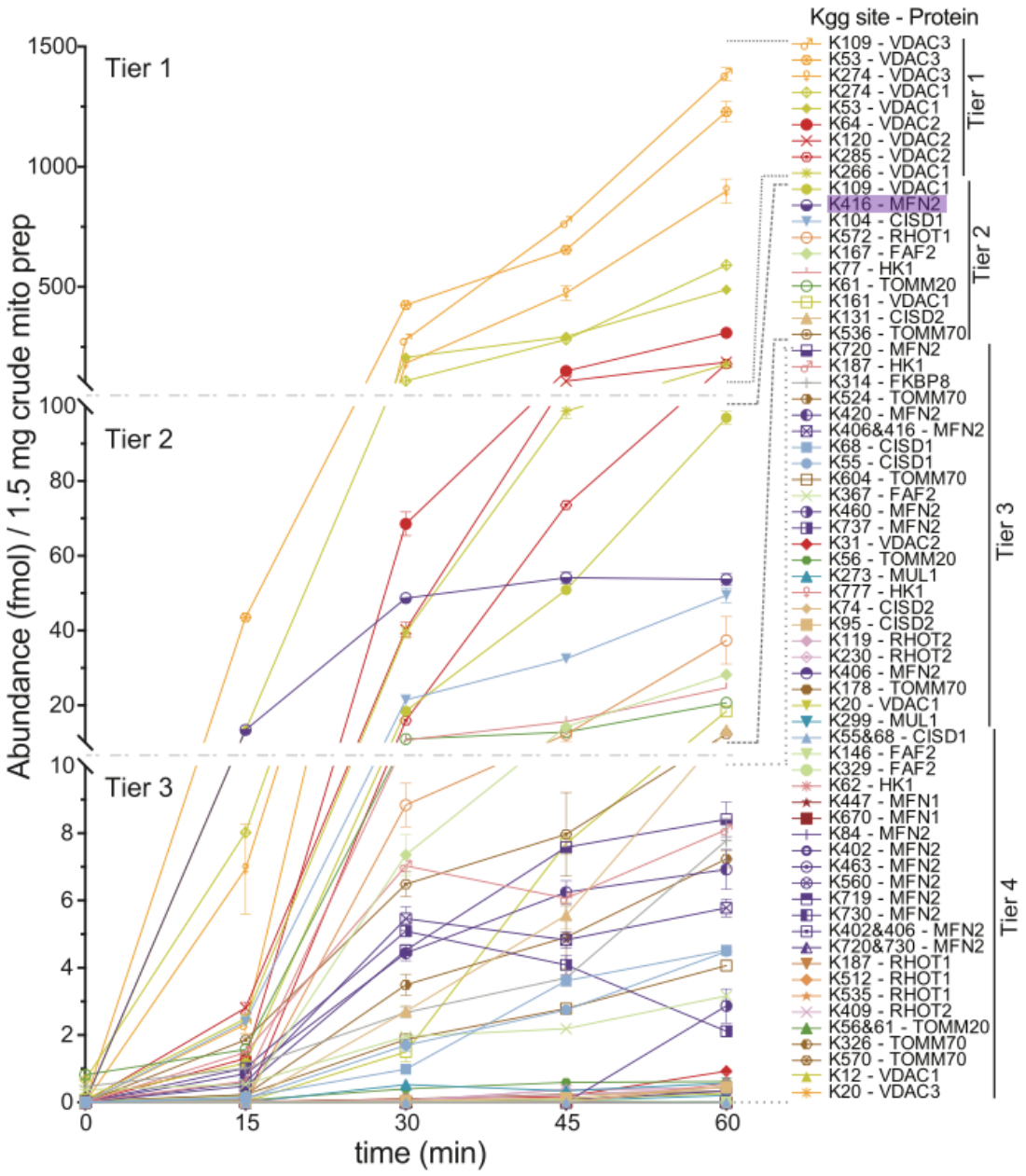

Figure 5: Kinetics of Parkin-dependent mitochondrial proteins ubiquitination. Quantitative proteomics studies measured the abundance of ubiquitinated substrates (y-axis) over time (x-axis). The detected proteins and their respective ubiquitinated lysine sites are classified into tiers from the most to the least ubiquitinated (shown on the right). All three isoforms of VDAC and Lys416 of Mfn2 (highlighted in purple) are the most ubiquitinated. Kgg: a diglycine peptide remnant on the conjugated lysine after trypsinolysis shows that ubiquitination has previously occurred. Figure reproduced from Ordureau et al. (2018).

Mitofusin-2 Modulation by Other E3 Ligases

Although Parkin is a well-characterized E3 ligase that acts on Mfn2, studies over the years have identified three other mitochondrial E3 ligases that are regulating Mfn2's activity as a response to physiological stress conditions. Here, we will briefly expand on each of those ligases by focusing on how they target Mfn2 and the role of these modifications.

The E3 ligase March5 (membrane-associated RING finger protein 5), also known as MITOL (mitochondria-associated ligase) is implicated in the regulation of mitochondria morphology (Karbowski et al. 2007) and the maintenance of ER-mitochondria contacts via Mfn2 (Sugiura et al. 2013). March5 is an OMM protein with four transmembrane domains and a RING finger domain at its N-terminus (Nakamura et al. 2006; Yonashiro et al. 2006). March5 regulates mitochondrial dynamics and morphology by inhibiting mitochondrial fission, thereby promoting tubulation of healthy mitochondria (Xu et al. 2016). March5 was shown to regulate ER-mitochondria tethering by activating Mfn2 through ubiquitination at its K192 position, which is located in the GTPase domain of Mfn2 (Sugiura et al. 2013). This in turn promotes the dimerization and the formation of Mfn2 oligomers that are important for the maintenance of ER-mitochondria appositions. Consistent with this observation, a K192R mutation or a March5 knockdown prevented Mfn2 complex formation and proper localization to the MAMs. Recent studies from the Matsuda group suggest that March5 facilitates Parkin recruitment following mitochondrial damage and that, conversely, silencing March5 led to a delay in ubiquitination of OMM substrates (Koyano et al. 2019). More recently, March5 was also shown to ubiquitinate mitochondrial protein precursors imported through the TOM complex, and a loss of March5 leads to a reduced pUb production on damaged mitochondria (Phu et al 2020).

Similar to March5, the E3 ligase MUL1 (mitochondrial ubiquitin ligase 1), also known as MULAN or MAPL (mitochondria-anchored protein ligase), is also an OMM protein that regulates mitochondrial dynamics. MUL1 has two transmembrane domains, with its C-terminal RING finger domain facing the cytosol. MUL1 was first described as a SUMO E3 ligase that regulates mitochondrial fission (Braschi et al 2007) and actively contributes to the formation of mitochondria-derived vesicles targeted to the peroxisomes (Neuspiel et al. 2008). In addition, MUL1-dependent SUMOylation of Drp1 stabilizes the ER-mitochondria contact sites, and this process is essential for proper cytochrome c (CytC) release and activation of apoptosis (Prudent et al. 2015). MUL1 can compensate for the loss of Parkin/PINK1 pathway by ubiquitinating Mitofusin in Drosophila and thereby promoting mitophagy. In addition, MUL1 overexpression can rescue the defects caused by an increase in Mitofusin abundance seen in dopaminergic neurons and in muscles of Parkin/PINK1 mutant flies (Yun et al. 2014). Furthermore, it has been shown that MUL1 plays a role in the context of dopaminergic (DA) neurons loss that is closely related to PD. In fact, PD-linked mutation of vacuolar protein sorting-35 (VPS35), a retromer component for endosomal trafficking, led to an increase in MUL1, thereby causing Mfn2 degradation by the proteasome, subsequent mitochondrial fragmentation and an impairment in oxidative phosphorylation (Tang et al. 2015). Conversely, MUL1 inhibition re-established Mfn2 levels, therefore suggesting that MUL1 is directly ubiquitinating Mfn2 (Tang et al. 2015).

Huwe1 is another ligase that ubiquitinates Mfn2. Huwe1 is a HECT domain E3 ligase that assembles a variety of ubiquitination types including: K48- and K63-linked polyubiquitination, K11- and K6-linked ubiquitination and monoubiquitination (Adhikary et al. 2005; Parsons et al.

2009; Michel et al. 2017). Indeed, Huwe1 is a main source of cellular K6 ubiquitin chains and Mfn2 is modified by K6-linked chains in a Huwe1-dependent fashion (Michel et al. 2017). Huwe1 has been shown to regulate Mfn2 in response to genotoxic stress, upon the activation of the c-Jun N-terminal kinase (JNK) (Leboucher et al. 2012). Indeed, phosphorylated Mfn2 by JNK led to the recruitment of Huwe1, which in turn promotes Mfn2 degradation and downstream mitochondrial fragmentation and apoptosis (Leboucher et al. 2012; Senyilmaz et al. 2015).

In conclusion, while Parkin remains the most studied E3 ligase that ubiquitinates Mfn2, there are undeniably other mitochondria-associated ligases that also actively play a role in regulating Mfn2's function. As such, Mfn2 ubiquitination by other E3 ligases such as March5/Mitol, MUL1/MULAN/MAPL and Huwe1 has been associated with morphological changes of mitochondria, alterations of mitophagy and promotion of apoptosis. The intertwinement between these E3 ligases and the Parkin/PINK1 pathway is still subject to further research, and will be explored in later sections of this thesis.

Polyubiquitination, Proteasomal Degradation and Autophagy

Polyubiquitination of proteins is a triggering signal that leads to the target protein degradation by the proteasome. While Parkin ubiquitinates OMM substrates, it can also build up large polyubiquitin chains on any of the seven lysines residues on Ub itself, among which Lys48- and Lys63-linked polyubiquitin chains are found to be enriched on mitochondria following depolarization in a Parkin-dependent manner (Chan et al. 2011; Durcan et al. 2014; Ordureau et al. 2014). Given that Parkin can make any type of polyubiquitin chains, this further consolidates the notion that Parkin does not have a substrate specificity and will ubiquitinate any accessible

lysine residues. It has been demonstrated that different polyubiquitin chains will lead to different outcomes with respect to their conjugated substrates. For instance, Parkin-mediated Lys48-linked polyubiquitin chains binds to the receptors of the 26S proteasome such as Rpn10 and Rpn13 to facilitate the proteasome recruitment to the damaged mitochondria (Husnjak et al. 2008). Moreover, the formation of polyubiquitin chains by Parkin will initiate the recruitment of autophagy receptors such as 1) optineurin (OPTN), which recruits microtubule-associated protein 1A/1B-light chain 3 (LC3) through its LC3-interacting region (LIR); 2) p62 (Sequestome 1), an adaptor protein that binds to Lys63 polyubiquitin chains; and 3) nuclear dot protein 52 (NDP52), which directs autophagy targets to autophagosomes by interacting with the cargo and LC3 (Lazarou et al. 2015; Viret et al. 2018; Pickles et al. 2018; Stolz et al. 2014). Although it was previously established that these autophagy receptors bind to ubiquitinated cargo and initiate mitochondrial clearance (Tanida et al. 2008), recent studies using knockdown assays in HeLa cells suggested that NDP52 and optineurin are the two primary receptors involved in Parkin/PINK1-mediated mitophagy. Consequently, knocking out optineurin and NDP52 severely impaired mitophagy (Lazarou et al. 2015).

In addition, polyubiquitin chains generated by Parkin will also recruit RABGEF1, a guanosine nucleotide exchange factor (GEF) for Rab proteins, which will bind to ubiquitinated chains and switch Rab5-GDP to Rab5-GTP (Yamano et al. 2014). Rab5 in turns stimulates MON1/CCZ1 complex, which is a Rab7 GEF that will activate Rab7 to Rab7-GTP, which altogether stimulate the formation and maturation of autophagosomes (Nordmann et al. 2010; Yamano et al. 2014). Nascent autophagosomes undergo a series of regulated steps for maturation prior to the fusion

with the degradative compartments, and this final step requires the assistance of the SNARE-like protein complex to catalyze the autophagosome-lysosomal fusion (Dikic, 2017).

Overall, Parkin-mediated polyubiquitination typically leads to the degradation of substrate proteins, either through the ubiquitin-proteasome system or autophagy. However, accumulating evidence shows that Parkin can also mediate a non-degradative and regulatory role. Quantitative proteomics show that OMM substrates levels, including Mfn2, remain unchanged following OA treatment in cell systems expressing endogenous levels of Parkin (Ordureau et al. 2018; Rakovic et al. 2013). Indeed, Mfn2 proteasomal degradation has only been observed in systems with Parkin overexpression. Although this might be an artifact of overexpression, it is however possible that the degradation is occurring locally and not affecting the bulk pool of Mfn2. Regardless, this suggests that Parkin may fulfill other non-degradative roles in addition to its implication in MQC.

Parkin and PINK1 Beyond Autophagy

Parkin and PINK1 are undoubtedly playing a critical role in the regulation of autophagic MQC pathways, but research from other fields now have shown they exhibit a broader implication and do not necessarily lead to mitophagy or the destruction of a whole damaged mitochondrion. Indeed, Parkin and PINK1 signalling can lead to the formation of mitochondrial-derived vesicles (MDVs) (Soubannier et al. 2012; Sugiura et al. 2014; McLelland et al. 2016). MDVs contain selective mitochondria cargo that are misfolded protein aggregates and oxidized components of mitochondrial matrix, which will be sent to the late endosomes/lysosomes in a SNARE protein syntaxin-17-dependent fashion for degradation (Soubannier et al. 2012; McLelland et al. 2014,

2016). Unlike mitophagy, MDVs bud off from mitochondria independently from the fission protein Drp1 and do not rely on the canonical macroautophagy machinery (Soubannier et al. 2012). It is therefore thought that MDVs help with the removal of selected and focal sites of damage and are indeed less drastic than bulk mitophagy. While the ubiquitin ligase activity of Parkin is required for the formation of a subset of MDVs, the substrates of Parkin involved in this process are unknown.

In contrast, Parkin and PINK1 have also been found to inhibit the formation of a subset of MDVs that are required for mitochondrial antigen presentation (MitAP) in immune cells, a process where self-antigens that are extracted from mitochondria via MDVs can present their cargo to the major histocompatibility (MHC) class I proteins, which are sent to the cell surfaces to be recognized by T cells (Matheoud et al. 2016). MitAP requires the recruitment of important effector proteins to the mitochondria: 1) Rab9, a GTPase regulating vesicle release from late endosomes (Kucera et al. 2016); and 2) Sorting nexin 9 (Snx9), a dynamin binding protein essential for clathrin-mediated endocytosis (Lundmark and Carlson, 2009). However, Parkin and PINK1 negatively regulate this MDV pathway and suppress MitAP (Matheoud et al. 2016). A new hypothesis that arises from this observation is that defects in Parkin and PINK1 can lead to the overactivation of MitAP and therefore, PD caused by mutations in Parkin and PINK1 could be an autoimmune disease. Regardless, further research is needed to reconcile the differentiation between MDVs that are promoted versus the ones are that suppressed by Parkin/PINK1.

Parkin and PINK1 have also been shown to be implicated in the regulation of inflammation. Indeed, Parkin and PINK1 homozygous knockout mice exhibit strong inflammatory phenotypes

following exhaustive exercise. These mice had significant higher levels of interleukin-6 (IL-6) and Interferon β1 (IFNβ1) in comparison to wild type mice (Silter et al. 2018). Additionally, these mutant mice also showed an increased circulating level of mtDNA. Presumably, a leak of mtDNA into the cytosol leads to an aberrant inflammatory response mediated by STING (Stimulator of Interferon Genes), which is achieved by the production of cGAMP synthase (cGAS) and NF-κB activation (Barber, 2015). Consequently, a loss of STING led to an attenuation of the observed inflammatory response to a level that is comparable to the WT mice (Silter et al. 2018). These altogether suggest that Parkin and PINK1 are essential for the removal of damaged mitochondria punctually before their DNA leaks in the cytosol and triggers a downstream STING-mediated inflammation.

Parkin and PINK1 are not only essential components of the MQC pathway, they are also ubiquitously expressed in many cell types and organs where they may fulfill different biological functions. Parkin has been shown to modulate cardiac health and provide protective roles in cardiac contractile dysfunction (Piquereau et al. 2013). Interestingly, studies suggest that Parkin/PINK1-mediated mitophagy in cardiac homeostasis is most likely to be an inducible cardiac stress-response mechanism rather than a housekeeping role (Dorn, 2016). Furthermore, growing evidence suggests that Parkin also functions as a tumor suppressor and it is linked in various cellular processes implicated in tumorigenesis (Wahabi et al. 2018). Parkin is shown to regulate many of the hallmarks of cancer such as cell cycle, cell proliferation, apoptosis and metabolic reprogramming (Checler et al. 2014; Veeriah et al. 2010). There is no doubt that mutations of Parkin and PINK1 have consequences on diverse physiological processes such as immunity,

metabolism and inflammation. Therefore, the implication of Parkin/PINK1 beyond their roles as neuroprotectants requires further investigation. Future research is essential to uncover the cell-to-cell variation in their biological roles and most importantly, to elucidate Parkin/PINK1's implication in other pathologies.

Hypothesis and Objectives

Despite several lines of evidence showing that Mfn2 is a preferred substrate of Parkin, the exact underlying cause of this substrate selectivity has not yet been uncovered. Therefore, the goal of this project is to elucidate the mechanism underlying Parkin's substrates specificity at the onset of mitochondrial damage, more specifically how it preferentially ubiquitinates Mfn2 over other OMM substrates. We hypothesize that Parkin preferentially ubiquitinates Mfn2 because it is the first protein to be tagged with pUb by virtue of its proximity to PINK1. We therefore posit that PINK1 builds up at ER-mitochondria contact sites near Mfn2.

Our goal was to first confirm Parkin's substrates selectivity towards Mfn2. We first confirmed this substrate preference by assessing the rate of Mfn2 ubiquitination by Parkin in comparison to other OMM substrates using *in vitro* reconstitution assays coupled to western blotting techniques. Proximity ligation assays (PLA) were then performed to determine the cellular localization of Mfn2 with respect to PINK1 in cells. Finally, ubiquitinated substrates pulldown from mitochondrial cell lysates and siRNA-mediated knockdown assays were completed to identify the E3 Ub ligase(s) that is/are "priming" Mfn2 at the onset of mitochondrial damage.

MATERIALS AND METHODS

Cell Cultures – Hela, U2OS (WT, Mfn2 KO, PINK1 KO) Monolayers

Cells were cultured in Dulbecco's Modified Eagle Medium (DMEM; Wisent Bioproducts) to which 5% (v/v) Fetal Bovine Serum (Wisent Bioproducts) and 1% (v/v) penicillin-streptomycin (Invitrogen) were supplemented. The cells were maintained at 37 °C with 5% CO_2 and 95% relative humidity. U2OS cell lines were a generous gift from the Edward Fon lab at the Montreal Neurological Institute.

WT and H433F *Rattus norvegicus* Parkin Purification

WT and H433F mutant Parkin DNA were codon-optimized for *Escherichia coli* expression and subcloned into pGEX6P-1. Parkin constructs were overexpressed in E. coli BL21 codon plus competent cells and grown at 37 °C in LB containing 50 mg/liter ampicillin until an A_{600} of 1.0 was reached. Protein expression was induced by adding 25 μM of isopropyl β-D-1-thiogalactopyranoside (IPTG), along with 500 μM $ZnCl_2$. Cells were allowed to grow overnight at 16 °C. Cells were harvested the next day, lysed and sonicated on ice in 50 mM Tris-HCl (pH 7.4), 120 mM NaCl, 2.5 mM dithiothreitol (DTT) buffer supplemented with EDTA-free protease inhibitor cocktail (Roche), 0.5 mg/ml lysozyme, 0.3 mg/ml DNAase, 5 mM $MgCl_2$ and 0.5% Triton-X. Clarified supernatant was collected after centrifugation at 15,000 RPM for 45 min. GST-Parkin was purified by GST-Sepharose 4B (GE healthcare) and eluted with 20 mM reduced glutathione in 50 mM Tris-HCl, 120 mM NaCl, 2.5 mM DTT, pH 7.4. Eluted proteins were cleaved overnight with HRV-3C protease at 4 °C and applied onto Superdex 75 16/60 (GE healthcare) in in 50 mM Tris-HCl, 120 mM NaCl, 2.5 mM DTT, pH 7.4 for gel filtration. Purified Parkin was concentrated

using Amicon Ultra concentrators with a mass cut-off of 10 kDa (Millipore). The purity and mass of the purified proteins were validated using mass spectrometry.

Mitochondria Isolation and *In Organello* Ubiquitination Assay (Adapted from Tang et al, 2017)

HeLa cells treated with 10 μM CCCP or dimethylsulphoxide (DMSO) for 3h were resuspended in mitochondrial isolation buffer (20 mM HEPES, 220 mM Mannitol, 10 mM potassium acetate, 70 mM sucrose, pH 7.4) at 4 °C. Harvested cells were disrupted by nitrogen cavitation techniques and cell homogenates were centrifuged at 500 g for 5 min at 4 °C. Intact mitochondria were obtained after two further rounds of centrifugation steps carried at 12,000 g for 15 min at 4 °C. The concentration of mitochondria pellets was determined by BCA protein assay (Pierce) and whole mitochondria were stored in mitochondria isolation buffer at a concentration of 1 mg/ml. CCCP- or DMSO-treated mitochondria were supplemented with an ubiquitination reaction mix: 20 nM Ub-activating enzyme (E1), 100 nM of Ub-conjugating enzyme 2 (E2), 5 μM Ub, 1 mM ATP, 5 mM $MgCl_2$, 50 μM TCEP in mitochondria isolation buffer, and recombinant RnParkin at 0, 0.1, 1 or 10 μM. After a 15-minute incubation at 37 °C, reactions were stopped with 3X sample buffer with 100 mM DTT and analysed by western blotting. Reactions were loaded on a 12% polyacrylamide sodium dodecyl sulphate gel (SDS-PAGE; Laemmli). Electrophoretically separated proteins were transferred onto a PVDF membrane (BioRad) in a 50 mM Tris, 40 mM glycine, 20%(v/v) methanol, pH 8.0, and stained with Ponceau. Non-specific binding was blocked using 5% bovine serum albumin (BSA) in phosphate buffered saline with 0.05% Tween (PBS-T). Membranes were incubated at 4 °C overnight with rabbit anti-mitofusin 2 (1:2,000, mAb D2D10, Cell Signaling), rabbit anti-mitofusin 1 (1:2,000, mAb 13196S, Cell Signaling), rabbit anti-Miro1

(1:2,000, mAb 14016S, Cell Signaling), rabbit anti-HK1 (1:2,000, mAb C35C4, Cell Signaling), rabbit anti-HK2 (1:2,000, mAb C64G5, Cell Signaling), rabbit anti-VDAC (1:5,000, mAb D73D12, Cell Signaling), rabbit anti-TOM20 (1:2,000, pAb FL-145, Santa Cruz Biotechnology), rabbit anti-TOM70 (1:1,000, pAb C-18, Santa Cruz Biotechnology), rabbit anti-Parkin (1:2,000, mAb Prk8, Cell Signaling) diluted in PBS-T with 3% BSA. Membranes were washed with PBS-T and incubated with HRP-coupled goat anti-mouse or anti-rabbit igG antibodies (1:10,000, Cell Signaling). Immunodetection was performed after extensive washing with PBS-T and exposed using ECL blotting substrates including peroxide solution and luminol/enhancer solution (Biorad) and visualized using ImageQuant LAS 500 station (GE Healthcare).

UbcH7 Charging and Substrate Ubiquitination Assay Using Parkin WT or H433F

E2 enzymes UbcH7 (100 nM) were charged by incubating with 5 μM Ub, 20 nM Ub-activating enzyme (E1), 1 mM ATP, 5 mM $MgCl_2$ in ubiquitination buffer (50 mM Tris, 120 mM NaCl, 1 mM TCEP, pH 7.4). The reaction was incubated for 60 min at 37 °C to allow the formation of UbcH7~Ub. UbcH7~Ub (1, 3, or 10 μM) was mixed with 20 μg of CCCP-treated mitochondria, 0.2 μM of WT or H433F RnParkin in mitochondria isolation buffer. After a 15-minute incubation at 37 °C, reactions were stopped with 3X sample buffer with 100 mM DTT and analysed by western blotting, as previously described, with primary antibodies targeting for Mfn2 (1:2,000, rabbit mAb D2D10, Cell Signaling), Parkin 1:2,000, rabbit mAb Prk8, Cell Signaling) and VDAC (1:5,000, rabbit mAb D73D12, Cell Signaling).

Proximity Ligation Assay for Proteins Interaction Studies

Protein-protein interactions were analyzed using Duolink in situ orange starter fluorescence kit (mouse/rabbit, Sigma-Aldrich) in human osteosarcoma U2OS cells (WT, Mfn2 KO and PINK1 KO). Cells were grown to confluency on coverslips (Fisherbrand) and 5 μg pCMV(d1) TNT PINK1(WT)-3HA plasmids, obtained from Noriyuki Matsuda for attenuated PINK1 expression, were transfected using Lipofectamine 3000 Reagent (ThermoFisher Scientific). Cells were grown for an additional 48 hours post transfection. Cells were treated with 10 μM CCCP or DMSO for 3 hours before fixation and permeabilization using 4% PFA/0.1% Triton-X-100 for 10 min at room temperature. Samples were blocked using Duolink blocking solution in a preheated humidified chamber at 37 °C for one hour. Primary antibody solution mix contains two primary antibodies raised in two different species (mouse and rabbit) targeting the proteins of interest: rabbit anti-mitofusin 2 (1:50, mAb D2D10, Cell Signaling), rabbit anti-VDAC (1:200, mAb D73D12, Cell Signaling), mouse anti-HA (1:100, mAb D73D12, Cell Signaling), rabbit anti-mitofusin 1 (1:100, mAb 13196S, Cell Signaling), rabbit anti-Miro1 (1:50, mAb 14016S, Cell Signaling), rabbit anti-pUb (1:100, mAb 37642S, Cell Signaling), or mouse anti-mitofusin 2 (1:50, mAb 661-757, Abnova) was added for overnight incubation at 4 °C. The next day, cells were incubated with proximity ligation assay probes PLUS and MINUS diluted 1:5 for one hour at 37 °C. After ligation, the samples were incubated with amplification polymerase solution for 100 min at 37 °C, protected from light. The endoplasmic reticulums were stained using an Alexa488-coupled anti-calnexin (1:200, mAb AF18, ThermoFisher Scientific) in 10% goat serum overnight at 4 °C. Cell nuclei were stained using DAPI (1:1000, ThermoFisher Scientific) for 10 min at room temperature. All samples were mounted

with mounting medium (Dako, Agilent). Images were acquired with a 40x Plan Apo oil-immersion objective using a TCS SP8 confocal microscope (Leica).

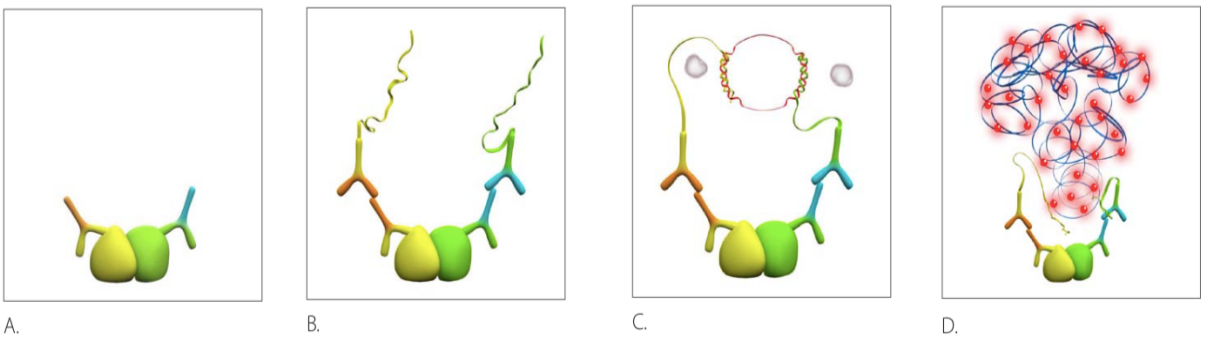

Figure 6: Schematic of proximity ligation assay (adapted from Sigma-Aldrich). A) The yellow and green shapes represent the two proteins of interest that are located in close proximity within 40 nm. Two primary antibodies raised in different species recognize the proteins of interest in the cell. B) Secondary antibodies that are coupled with PLA ligation probes bind to the primary antibodies. C) The PLA ligation probes, if located in close proximity, will ligate to form a circular DNA template to be amplified by DNA polymerase. D) Fluorophores hybridize to the template and amplify to generate detectable fluorescent signals by microscopy.

Tandem Ubiquitin Binding Entities (TUBE) Pulldown

Tandem ubiquitin binding entities (TUBE) pulldown was performed as described in the manufacturer's protocol with slight modifications. Agarose TUBE resin (UM401, LifeSensors) were allowed to equilibrate to 4 °C and resuspended in TBS-T prior to the actual pulldown assay. CCCP- or DMSO-treated mitochondria were isolated as described above and lysed in 50 mM HEPES pH 7.5, 150 mM NaCl, 1 mM EDTA, 1% NP40 or Triton X-100, 10% glycerol, EDTA-free protease inhibitor cocktail (Roche), phosphatase inhibitors (Roche) and 50 uM chloroacetamide. Cleared supernatant after centrifugation at 14,000 RPM for 10 min were added to control

uncoupled agarose (UM400, LifeSensors) for 30 min at 4 °C on a rocker platform. Control uncoupled agarose were removed by centrifugation and the supernatant was added to agarose TUBE resin to allow binding at 4 °C for an hour. Samples were spun down after incubation and washed with TBS-T before being eluted in 100 μl of 6 M urea and 50 mM tetraethylammonium bromide (TEAB) pH 8.5.

GST-R0RBR Purification

GST-R0RBR was expressed as a fusion protein subcloned into pGEX6P-1 vectors and overexpressed in E. coli BL21 competent cells. Cells were grown at 37 °C in 1 liter of LB containing 50 mg of ampicillin until an A_{600} of 1.0 was reached. Protein expression was induced by adding 25 μM of isopropyl β-D-1-thiogalactopyranoside (IPTG), along with 500 μM $ZnCl_2$. Cells were allowed to grow overnight at 16 °C. Cells were harvested the next day, lysed and sonicated on ice in 50 mM Tris-HCl (pH 7.4), 120 mM NaCl, 2.5 mM dithiothreitol (DTT) buffer supplemented with EDTA-free protease inhibitor cocktail (Roche), 0.5 mg/ml lysozyme, 0.3 mg/ml DNAase, 5 mM $MgCl_2$ and 0.5% Triton-X. Clarified supernatant was collected after centrifugation at 15,000 RPM for 45 min. GST-R0RBR was purified by GST-Sepharose 4B (GE healthcare) and eluted with 20 mM reduced glutathione in 50 mM Tris-HCl, 120 mM NaCl, 2.5 mM DTT, pH 7.4. Purified GST-R0RBR was concentrated using Amicon Ultra concentrators with a mass cut-off of 10kDa (Millipore). Purified samples were ran on a 12% poly-acrylamide gel and stained overnight with 0.125% w/v Coomassie G250 (Bio Basic Canada Inc.) in 45% methanol, 10% acetic acid. Gel was destained using 25% methanol, 0.75% acetic acid for at least 24 h. Band intensities for destained poly-acrylamide gel were imaged using ImageQuant LAS 500 station (GE Healthcare).

Mass Spectrometry Analysis

Samples' cysteine residues were reduced using 10 mM DTT for 15 min at 50 °C and alkylated with 25 mM chloroacetamide for 30 min at room temperature, protected from light. Mitochondrial proteins were extracted by methanol-chloroform precipitation: to one volume of mitochondria suspension, four volumes of methanol, one volume of chloroform and three volumes of water were added and vortexed. The mixture was centrifuged for 5 min at 13,000 g at room temperature and the upper aqueous phase was discarded. Three volumes of methanol were added, and the mixture was centrifuged after vortexing. Protein pellets were dried by evaporation and resuspended in 100 mM TEAB pH 8.5, 0.1% RapiGest, 10% acetonitrile (ACN). Protein samples were digested with 1:100 trypsin (Sigma) overnight at room temperature. Digested peptides were purified using C18 Spin Columns (ThermoFisher) and resuspended in 5% ACN and 1.5% trifluoroacetic acid-containing loading buffer. 2 μg of peptides were captured and eluted from an Acclaim PepMap100 C18 column with a 2h gradient of acetonitrile in 0.1% formic acid at 200 nl/min. The eluted peptides were analysed with an Impact II Q-TOF spectrometer equipped with a Captive Spray nanoelectrospray source (Bruker). Data were acquired using data-dependent automatic tandem mass spectrometry (auto-MS/MS) and analysed with MaxQuant using a standard search procedure against the human proteome.

Intact Protein Mass Spectrometry Analysis

Purified proteins were diluted to 0.1 mg/ml in 0.05% TFA and 2% ACN, and 20 μL was injected on a Dionex C4 Acclaim 1.0/15 mm column at a 10 minute 4-50% gradient of ACN in 0.1% formic acid with a flow rate of 40 μL/min. The eluate was analyzed on a Bruker Impact II Q-TOF mass

spectrometer equipped with an ion funnel ESI source. Multiple charged ions were deconvoluted at 10,000 resolution to yield the isotopically resolved mass spectra.

March5, MUL1 and Huwe1 RNA Interference

siRNA oligos for MUL1, Huwe1 and MARCH5 were purchased from QIAGEN. The target individual sequences for March5, Huwe1 and MUL1 are the following:

Protein Target	Target Sequence
March5 (Hs)	5’-TGGCGCAAATACTCGAATAAA-3’; 5’-CAGGAATAATGGTCGGCTCTA-3’; 5’-AACCATTATCTTAGCATGGTA-3’; 5’-CAGGTTGTAGGTCATAAAGAA-3’;
Huwe1 (Hs)	5’-AAGCAGCTTATGGAGATTAAA-3’; 5’-CCGGGCTAACAAGAAAGCCAA-3’; 5’-CAGGTTGTTGGTACAGAGGAA-3’; 5’-CCGGCTTTCACCAGTCGCTTA-3’;
MUL1 (Hs)	5’-CCGCGCCTTGCCAGAGCCCAA-3’; 5’-TGCGTGCCTTATGCTGTTATA-3’; 5’-CTGTGCGGTCTGTTAAAGAAA-3’; 5’-CCGGGTCTCCCAAGAGCTCAA-3’;

siRNAs were transfected into HeLa cells using Lipofectamine 3000 (ThermoFisher Scientific) according to the manufacturer's protocol. The media was changed 6 hours following transfection and the cells were grown for 48 hours before drug treatment. Cells were harvested post 3 hours CCCP treatment and lysed in HEPES buffered saline (HBS) complemented with 0.2% SDS, 1% Triton-X, EDTA-free protease inhibitor cocktail (Roche) and phosphatase inhibitors (Roche). Lysed cells were spun at 40 min at 14,000 RPM and supernatant was collected. Protein concentrations of supernatants were determined with a BCA protein assay kit (Pierce), and 5 μg of the sample were ran on a 12% polyacrylamide sodium dodecyl sulphate gel (SDS-PAGE; Laemmli). Electrophoretically separated proteins were transferred onto a PVDF membrane (BioRad) in a 50 mM Tris, 40 mM glycine, 20%(v/v) methanol, pH 8.0, and stained with Ponceau-S. Non-specific binding was blocked using 5% bovine serum albumin (BSA) in phosphate buffered saline with 0.05% Tween (PBS-T). Immunodetection was performed after extensive washing with PBS-T. The membranes were incubated with the primary antibodies diluted in PBS-T at 4 °C overnight: rabbit anti-March5 (1:1,000, pAb SAB2103803, Sigma), mouse anti-Huwe1 (1:2,000, mAb AX8D1, Cell Signalling) and rabbit anti-MUL1 (1:1,000, pAb A89945, Atlas Antibodies). The next day, membranes were washed for 30 minutes with PBS-T at room temperature. The membranes were then incubated with HRP-coupled goat anti-mouse or anti-rabbit igG antibodies (1:10,000, Cell Signaling). Membranes were washed for 30 minutes with PBS-T at room temperature. Immunoblots were exposed using ECL reagent (Pierce) and visualized using ImageQuant LAS 500 station (GE Healthcare).

Statistical Analyses

All data were expressed as mean ± SEM. No statistical methods were used to predetermine sample size, and they are solely based on experimental feasibility and sample availability. Samples were processed in a random order and PLA signal counts were measured in a blinded fashion. Comparisons between groups were analysed using independent t-tests followed by Bonferroni corrections post-hoc test on Prism GraphPad 8 and $P < 0.05$ was considered as statistically significant.

RESULTS

Purifying Recombinant WT and H433F RnParkin

In order to test the effects of Parkin on Mfn2 ubiquitination in *in organello* assays, recombinant WT and H433F RnParkin were purified. The H433F mutation was selected because it impairs the transfer of Ub to a substrate's lysine, thus providing mechanistic insights. Constructs were expressed in BL21 DE3 E. coli and purified using its GST tag. Following incubation with glutathione sepharose beads for affinity purification, overnight treatment with HRV-3C cleavage and size exclusion chromatography (SEC) (figure 7), WT and H433F RnParkin were successfully purified.

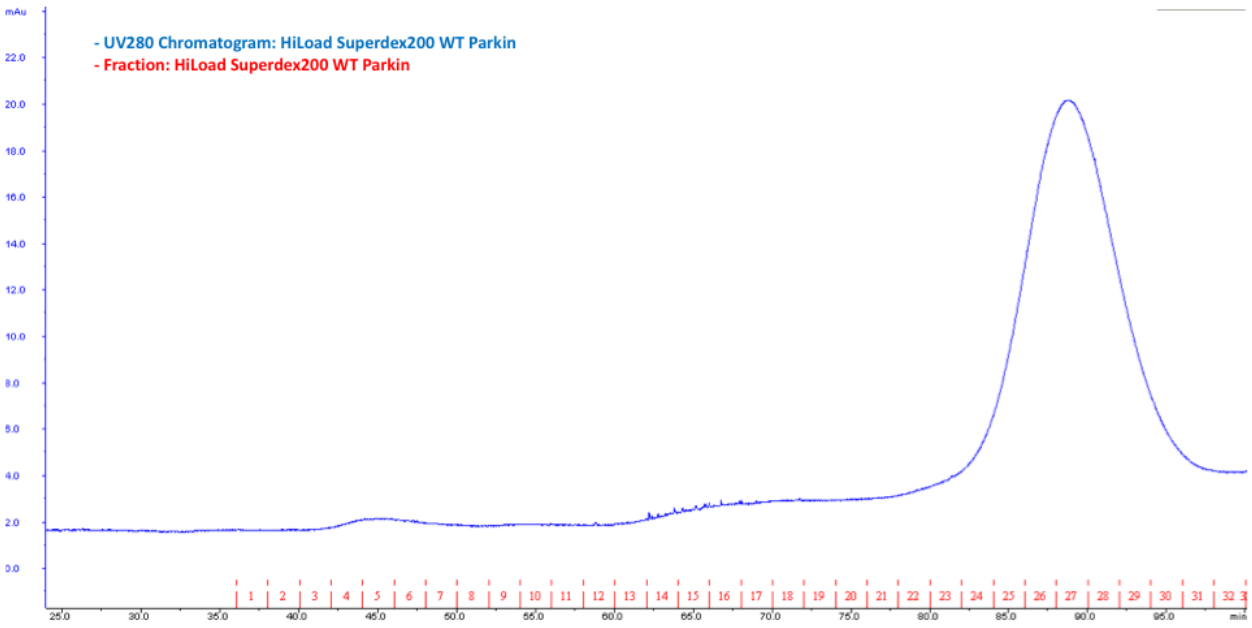

Figure 7: WT Parkin is separated from GST and HRV-3C by SEC following overnight HRV-3C cleavage. The SEC fractions and the elution time are shown on the x-axis, and the UV absorbance (at 280 nm) is shown on the y-axis. The main peak at 20 mAU and eluted in fractions 26 to 29 corresponds to WT Parkin. *(A similar SEC chromatogram elution profile was obtained for H433F Parkin purification; data not shown).* mAU: milli-absorbance units.

To confirm the molecular weights and identities of each protein, we performed intact mass spectrometry analysis (figure 8). The observed masses matched the predicted masses within 1 Da.

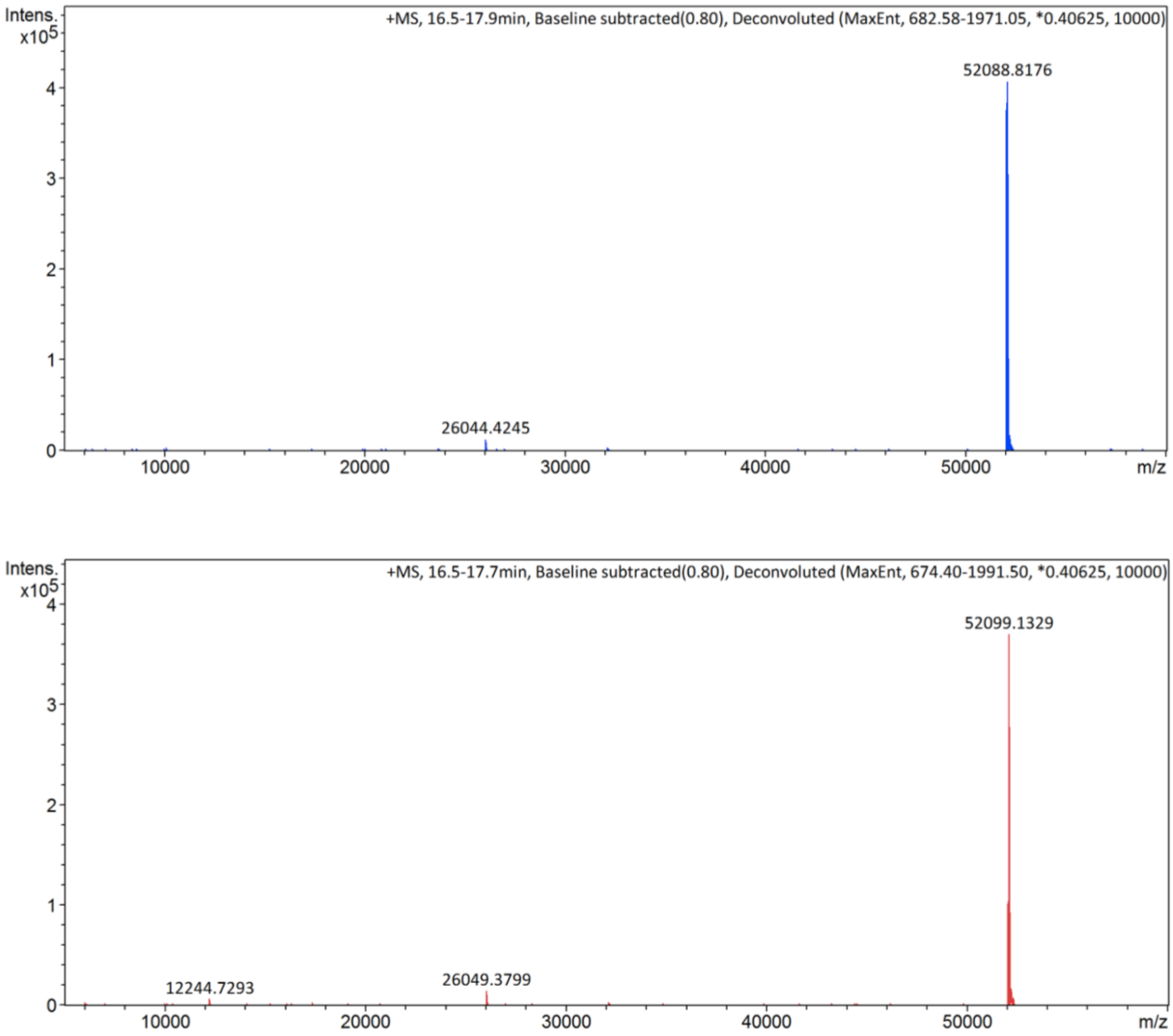

Figure 8: WT and H433F RnParkin were purified recombinantly in E. coli. Deconvoluted spectra (see Materials and Methods section for more details) shows the mass to charge ratio (m/z) on the x-axis and the detected intensities (x10^5) on the y-axis. The detected peak at 52088.8176 and 52099.1329 represent the expected molecular mass for WT (in blue) and H433F (in red) RnParkin, respectively.

Testing the Effects of Parkin Mutant on Mfn2 Ubiquitination

An *in organello* assay was performed to test the effects of Parkin His433 mutant on Mfn2, VDAC and Parkin autoubiquitination. *In organello* assay consists of using extracted mitochondria from CCCP-treated HeLa cells that contain accumulated HsPINK1 on the OMM, which will be extracted simultaneously. DMSO-treated mitochondria from HeLa cells are used as HsPINK1 lacking controls. The isolated mitochondria were used as reagents for *in vitro* ubiquitination assays with recombinant Parkin (see Materials and Methods for detail), and Parkin substrates ubiquitination was then assessed by immunoblotting. Given that the acyl transfer step of Parkin ubiquitination is heavily dependent on the presence of His433 acting as a base to deprotonate the catalytic Cys431, we set out to evaluate whether His433 mutation will cause an ineffective ubiquitination of OMM substrates including Mfn2, VDAC and Parkin itself (figure 9). As expected, His433 mutant heavily diminished ubiquitination level for poor substrates such as VDAC and Parkin itself. However, we have noticed that Mfn2 ubiquitination is not affected by the mutation.

Testing the Effects of Parkin Mutant on Mfn2 Ubiquitination When Transthiolation Is Not Rate Limiting

Mfn2 ubiquitination is unaffected by the His433 mutant suggested that it is indeed a preferred substrate of Parkin and that its ubiquitination rate is independent of the rate limiting acyl transfer step, where His433 is implicated. As such, the global rate of Mfn2 ubiquitination should solely depend on the transthiolation step (figure 3). To prove this model, we set out to test the level of Mfn2 ubiquitination when the transthiolation step is no longer rate limiting by precharging E2 enzymes with Ub (UbcH7~Ub) (figure 10).

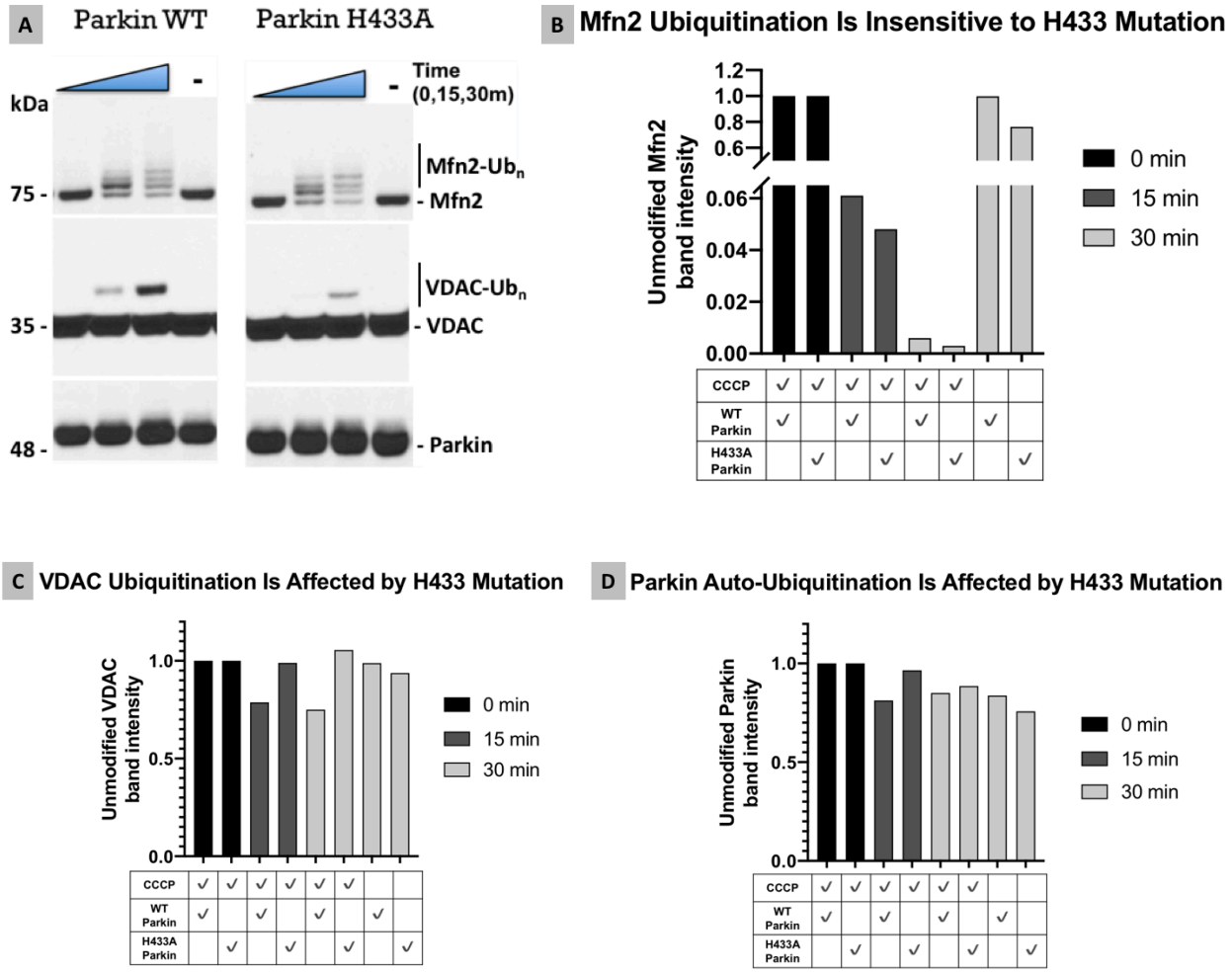

Figure 9: Mfn2 is insensitive to His433 mutation (performed by Dr. Jean-François Trempe). Mfn2's ubiquitination rate is unaffected by H433 mutation at all tested time points (15 and 30 min) in *in vitro* reconstitution assays (Panel A and B). VDAC ubiquitination and Parkin autoubiquitination are heavily affected by the His433 mutation (Panel C and D, respectively), and a drastic decrease was observed in comparison to Parkin WT. Ubiquitination of Mfn2 is represented by the appearance of the smear-like upper bands above the 75 kDa bands.

As expected, by precharging E2 enzymes with Ub, which renders the transthiolation step no longer rate limiting, *in organello* assay revealed a reduced level of Mfn2 ubiquitination in Parkin His433 mutant compared to Parkin WT at low concentration of UbcH7~Ub, and this difference in

ubiquitination vanishes at high UbcH7~Ub concentration such as 10 μM (figure 10). VDAC, on the other hand, was not ubiquitinated by Parkin at any given UbcH7-Ub concentration (figure 10). Taken together, the above observations suggest that 1) Mfn2 is a preferred substrate of Parkin given that it is insensitive to the His433 mutant, and 2) the rate limiting step of Mfn2 ubiquitination is not the acyl transfer step.

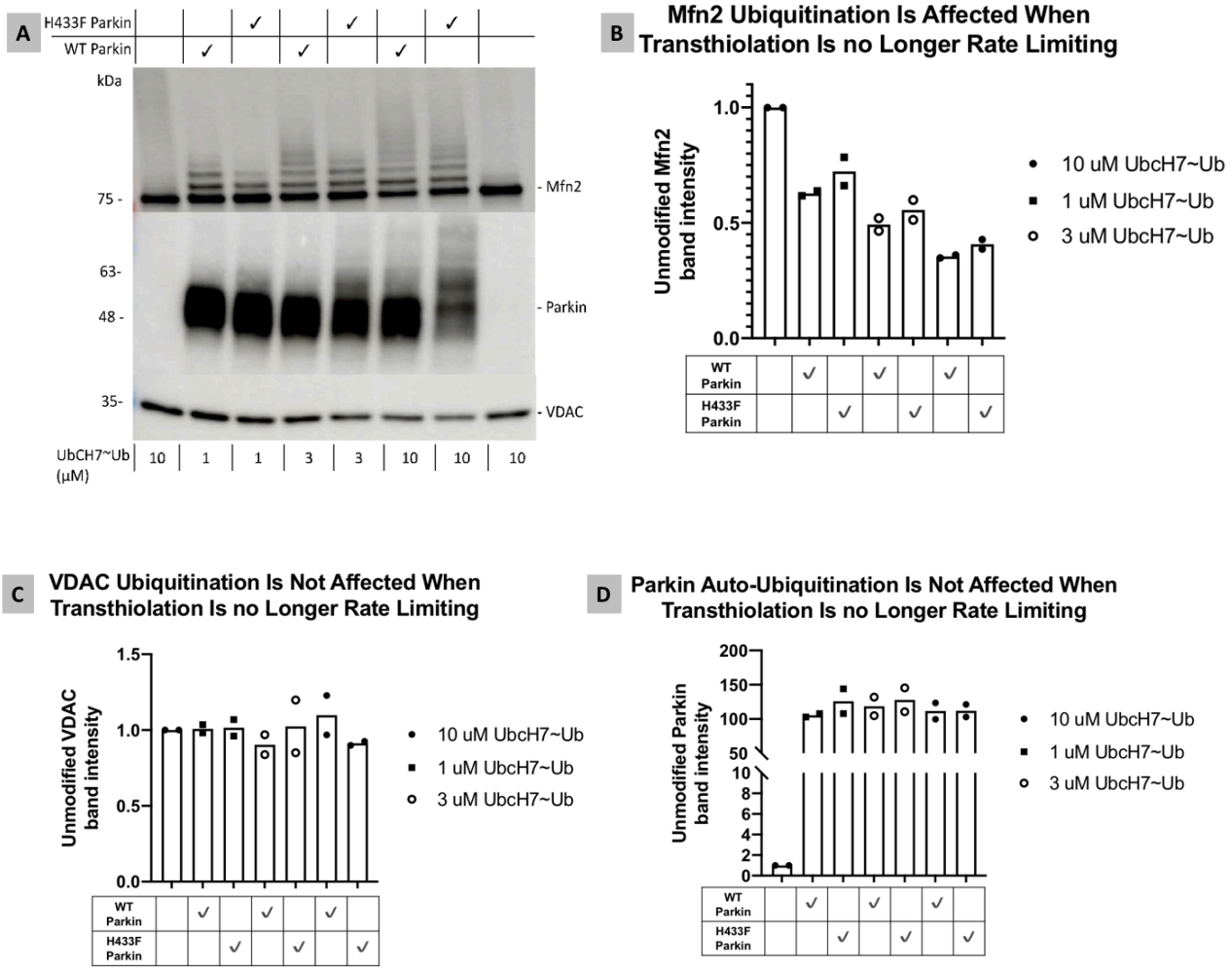

Figure 10: Mfn2 ubiquitination is affected by His433 mutant when transthiolation is no longer rate limiting. Immunoblots of Mfn2, Parkin and VDAC for various concentrations of UbcH7~Ub show that Mfn2 is readily ubiquitinated at all tested concentrations (1, 3 or 10 μM of UbcH7~Ub)

(Panel A). A difference in Mfn2 ubiquitination between Parkin WT and H433F is only observed after precharging UbcH7 with Ub, which makes transthiolation no longer rate limiting. The unmodified bands for Mfn2, VDAC and Parkin are quantified in panel B, C and D, respectively. Ubiquitination of Mfn2 is represented by the appearance of the smear-like upper bands above the 75 kDa bands.

Evaluating OMM Substrates Ubiquitination by Recombinant Parkin Using *In Organello* Assay

Given that Mfn2 is readily ubiquitinated *in vitro*, we next sought to evaluate whether other OMM proteins are also ubiquitinated by Parkin. To this end, an *in organello* assay using WT Parkin (concentrations ranging from 0 to 10 μM) was performed and nine OMM substrate proteins were blotted to assess their ubiquitination. The *In organello* assay revealed that Mfn2 is readily ubiquitinated for concentration of Parkin as low as 0.1 μM (figure 11). Likewise, Mfn1 is also ubiquitinated in a similar fashion, though its ubiquitination pattern is less prominent than Mfn2. The remaining substrates are not ubiquitinated and remain unmodified even at higher Parkin concentration (10 μM) (figure 11). This further consolidates previous observations that Mfn2 is a preferred substrate of Parkin.

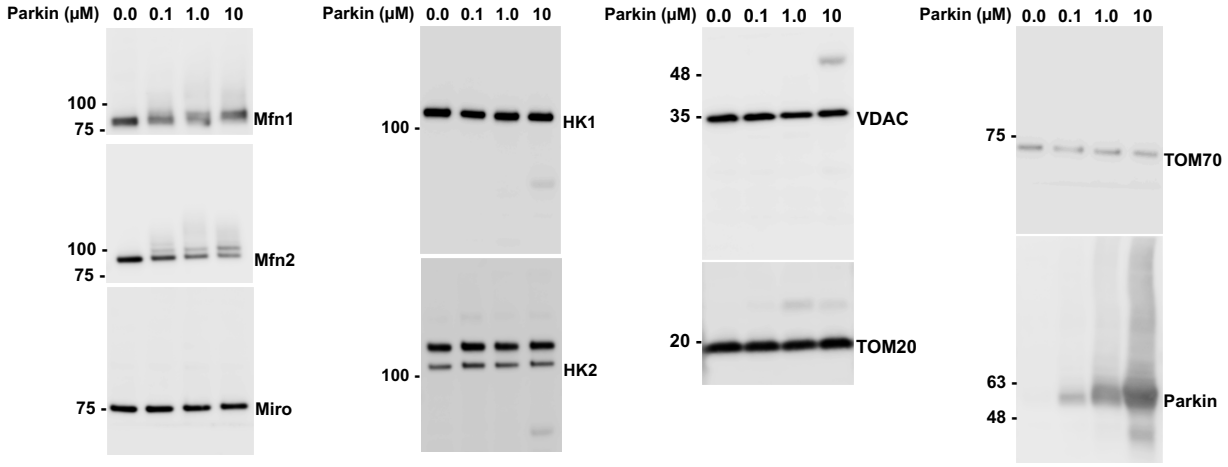

Figure 11: Parkin preferentially ubiquitinates Mfn2 over other OMM substrates. Ubiquitination of a given protein is represented by the appearance of the smear-like upper bands above the main non-modified molecular weight band. Mfn2's unmodified molecular weight is around 75kDa. Molecular weight in kDa are shown on the left.

Assessing the Cellular Localization of Mfn2 In Close Proximity to PINK1

Given that Mfn2 is a preferred substrate of Parkin, we next sought to validate whether its cellular localization plays a role in dictating its substrate specificity. Since Parkin is recruited to the damaged OMM and activated by pUb, which can only be generated by PINK1, we hypothesized that any substrate located into proximity of PINK1 will be preferentially ubiquitinated by Parkin. As such, we set out to validate whether Mfn2 is localized in proximity to PINK1, and if so, whether this interaction occurs at the interface between the ER and the mitochondria. In order to quantitatively assess whether Mfn2 is localized in close proximity to PINK1, proximity ligation assays (PLA) were performed in various U2OS cell lines. PLA is an antibody-based assay that detects close contact sites between proteins by producing fluorescent signals are the sites of

interaction, which can be visualized with confocal microscopy (see Materials and Methods for detail). U2OS cell lines have been transfected with CMV(d1) promoter-driven PINK1-HA to recapitulate endogenous levels of PINK1 in cells (Matsuda et al. 2012). However, we observed that the construct still had a higher PINK1 expression in comparison to the endogenous level (figure 12). However, it is noteworthy to mention that the transfected PINK1-HA is unlikely to be entirely expressed at the mitochondria and by default, some will not be active. Nevertheless, previous studies have shown that the active pool of transfected PINK1-HA show mitochondrial localization upon CCCP treatment (Okatsu et al. 2012). U2OS Mfn2 KO and PINK1 KO cell lines are used as negative controls to monitor nonspecific fluorescent signals. Confocal microscopy images revealed, on average per cell, 17 fluorescent PLA spots situated around the nucleus and within the contour of ER (Figure 13, Panel E), suggesting that Mfn2 is indeed localized in proximity to PINK1 in cells. This data was statistically significant when compared to the tested negative controls (figure 14). Indeed, an average of less than 5 PLA spots were observed in negative controls where either PINK1 or Mfn2 is absent (Figure 13, Panel A and B, respectively). A lack of PLA signal is also observed in cells that have not been treated with CCCP, therefore there is no mitochondrial depolarization to cause PINK1 buildup (Figure 13, Panel D). In the U2OS WT cell line that has been transfected with CMV(d1) promoter-driven PINK1-HA, an average of 13 PLA spots per cell were counted (Figure 13, Panel C).

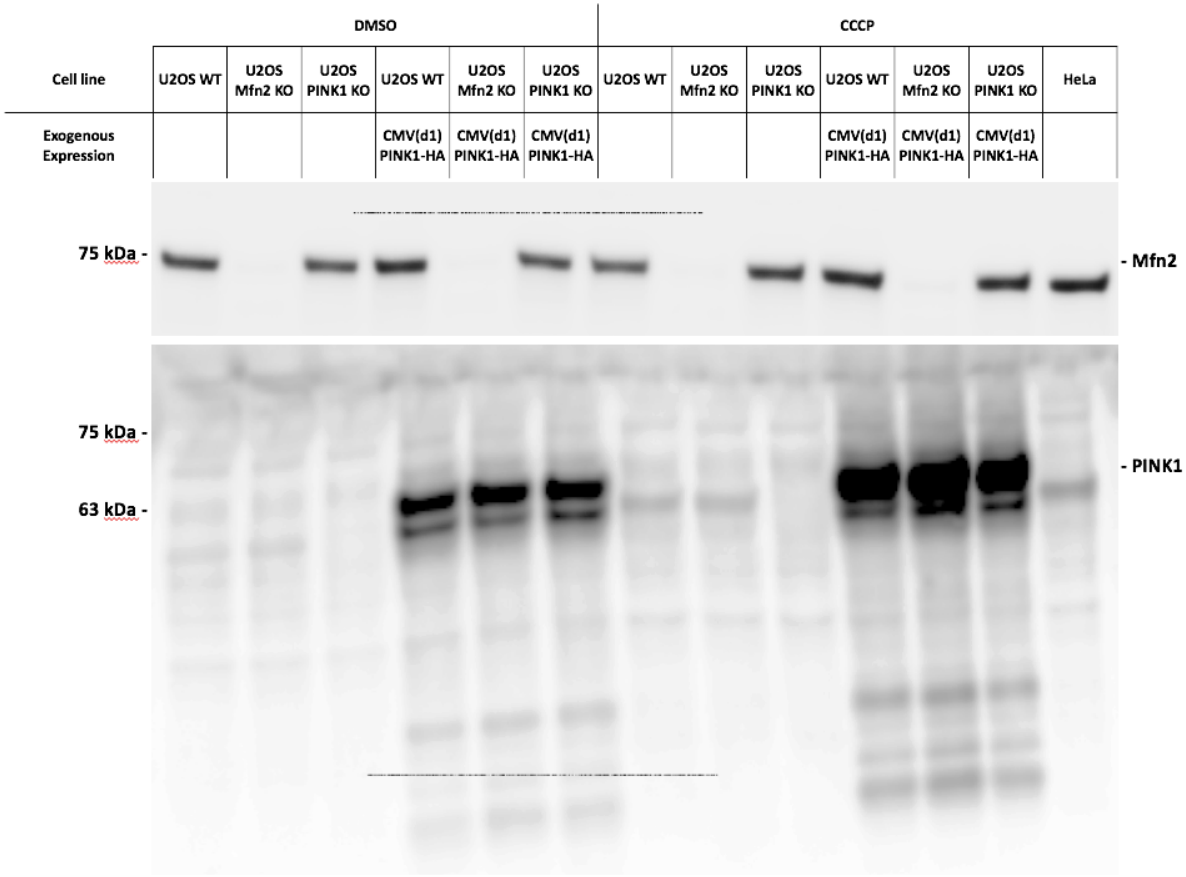

Figure 12: Validation of the efficiency of Mfn2 and PINK1 knockout in HeLa and various U2OS cell lines. The efficiency of protein knockout in each cell line was validated prior to performing all the subsequent PLA assays. The exogenous expression of PINK1 was achieved by transfecting a desired cell line with a CMV(d1) promoter-driven PINK1-HA. Molecular weight in kDa are shown on the left.

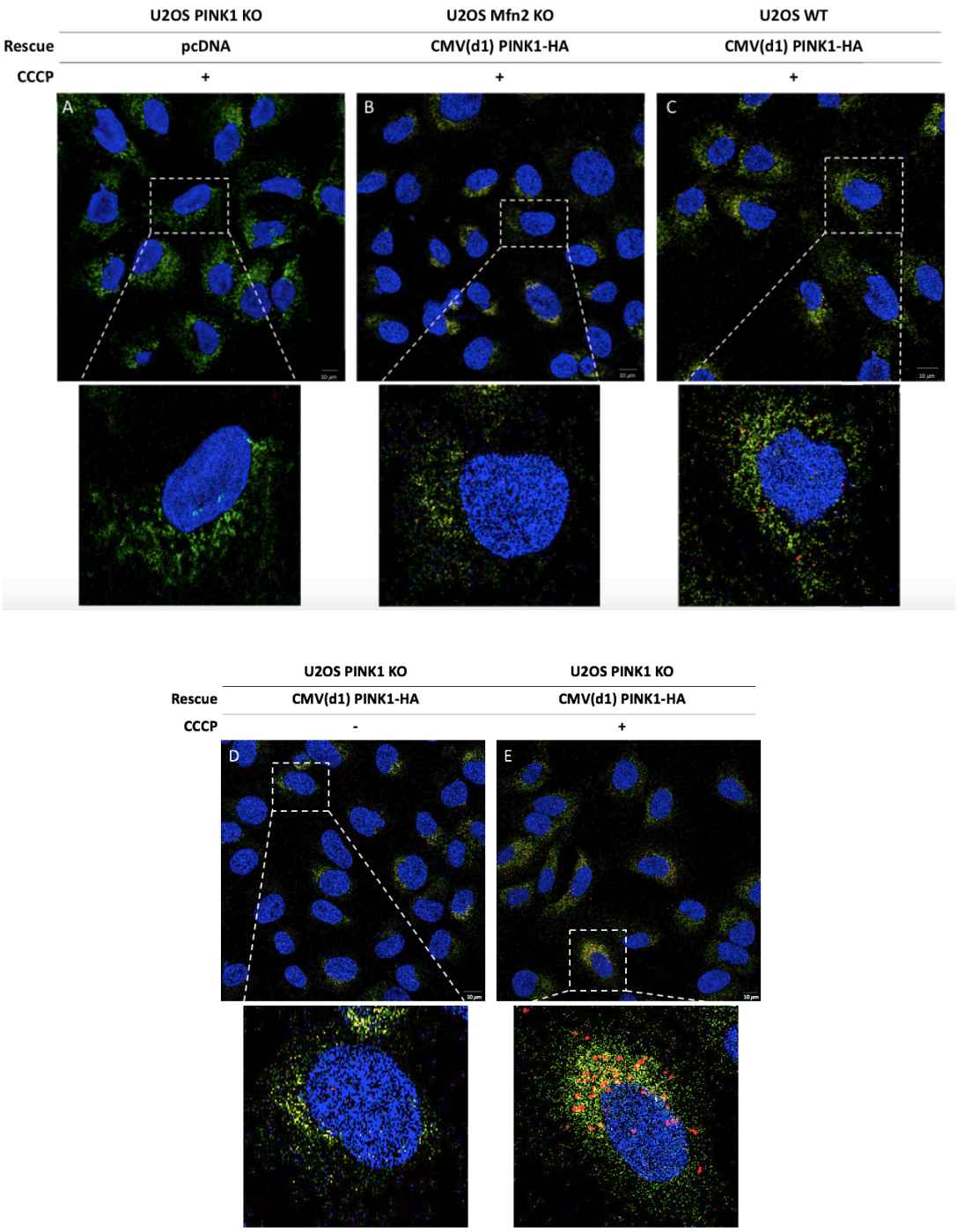

Figure 13: Mfn2 is located in proximity to PINK1. Proximity ligation assay (PLA) targeting Mfn2 and PINK1 was performed in various U2OS cell lines: WT, Mfn2 KO, PINK1 KO transfected with or without CMV(d1) promoter-driven PINK1-HA. PLA spots (red) are located around the nuclei (blue) and within the contour of the ER (green). Each PLA spot represents an interaction between Mfn2 and PINK1.

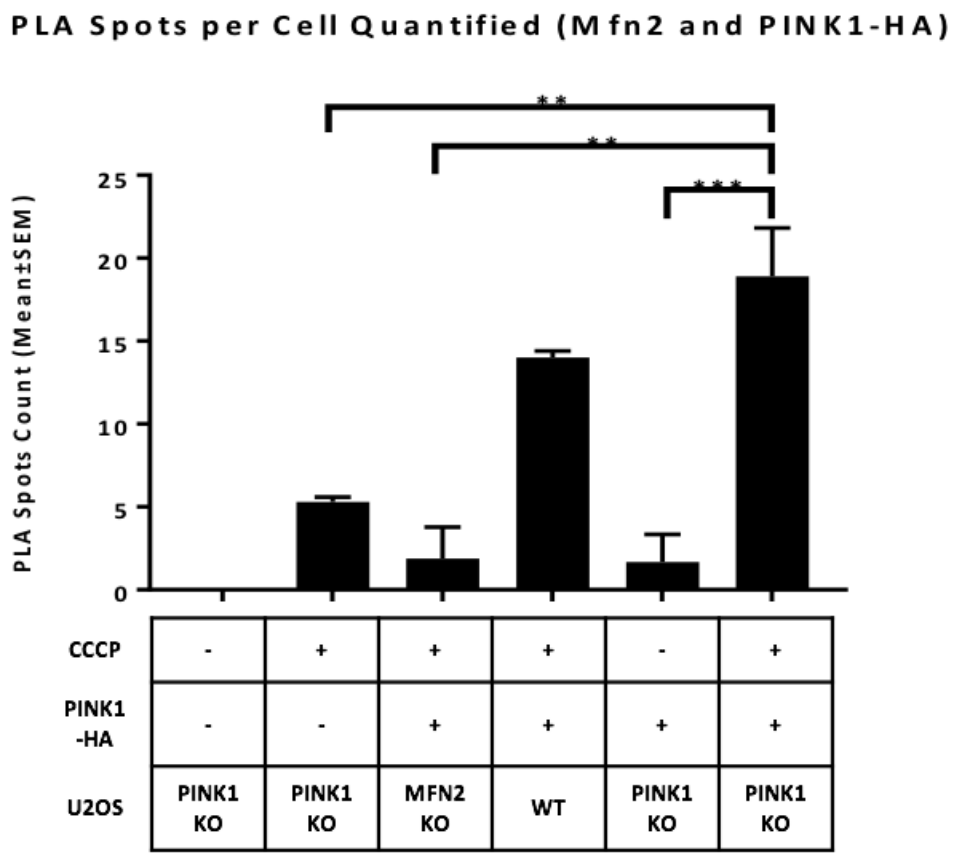

Figure 14: Quantification of the number of PLA spots per cell representing Mfn2 and PINK1 interaction in various U2OS cell lines. Quantification of PLA spots per cell shown in figure 13, in which the total number of detected PLA signals within each defined cell were computed using confocal microscope. Three biological replicates were performed for each condition. Statistical significances were determined using independent t-tests with Bonferroni corrections post-hoc test. ** $P < 0.01$. *** $P < 0.001$.

Assessing the Cellular Localization of Other OMM Substrates in Close Proximity to PINK1

Given that Mfn2 is located into proximity to PINK1, which explains its substrate specificity, we next sought to evaluate whether additional Parkin substrates are also located in the vicinity of

PINK1. PLA was employed to assess the interaction between PINK1 and the following three OMM proteins: Mitofusin-1 (Mfn1), voltage-dependent anion channel (VDAC), and Miro1. The following assay is entirely performed in U2OS PINK1 KO cells transfected with CMV(d1) promoter-driven PINK1-HA to recapitulate endogenous levels of PINK1. The total number of detected PLA signals were computed using confocal microscopy and our data indicate that none of the three tested OMM proteins is located or enriched in close proximity to PINK1. PLA targeting Mfn1 and PINK1 showed a nearly undetectable number of signals in both the negative control and the CCCP-treated experimental condition (figure 15). A similar observation was acquired with PLA targeting Miro and PINK1 (figure 16). We observed around 35 PLA signals when assessing VDAC and PINK1. However, a large number of signals were also present in the respective negative control, suggesting that although VDAC is abundantly present on the OMM, it is however not enriched in proximity to PINK1 (figure 17). None of the three tested conditions was statistically significant when compared to their respective untreated control (figure 18). We have demonstrated that Mfn2‘s cellular localization in close proximity to PINK1 is a unique property of Mfn2 and that other tested OMM substrates do not share this feature.

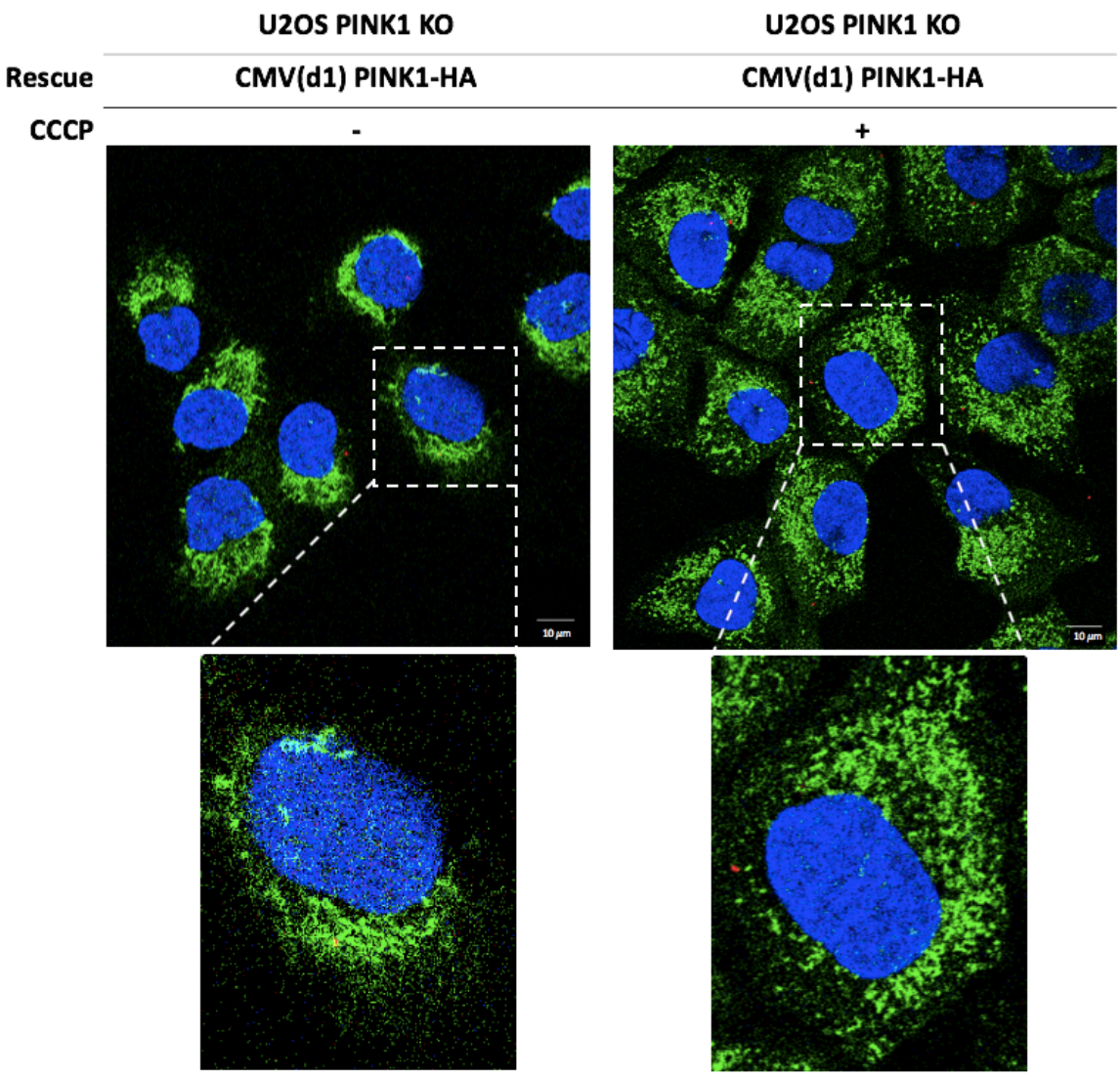

Figure 15: Mfn1 is not located in close proximity to PINK1. Proximity ligation assay (PLA) targeting Mfn1 and PINK1 was performed in U2OS PINK1 KO cells transfected with CMV(d1) promoter-driven PINK1. Untreated cells (-CCCP) are employed as negative controls. PLA spots (red) are located around the nuclei (blue) and within the contour of the ER (green). Each PLA spot represents an interaction between Mfn1 and PINK1, which are nearly undetectable.

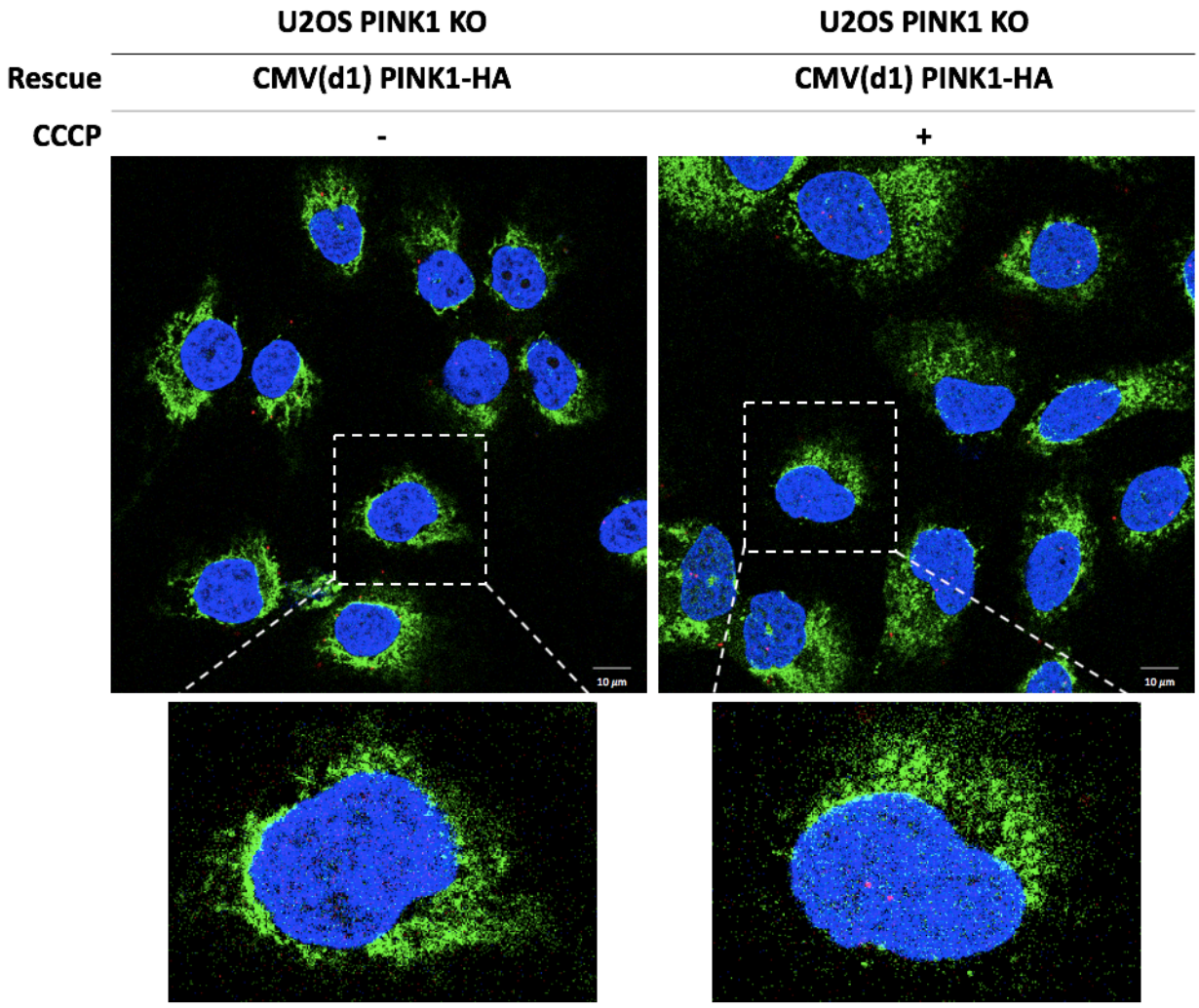

Figure 16: Miro is not located in close proximity to PINK1. Proximity ligation assay (PLA) targeting Miro and PINK1 was performed in U2OS PINK1 KO cells transfected with CMV(d1) promoter-driven PINK1. Untreated cells (-CCCP) are employed as negative controls. PLA spots (red) are located around the nuclei (blue) and within the contour of the ER (green). Each PLA spot represents an interaction between Miro and PINK1, which are indiscernible.

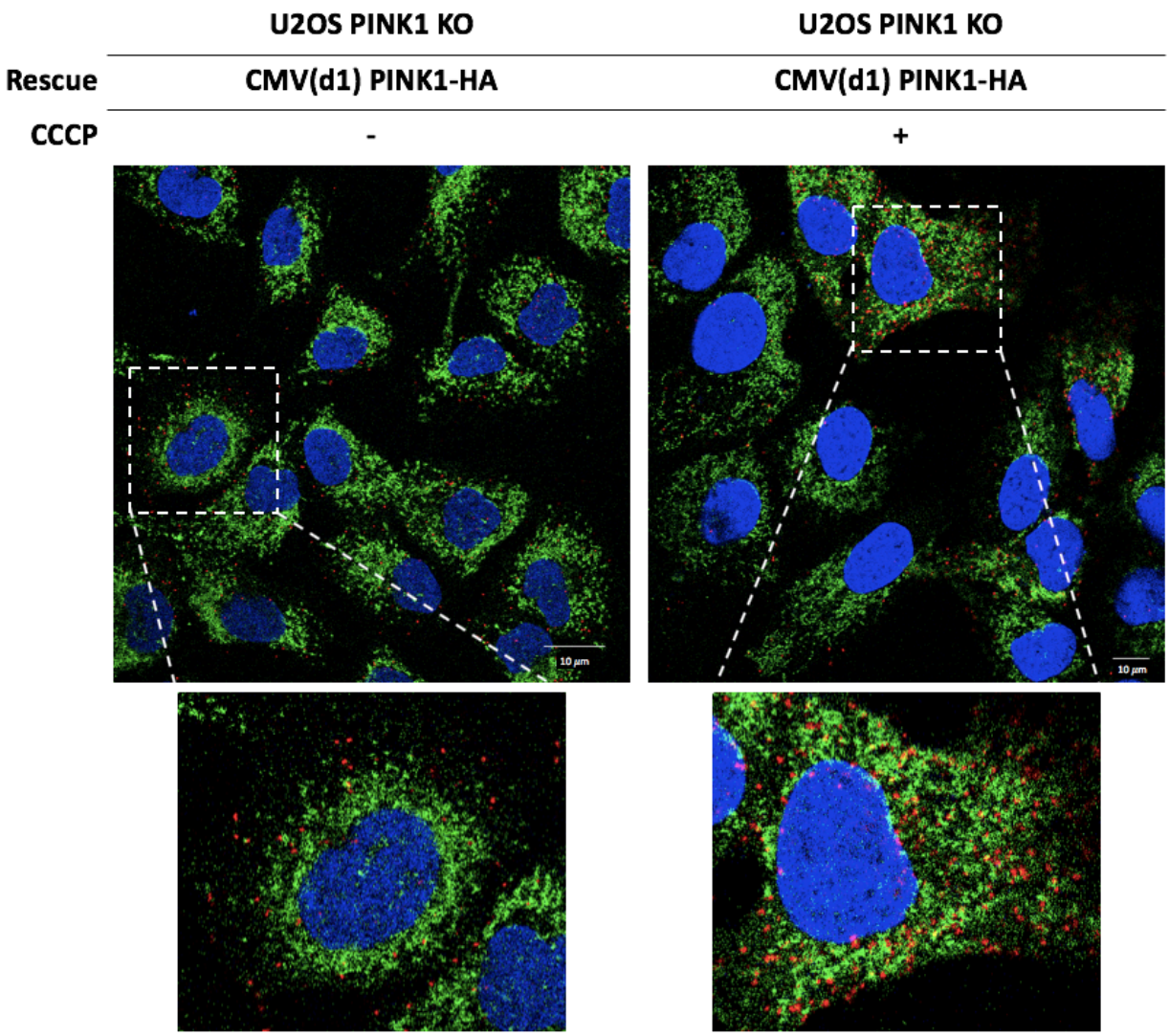

Figure 17: VDAC is abundantly located on the OMM, but is not enriched in proximity to PINK1. Proximity ligation assay (PLA) targeting VDAC and PINK1 was performed in U2OS PINK1 KO cells transfected with CMV(d1) promoter-driven PINK1. Untreated cells (-CCCP) are employed as negative controls. PLA spots (red) are located around the nuclei (blue) and within the contour of the ER (green). Each PLA spot represents an interaction between VDAC and PINK1, which are detected at high abundance in both CCCP-treated experimental condition and the DMSO-treated negative control.

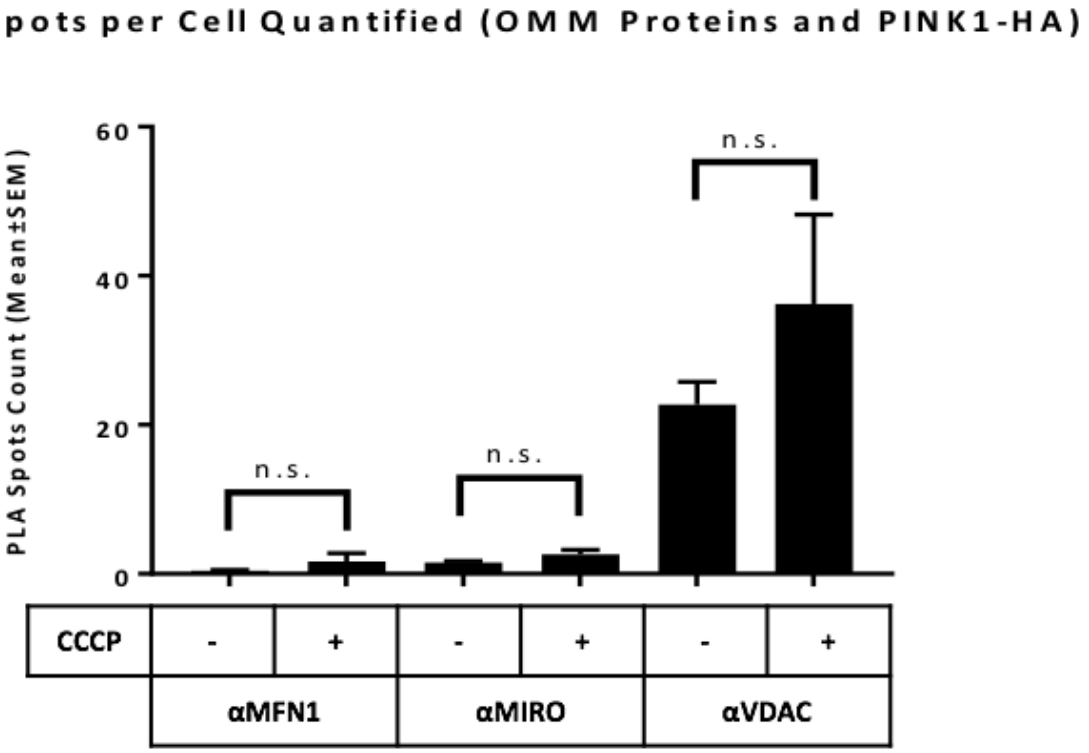

Figure 18: Quantification of the number of PLA spots per cell between PINK1 and other OMM substrate proteins in U2OS PINK1 KO cells. Quantification of PLA spots per cell shown in figure 15, 16 and 17, in which the total number of detected PLA signals within each defined cell were computed using confocal microscopy. Three biological replicates were performed for each condition. Statistical significances were assessed for each CCCP-treated condition to the respective DMSO-treated negative control and p values were calculated using independent t-tests with Bonferroni corrections post-hoc test. n.s. not significant.

Assessing the Cellular Localization of Mfn2 In Close Proximity to pUb

Finding Mfn2 in close proximity to PINK1 justifies the reason behind which it is preferentially ubiquitinated by Parkin. To further consolidate our observation, we sought to assess whether Mfn2 is found in close proximity to pUb, which is the direct output of PINK1. The antibody for PINK1 could not be used in this experiment because the two primary antibodies targeting PINK1

and Mfn2 are both raised in the same species (see Materials and Methods for detail). The following PLA assay is performed without employing an ectopic overexpression system (i.e. transfecting exogenous PINK1-HA) to critically evaluate the interaction between proteins of interest at endogenous levels of PINK1 in cells. The total number of detected PLA signals were computed using confocal microscopy and our data indicate that Mfn2 is also found in proximity to pUb in cells. PLA signals were only observed in the condition where both Mfn2 and pUb are present (figure 19, panel D), and this data was statistically significant (figure 20) when compared to the untreated control (figure 19, panel B), or in conditions where either Mfn2 or PINK1 is absent (figure 19, panel A and panel C, respectively).

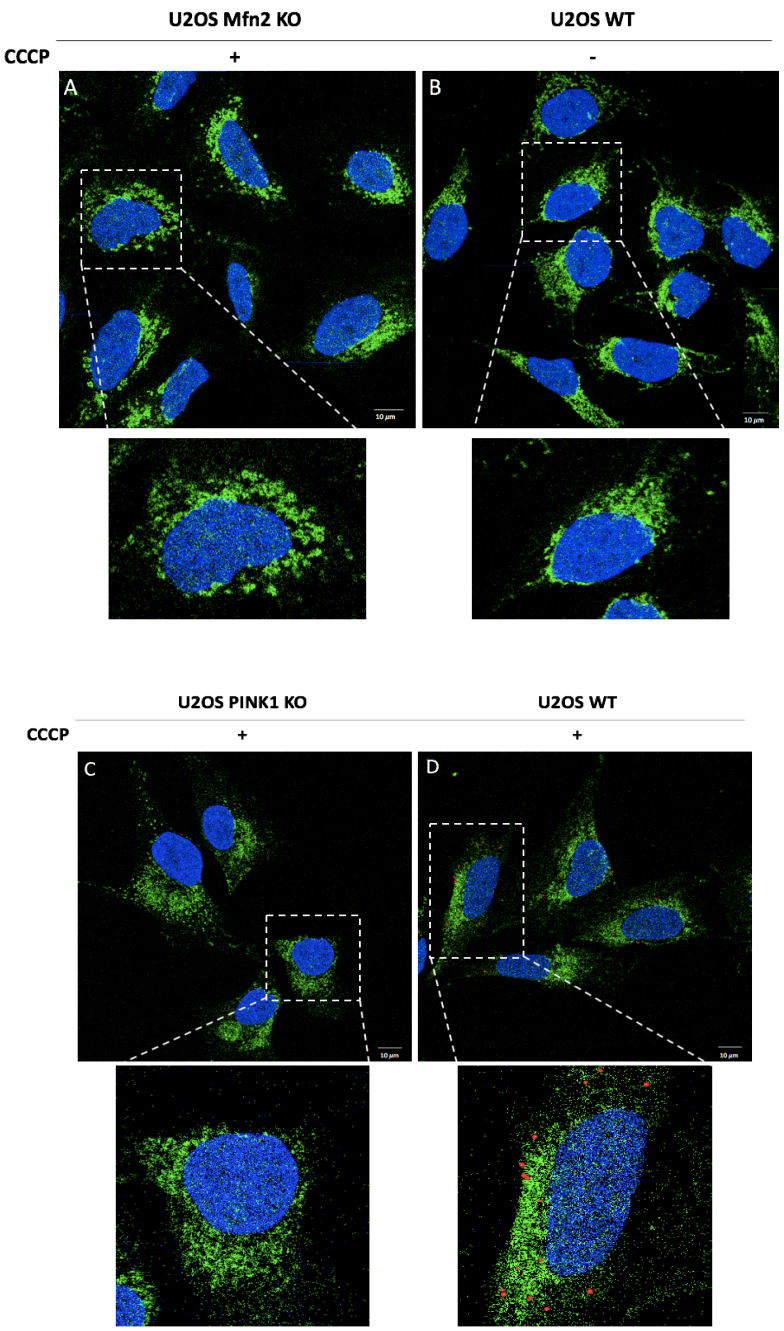

Figure 19: Mfn2 is located in proximity to pUb. Proximity ligation assay (PLA) targeting Mfn2 and pUb was performed in U2OS cell lines without exogenous expression of PINK1. PLA spots (red) are located around the nuclei (blue) and within the contour of the ER (green). Untreated cells (-CCCP) are employed as negative controls. Each PLA spot represents an interaction between Mfn2 and pUb. An average of 12 PLA spots are observed in the experimental condition where both Mfn2 and PINK1 are present (Panel D). In negative controls where either Mfn2 is absent (Panel A), PINK1 is absent (Panel C) or DMSO-treated cells (Panel B), PLA signals are nearly undetectable.

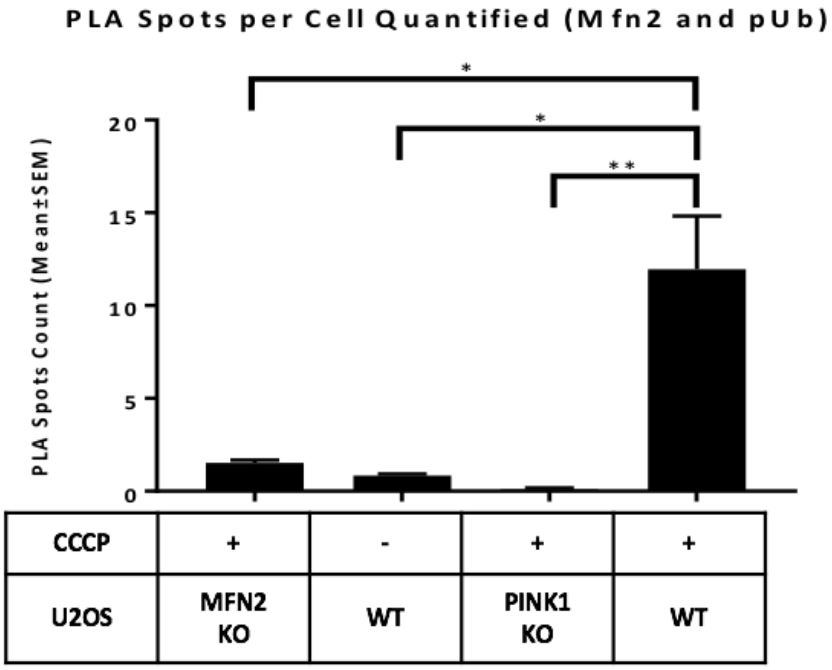

Figure 20: Quantification of the number of PLA spots per cell representing Mfn2 and pUb interaction in various U2OS cell lines. Quantification of PLA spots per cell shown in figure 19, in which the total number of detected PLA signals within each defined cell were computed using confocal microscope. Three biological replicates were performed for each condition. Statistical significances were determined using independent t-tests with Bonferroni corrections post-hoc test. * $P < 0.05$. ** $P < 0.01$.

Assessing the Existence of Mfn2-pUb Complexes in Parkin-Null HeLa Cells

Although previous studies have already established the existence of pUb-associated Mfn2 complexes in cells expressing Parkin (McLelland et al. 2018), it is however unclear which substrates harbor pre-existing pUb chains that serve as recruitment signals for Parkin. Therefore, a Tandem Ubiquitin Binding Entities (TUBE) pulldown assay was performed to validate whether Mfn2 is coupled to pUb in the absence of Parkin. TUBE resin will allow for the enrichment of

ubiquitinated species by selectively binding to ubiquitin moieties in Parkin-null HeLa cells' mitochondrial lysates via their ubiquitin binding associated domains (UBAs). Tandem liquid-chromatography mass spectrometry (LC-MS) analysis have identified massive enrichment for ubiquitinated species mainly including Ub-associated ribosomal proteins as one of the highest hits (figure 21). Interestingly, total pUb levels were detected in the CCCP-treated mitochondrial cell lysates, which were absent in the DMSO control condition (figure 22). However, we were unable to identify Mfn2, or any other proteins conjugated to pUb.

Protein Names	LFQ Intensity
Ubiquitin-60S ribosomal protein L40;Ubiquitin;60S ribosomal protein L40;Ubiquitin-40S ribosomal protein S27a;Ubiquitin;40S ribosomal protein S27a;Polyubiquitin-B;Ubiquitin;Polyubiquitin-C;Ubiquitin	468850000
60 kDa heat shock protein, mitochondrial	278590000
Small ubiquitin-related modifier 3;Small ubiquitin-related modifier 2	206570000
Stress-70 protein, mitochondrial	157430000
Transitional endoplasmic reticulum ATPase (VCP)	150660000
ATP synthase subunit beta, mitochondrial	126910000
ATP synthase subunit alpha, mitochondrial	114380000
Glyceraldehyde-3-phosphate dehydrogenase (GAPDH)	84353000
Ubiquilin-1;Ubiquilin-4;Ubiquilin-2	70351000
Voltage-dependent anion-selective channel protein 1	46813000

Figure 21: Identification of TUBE pulldown-enriched proteins. Tandem liquid-chromatography mass spectrometry (LC-MS) analysis have identify massive enrichment for ubiquitinated species following TUBE pulldown in CCCP-treated HeLa cells lysates. The first ten identified proteins are listed in order of their LFQ intensity, which represents the average of total detected peptides intensities for one given protein of interest.

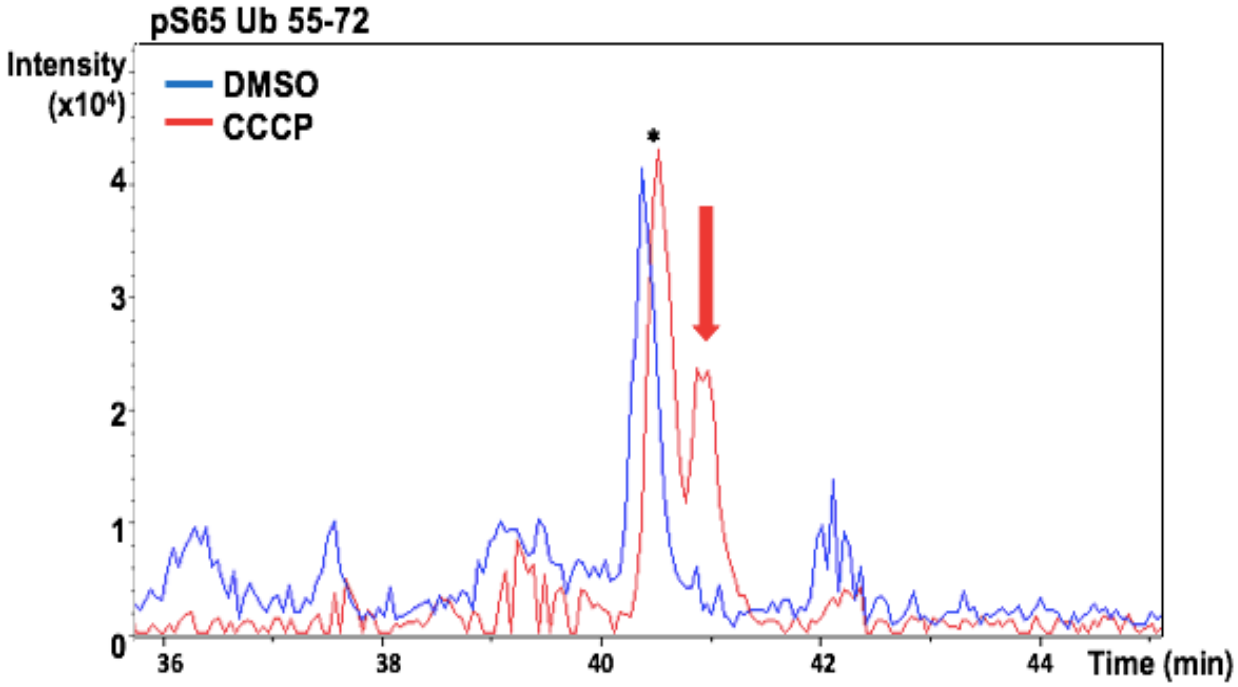

Figure 22: Identification of pUb in Parkin-null cell lysates. ESI-Q-TOF extracted ion chromatogram shows time of elution on the x-axis and intensity on the y-axis. After enriching for ubiquitinated species using Tandem Ubiquitin Binding Entities (TUBE) pulldown, identified pS65 Ub peptide is only present in the CCCP-treated HeLa cell lysates (red arrow), which is absent in the DMSO-treated control condition (blue line). *Unknown peptide.

Identifying E3 Ub Ligases Acting Upstream to Parkin/PINK1 Activation

Given that we have found total pUb in the absence of Parkin, we next to sought to identify which mitochondrial E3 ligase(s) is/are catalyzing the addition of pre-existing Ub chains on mitochondrial substrates such as Mfn2, prior to Parkin and PINK1 activation. Small interfering RNAs (siRNAs) were used to knock down three mitochondrial Ub ligases: March5, MUL1 and/or Huwe1 in Parkin-null HeLa cells and the effect of the knockdown on pUb levels is assessed by western blotting. Successful knockdown of Huwe1 and March5 were observed (figure 23 and

figure 24, respectively). Because we were not able to successfully detect MUL1 with a commercial antibody, we are currently testing another antibody in order to determine if MUL1 is knocked down (data not shown). When we assessed the level of total pUb upon mitochondrial depolarization following the knockdown of March5, MUL1 and/or Huwe1, we have observed a decreased level of pUb only when March5 and/or Huwe1 is/are knocked down (figure 25).

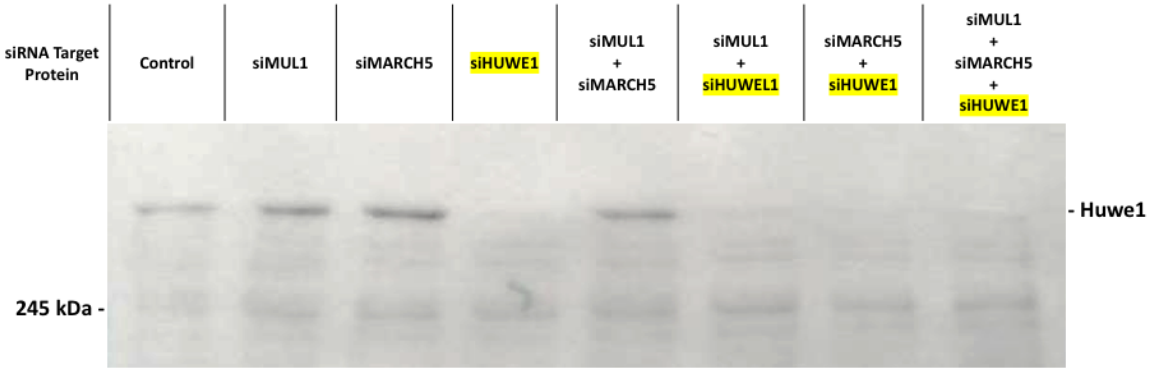

Figure 23: Huwe1 was successfully knocked down using siRNA in HeLa cells. Western blotting demonstrated that transfecting siRNA for Huwe1 alone, or in combination with March5 and/or MUL1 in HeLa cells successfully abolished its protein expression. Molecular weight in kDa are shown on the left.

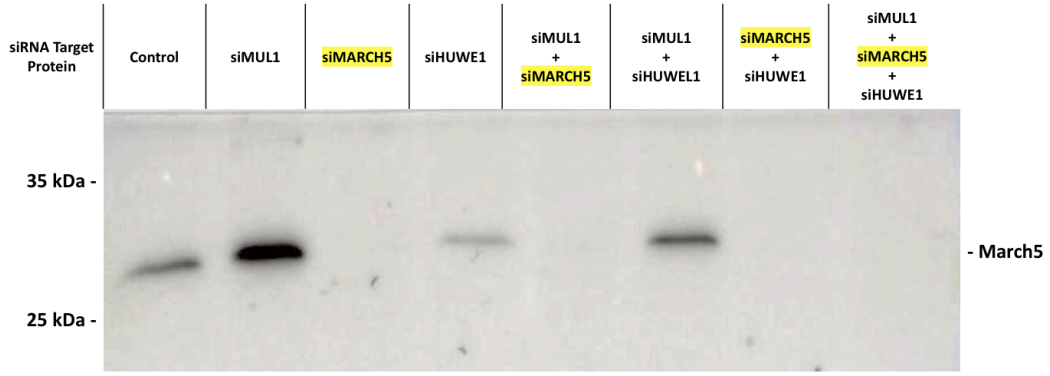

Figure 24: March5 was successfully knocked down using siRNA in HeLa cells. Western blotting demonstrated that transfecting siRNA for March5 alone, or in combination with Huwe1 and/or MUL1 in HeLa cells successfully abolished its protein expression. Molecular weight in kDa are shown on the left.

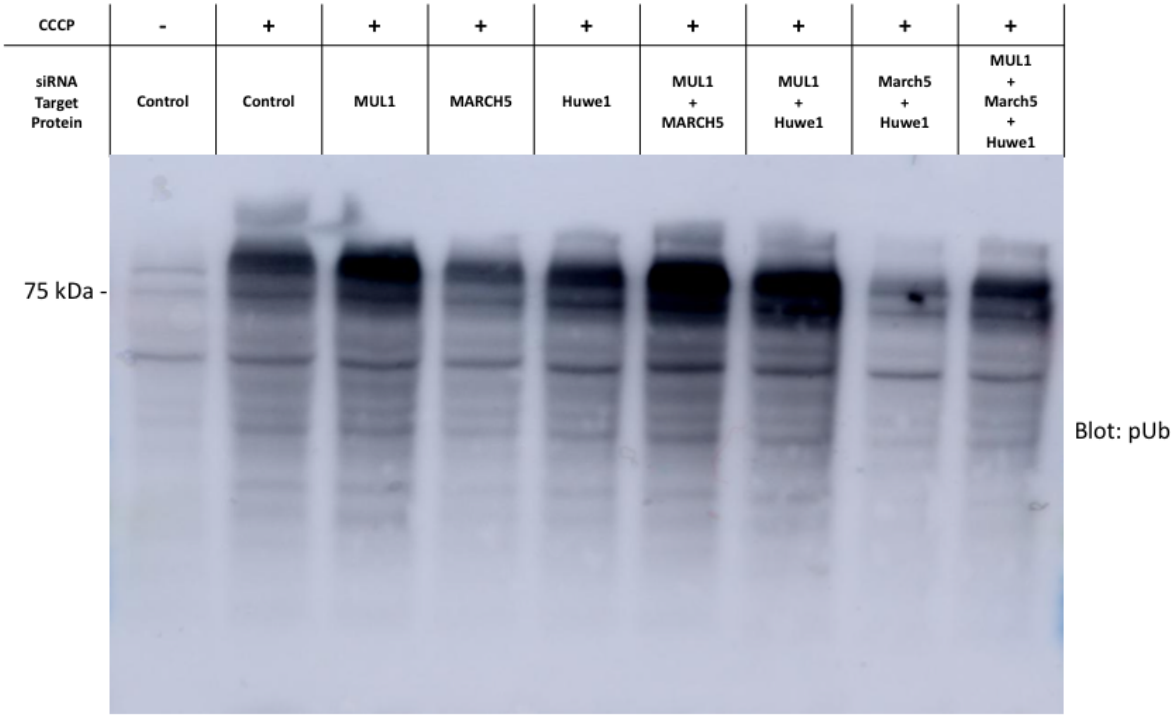

Figure 25: pUb level is reduced when March5 and/or Huwe1 is/are knocked down in HeLa cells. Production of pUb (in the form of large chains (>75 kDa)) in HeLa cells following CCCP treatment is diminished upon March5 and/or Huwe1 knockdown. This reduction in pUb level is especially prominent when both March5 and Huwe1 are knocked down. Molecular weight in kDa are shown on the left.

DISCUSSION

Mitofusin-2 Is A Preferred Substrate of Parkin

Previous work by our group and many others has established that, upon recruitment to depolarized mitochondria, Parkin will catalyse the addition of ubiquitin chains onto mitochondrial substrates. Although many E3s do have stringent substrate specificity, Parkin is rather atypical. In fact, Parkin does not ubiquitinate its substrates by identifying a recognition sequence and there is lacking evidence showing Parkin interacting with its substrates. Nonetheless, over a hundred of Parkin substrates have been identified throughout the years, of which the most studied are VDAC, TOM20, Miro1, HK1 and Mfn2 (Rose, 2016). However, many questions remain to be elucidated: 1) Does Parkin ubiquitinate all the substrates at the same rate? And if not, 2) what is the kinetic model behind its substrate ubiquitination once it is recruited to the mitochondria? Our data from the recombinant ubiquitination assays confirmed that Parkin indeed preferentially ubiquitinates Mfn2 *in vitro*. In fact, given that the acyl transfer step of Parkin-mediated ubiquitination is heavily dependent on the presence of His433 acting as a base to deprotonate the catalytic Cys431, its mutation will lead to an ineffective ubiquitination of substrates such as VDAC or even itself. However, we have noticed that Mfn2 ubiquitination is not affected by the His433 mutation (figure 9). In fact, *in organello* assays performed on extracted depolarized mitochondria showed that Mfn2 ubiquitination was unaffected when Parkin's His433 is mutated, whereas ubiquitination of other substrates such as VDAC was highly reduced (figure 9). This observation proposed that 1) Mfn2 must be a preferred substrate of Parkin, and 2) the rate limiting step of Mfn2 ubiquitination is not the acyl transfer step.

Thus, the kinetic model of Parkin's substrates ubiquitination should be the following: for any substrate such as VDAC or Miro1, the rate limiting acyl transfer step will dictate the global rate of ubiquitination. For instance, any mutation impeding this step, including the mutation His433, will slow down the global rate of substrate ubiquitination by Parkin (figure 26, in orange). On the other hand, for a kinetically-preferred substrate such as Mfn2, the global rate of its ubiquitination will solely depend on the transthiolation step, shown by the unchanged ubiquitination rate with the His433 mutant (figure 26, in blue). To prove this model, we tested whether the global rate of Mfn2 ubiquitination would be affected when the transthiolation step is no longer rate limiting. Not to our surprise, by precharging E2 enzymes with Ub (i.e. UbcH7~Ub), *in organello* assays revealed a reduced Mfn2 ubiquitination levels in Parkin His433 mutant compared to Parkin WT (figure 10 and figure 26, in green). The above observations suggest that Mfn2 must be readily positioned in order to receive Ub from nearby Parkin, therefore explaining why its ubiquitination rate is independent of the acyl transfer step.

	Parkin	Transthiolation rate (E2-Ub → Parkin)	Acyl transfer rate (Parkin-Ub → Lysine)	Global rate
Kinetically-disfavored substrate (VDAC, Miro1)	WT	10	1	1
	H433F	10	0.1	0.1
Kinetically-preferred substrate (Mfn2)	WT	10	100	10
	H433F	10	10	10
Kinetically-preferred substrate + E2-Ub	WT	100	100	100
	H433F	100	10	10

Figure 26: A kinetic model of substrate ubiquitination by Parkin. The global rate of the two-step thioester intermediate model of Parkin ubiquitination dictates that the global rate of the reaction is the lowest (i.e. the rate limiting) of the two steps.

To further demonstrate that Mfn2 is indeed rapidly ubiquitinated by Parkin compared to a variety of OMM substrates, an *in organello* assay was performed using extracted depolarized mitochondria to which different concentrations of recombinant Parkin were added to allow *in vitro* ubiquitination of 9 OMM substrates (figure 11). As expected, Mfn2 was ubiquitinated even at low concentration of Parkin (0.1 μM), shown by the disappearance of the unmodified lower band and the appearance of the smear-like upper bands above 75 kDa, suggesting that protein ubiquitination has occurred. On the other hand, other OMM proteins, such as HK1, VDAC and Miro1, were not ubiquitinated, and remain unmodified even at higher Parkin concentrations such as 10 μM. Although Mfn1 is also very rapidly ubiquitinated, though less drastically than Mfn2, it is not considered as a preferred substrate of Parkin. Mfn1, despite its mitochondrial fusion activity, does not promote interorganellar tethering between the ER and the mitochondria (de Brito and Scorrano, 2008). Furthermore, silencing Mfn1 in U2OS:GFP-Parkin cells did not enhance

the recruitment of Parkin to the damaged mitochondria following CCCP treatment, nor did it promote Parkin-dependent mitophagy beyond single Mfn2 knockdown (McLelland et al. 2018). Taken altogether, these results suggest that 1) Mfn2 is indeed a preferred substrate of Parkin and 2) although previous studies have suggested that Mfn2 acts as the direct receptor for Parkin, this is rather unlikely because Mfn2 is rapidly extracted from the OMM by the AAA-ATPase p97 in a step that occurs concurrently with Parkin translocation to the damaged mitochondria (McLelland et al. 2018). Furthermore, incubation of mitochondria with a non-ionic detergent completely disrupts Mfn2 ubiquitination, suggesting that an intact membrane is critical to maintain the substrate specificity (appendix figure 1). We rather propose that Parkin's substrate specificity towards Mfn2 is most likely explained by its position in regard to receiving Ub from Parkin once the latter is recruited and activated on damaged mitochondria.

Mitofusin-2 Is Localized in Proximity to PINK1

Given that Mfn2 must be well positioned to receive Ub from Parkin at the onset of mitochondrial damage, this further implies that it must be decorated with pUb in order to attract Parkin upon its recruitment. Given that PINK1 is the only existing Ub kinase that generates pUb, we therefore evaluated whether Mfn2 is localized in proximity to PINK1, therefore justifying Parkin's substrate selectivity towards Mfn2. Our data from PLA showed that indeed, as we predicted in our hypothesis, Mfn2 is located in close proximity to PINK1 in cells. Distinct fluorescent spots were observed when PLA targeting Mfn2 and PINK1 was performed in U2OS PINK1 KO cells that have been transfected with CMV(d1) promoter-driven PINK1-HA to recapitulate endogenous levels of PINK1 in cells. Confocal microscopy images revealed, on average per cell, 17 fluorescent PLA spots situated around the nucleus and within the contour of ER (figure 13), suggesting that Mfn2 is found in proximity to PINK1. An average of less than 5 PLA spots were observed in negative controls where either Mfn2 or PINK1 is absent, using U2OS Mfn2 KO cells or U2OS PINK1 KO cells, respectively. A lack of PLA signal is also observed in cells that have not been treated with CCCP to cause mitochondria depolarization, whereby PINK1 accumulation and subsequent downstream Parkin recruitment have been halted. An interesting observation arises in the condition where PLA targeting Mfn2 and PINK1 in U2OS WT cells resulted in an average of 13 PLA spots per cell. This damped down, yet still present signal is most likely caused by the competition between endogenous PINK1 in U2OS WT cells and the transfected PINK1-HA.

In order to ensure that the presence of PLA signals is unique and specific to Mfn2 and PINK1, follow-up PLA experiments were performed to evaluate whether other OMM proteins that have

been reported as Parkin substrates are also located into proximity to PINK1. To this end, Mitofusin-1 (Mfn1), voltage-dependent anion channel (VDAC), and Miro1 were chosen for very specific reasons: Mammals Mfn1 shares high sequence homology to Mfn2, and it also plays an important role in mitochondrial fusion activities. Unlike Mfn2, which plays a critical role in the initiation of mitophagy at the onset of cellular damage, McLelland et al. have recently shown that silencing Mfn1 will not enhance the kinetics of Parkin recruitment to damaged mitochondria (McLelland, 2018). Nonetheless, *in vitro* ubiquitination assays suggested that Mfn1, to some extent, also get rapidly ubiquitinated by recombinant Parkin (figure 11). It is therefore essential to validate whether Mfn1 is also located in proximity to PINK1. VDAC is a mitochondrial ion channel located on the OMM that allows for the exchange of anions and small molecules between the cytosol and the intermembrane space (IMS). VDAC was first reported to be a substrate of Parkin-mediated lysine (Lys)-27 polyubiquitination in 2010 (Geisler, 2010). A recent publication by Ordureau et al. used quantitative proteomics to measure the kinetics of OMM Parkin's substrates ubiquitination, where they identify all three isoforms of VDAC to be the kinetically-preferred substrates of Parkin, followed by other substrates such as Mfn2, Miro1, HK1 and TOM20. It is however noteworthy to state that: 1) VDAC is much more abundant than Mfn2 in cells, and in fact, the isoform VDAC1 alone is at least 100 times more abundant than Mfn2; 2) Mfn2 ubiquitination reaches its maximum 30 minutes following mitochondrial damage and plateaus thereafter (figure 5). This suggests that the entire pool of Mfn2 is ubiquitinated rapidly, which is in contrast to other OMM substrates, including VDAC. Nonetheless, it is still valuable to assess whether VDAC is also located in proximity to PINK1. Lastly, Miro1 is a GTPase that regulates mitochondrial transport by binding to Milton, a kinesin-binding protein. Miro1

mediates mitochondrial fusion and mitophagy along with Mfn2 and its degradation will lead to the production of fragmented and stationary mitochondria (Liu, 2009). Miro1 is also a substrate of Parkin, but unlike VDAC, its protein abundance is comparable to Mfn2 in cells, making it an interesting candidate to evaluate its cellular localization with respect to PINK1. Our PLA data showed that, as we predicted, neither Mfn1, VDAC nor Miro1 is enriched in close proximity to PINK1 given that their quantified PLA data were not statistically significant in comparison to their respective negative controls. In fact, PLA targeting Mfn1 and PINK1-HA showed barely any detectable PLA signals, and a similar result was observed for PLA targeting Miro1 and PINK1-HA. Although an average of nearly 35 PLA spots were observed between VDAC and PINK1-HA, these are most likely to be non-specific signals since more than 20 PLA spots were observed in the untreated negative control. In fact, giving that the highly abundant VDAC isoforms are inevitably also located nearby ER-mitochondria contact sites, they are most likely to be found near PINK1 when the latter is stalled on the OMM, thereby giving rise to this artifact.

In order to further consolidate our hypothesis that Mfn2 is located in proximity to PINK1, we evaluated whether Mfn2 is also found in the vicinity of pUb. In fact, given that PINK1 is the only so far known Ub kinase, pUb can therefore be considered as a molecular marker for PINK1 activity. Not to our surprise, PLA targeting Mfn2 and pUb also exhibit strong signals. We have computed an average of 12 PLA spots per cell that are located around the nucleus and within the contour of ER. This result was statistically significant when compared to the negative controls, in which cells were either untreated or lacking one of the targeted proteins (Mfn2 or pUb) (figure 19). It is worth mentioning that although previous PLA assays were performed in overexpression

systems in which exogenous PINK1-HA were transfected, the present PLA experiment was carried out in cell lines without transfection nor overexpression. Having proven that Mfn2 is also found in the vicinity of pUb further consolidates our hypothesis that Mfn2 must be localized into close proximity of PINK1, therefore rendering it a preferred substrate of Parkin. Ongoing experiments aim to colocalize the ER and the mitochondria to further demonstrate that not only Mfn2 is located into close proximity to PINK1, but this interaction occurs very specifically at the interface between the ER and the mitochondria.

In the current literature, Mfn2 has been shown to dimerize and to act as a tether at the interface of the ER and the mitochondria in cells, and silencing Mfn2 is enough to disrupt the ER morphology and to loosen the ER-mitochondria contact sites (de Brito OM, 2008). In 2018, McLelland et al. have shown that Mfn2 extraction from the ER-mitochondria juxtapositions by the p97 AAA+ ATPase and its downstream degradation by the proteasome is a key step in initiating bulk mitophagy (McLelland, 2018). In light of these observations, the cascade of events following mitochondrial damage should be the following: upon cellular damage, PINK1 is recruited to the mitochondria, more specifically at the interface between the ER and the mitochondria, where Mfn2 is located. Subsequent PINK1-catalyzed phosphorylation of nearby Ub moieties on Mfn2 will act as a signal for Parkin recruitment and activation. Once catalytically active, Parkin will ubiquitinate any lysine residues in its proximity, which confers to the pUb-tagged Mfn2 located at the ER-mitochondria appositions.

Mitofusin-2 Is Coupled to pUb In the Absence of Parkin

Finding Mfn2 in close proximity to pUb in our PLA assays demonstrated that the cellular localization of Mfn2 is indeed a critical factor in dictating its substrate specificity. Nonetheless, it was worthy to further investigate whether Mfn2 is actually decorated with those pUb chains prior to Parkin activation, thereby acting as a recruitment signal. Although previous reports in the literature have found pUb-conjugated Mfn2 in pulldown assays, most of those assays were performed in a cell system overexpressing Parkin (McLelland et al. 2018). We employed a TUBE pulldown assay in Parkin-null HeLa cells to show that Mfn2 is coupled to pUb even in the absence of Parkin. Following enrichment with TUBE resin and tandem liquid-chromatography mass spectrometry (LC-MS) analysis, we have successfully identified massive enrichment for ubiquitinated species mainly including Ub-associated ribosomal proteins, polyubiquitin-B and ubiquitin as the highest hits. Other mitochondrial proteins that we identified include the 60 kDa heat shock protein (HSP60), subunits alpha and beta of ATP synthase, VDAC1 etc. (Figure 21). Mfn2 was not detected as one of the ubiquitinated species in our assay mainly because 1) it has very low protein abundance in cells and 2) we are not employing a Parkin-overexpressed cell system. Nonetheless, we aim to attempt a different approach to validate our hypothesis. In fact, we can profit from the nanomolar affinity of the Parkin's R0RBR domain (appendix, figure 2) for pUb to employ a GST-R0RBR to pulldown the phospho-ubiquitinated species from HeLa cell lysates (Sauvé et al. 2015; McLelland et al. 2018). We have already successfully purified GST-R0RBR WT and A320R (appendix figure 3), which will be used to pulldown Mfn2 as a phospho-ubiquitinated species from CCCP-treated HeLa cells' mitochondrial lysates. The mutant A320R

will be used as a negative control given that it fails to bind pUb due to a disruption of hydrophobic interaction caused by the mutation from alanine to arginine.

It has been well established that the process of Parkin recruitment to the damaged mitochondria is dependent on the production of pUb. Indeed, as previously discussed, parkin is recruited to the depolarized mitochondria by pUb chains, which reciprocally, is dependent on Parkin activity for their production. This interconnectedness suggests that, at the onset of mitochondrial damage, there must be at least another E3 Ub ligase that is catalyzing the addition of Ub chains onto OMM substrates such as Mfn2 and this initial "seed" Ub will in turn be phosphorylated by PINK1, initiating the recruitment and activation of Parkin on the OMM. Parkin recruitment contributes to the positive feedback loop in which it will further ubiquitinate Mfn2, and other OMM substrates that will subsequently be phosphorylated by PINK1 and the positive feedback mechanism carries on. Interestingly enough, we have detected in our TUBE pulldown assay total pUb in the CCCP-treated HeLa cell lysates, which was absent in the DMSO control condition (Figure 22). Given that our experiment was performed in a Parkin-null cell line, detecting the presence of pUb further consolidates the existence of another E3 Ub ligase(s) that is/are acting upstream to PINK1 and Parkin activation. To date, there are three other mitochondrial Ub ligases that have been reported to ubiquitinate Mfn2: Huwe1, March5 and MUL1. These E3 ligases have been characterised to carry important functions in controlling mitochondrial dynamics via their interaction with Mfn2, as previously discussed. Hence, we validated whether Huwe1, March5 and/or MUL1 is/are implicated in catalyzing the addition of pre-existing Ub chains on OMM substrates, thereby priming Parkin recruitment and activation. Our siRNA knockdown assays

targeting the three above-mentioned Ub ligases in Parkin-null HeLa cells revealed a decrease level of pUb that is only observed when March5 and/or Huwe1 is/are knocked down in HeLa cells. This reduction in pUb level is especially prominent when both March5 and Huwe1 are absent (Figure 25). These promising data potentially suggest that March5 and/or Huwe1 is/are acting as the "priming" E3 ligase(s) that catalyze(s) the addition of the initial "seed" Ub on OMM substrates such as Mfn2. The reduced pUb levels in HeLa cells upon knockdown of March5 was also observed by a group at Genentech recently (Phu et al. 2020).

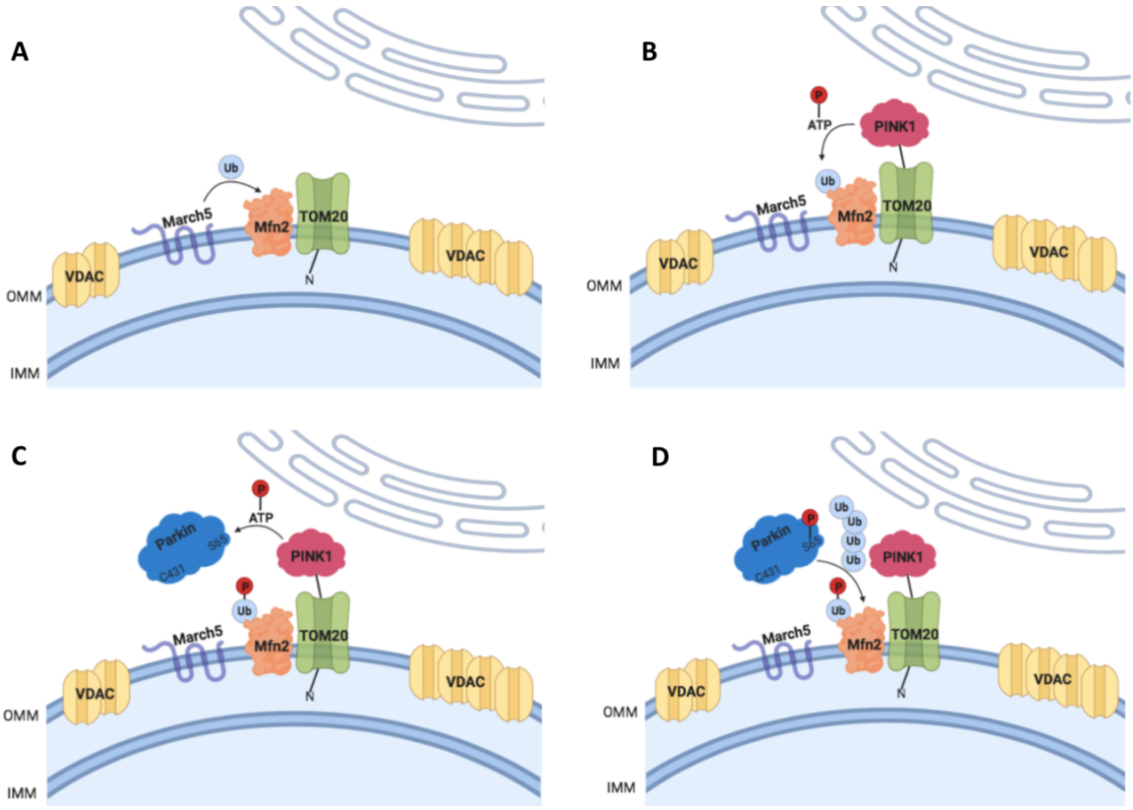

Figure 27: Schematic illustrating Parkin's substrates specificity towards Mfn2 at the onset of cellular damage. A) March5 acts as the priming E3 Ub ligase that catalyzes the addition of a "seed" Ub onto Mfn2. B) PINK1 is recruited to the damaged OMM and uses its kinase activity to phosphorylate the existing Ub moieties on the nearby Mfn2. C) The generation of pUb recruits Parkin, which becomes catalytically active upon PINK1 phosphorylation of its Ser65. D) Parkin

further catalyzes the addition of Ub moieties onto Mfn2, which in turn are phosphorylated by PINK1, and the feedback loop continues. Eventually, other abundant OMM substrates such as VDAC will be ubiquitinated.

We intent, in the future, to resolve the structural basis of Mfn2 recognition by March5. In fact, we are going to initially focus on March5 given that it has been proposed to 1) modulate the Parkin/PINK1 pathway (Koyano et al. 2019); 2) locate at the ER-mitochondria interface (Nagashima et al. 2014); 3) mediate polyubiquitination of mitochondrial Mfn2 (Sugiura et al. 2013). March5 is a 278 a.a. protein which consists of a N-terminal RING domain which binds to E2 Ub-conjugating enzymes, a TM domain with four helices and a disordered C-terminus. We will map the substrate binding site by performing a catalase-based proximity labeling assay with full-length or N-terminus truncated March5 in Parkin-null HeLa cells coupled with biotin pulldown followed by protein identification by mass spectrometry analysis (LC-MS). The collected data would confirm whether March5's N-terminus is required for binding to Mfn2. Given that no structural information is available for March5 in the current literature, we also intent to determine the crystal structure of soluble March5's RING domain by first expressing the recombinant protein in a glutathione-S-transferase (GST) fusion protein in E. coli, followed by its affinity purification by size exclusion chromatography and its structural determination by X-ray crystallography. These results altogether will further shed light on the mechanism underlying protein substrates (i.e. Mfn2) recognition and ubiquitination at the very early onset of mitochondrial damage. Given that Mfn2 acts as a gateway to initiate the clearance of other OMM substrates and downstream degradation of damaged mitochondria, understanding its regulation will provide us potential therapeutic targets, better defined biomarkers for disease detection and an improved model to understand the pathogenesis of PD.

CONCLUSION

The present project aimed to determine the mechanism underlying Parkin's substrates specificity towards Mfn2 at the onset of mitochondrial damage in the context of Parkinson's disease. We have confirmed that Mfn2 is rapidly and selectively ubiquitinated by Parkin *in vitro* recombinant assays, while other OMM substrates remain unmodified through a range of tested Parkin concentrations. Likewise, Mfn2 ubiquitination is unaffected by a mutation in Parkin's His433, which impedes the acyl transfer step of Parkin-catalyzed ubiquitination that would otherwise significantly affect other substrates' ubiquitination rate (i.e. VDAC). Our PLA data demonstrated that this substrate specificity arises from Mfn2's proximal localization to PINK1 and to its unique readout, pUb. Indeed, while Mfn2 was shown to be located in close proximity to PINK1 and to pUb, other well-characterized OMM substrates such as VDAC, Miro and Mfn1, are not. To demonstrate that Mfn2 is coupled with pUb prior to Parkin recruitment and activation, thereby conferring to its substrate specificity, an Ub-selective TUBE pulldown assay was performed with mitochondrial lysates from HeLa cells and massive enrichment for Ub was obtained. Additionally, we have successfully identified total pUb in Parkin-null HeLa cells, which implies the existence of a "priming" E3 Ub ligase(s) acting upstream to PINK1 and Parkin activation. Our latest data suggest that March5 and Huwe1 are most likely to be catalysing the addition of Ub chains on substrates such as Mfn2 at the onset of mitochondrial damage. Hence, we aim to first uncover the structural basis of Mfn2 recognition by March5 and to resolve March5's N-terminal crystal structure by X-ray crystallography. This will give us new insights into the mechanistic model of substrates recognition and specificity in the context of PD.

REFERENCES (in alphabetical order)

Adhikary, S., Marinoni, F., Hock, A., Hulleman, E., Popov, N., Beier, R., . . . Eilers, M. (2005). The ubiquitin ligase HectH9 regulates transcriptional activation by Myc and is essential for tumor cell proliferation. *Cell, 123*(3), 409-421. doi:10.1016/j.cell.2005.08.016

Ashrafi, G., Schlehe, J. S., LaVoie, M. J., & Schwarz, T. L. (2014). Mitophagy of damaged mitochondria occurs locally in distal neuronal axons and requires PINK1 and Parkin. *J Cell Biol, 206*(5), 655-670. doi:10.1083/jcb.201401070

Bae, Y. J., Park, K. S., & Kang, S. J. (2003). Genomic organization and expression of parkin in Drosophila melanogaster. *Exp Mol Med, 35*(5), 393-402. doi:10.1038/emm.2003.52

Barber, G. N. (2015). STING: infection, inflammation and cancer. *Nat Rev Immunol, 15*(12), 760-770. doi:10.1038/nri3921

Basso, V., Marchesan, E., Peggion, C., Chakraborty, J., von Stockum, S., Giacomello, M., . . . Ziviani, E. (2018). Regulation of ER-mitochondria contacts by Parkin via Mfn2. *Pharmacol Res, 138*, 43-56. doi:10.1016/j.phrs.2018.09.006

Bender, A., Krishnan, K. J., Morris, C. M., Taylor, G. A., Reeve, A. K., Perry, R. H., . . . Turnbull, D. M. (2006). High levels of mitochondrial DNA deletions in substantia nigra neurons in aging and Parkinson disease. *Nat Genet, 38*(5), 515-517. doi:10.1038/ng1769

Chan, N. C., Salazar, A. M., Pham, A. H., Sweredoski, M. J., Kolawa, N. J., Graham, R. L., . . . Chan, D. C. (2011). Broad activation of the ubiquitin-proteasome system by Parkin is critical for mitophagy. *Hum Mol Genet, 20*(9), 1726-1737. doi:10.1093/hmg/ddr048

Chang, D., Nalls, M. A., Hallgrimsdottir, I. B., Hunkapiller, J., van der Brug, M., Cai, F., . . . Graham, R. R. (2017). A meta-analysis of genome-wide association studies identifies 17 new Parkinson's disease risk loci. *Nat Genet, 49*(10), 1511-1516. doi:10.1038/ng.3955

Checler, F., & Alves da Costa, C. (2014). Interplay between parkin and p53 governs a physiological homeostasis that is disrupted in Parkinson's disease and cerebral cancer. *Neurodegener Dis, 13*(2-3), 118-121. doi:10.1159/000354075

Chen, H., Detmer, S. A., Ewald, A. J., Griffin, E. E., Fraser, S. E., & Chan, D. C. (2003). Mitofusins Mfn1 and Mfn2 coordinately regulate mitochondrial fusion and are essential for embryonic development. *J Cell Biol, 160*(2), 189-200. doi:10.1083/jcb.200211046

de Brito, O. M., & Scorrano, L. (2008). Mitofusin 2 tethers endoplasmic reticulum to mitochondria. *Nature, 456*(7222), 605-610. doi:10.1038/nature07534

Dikic, I. (2017). Proteasomal and Autophagic Degradation Systems. *Annu Rev Biochem, 86*, 193-224. doi:10.1146/annurev-biochem-061516-044908

Dorn, G. W., 2nd. (2016). Parkin-dependent mitophagy in the heart. *J Mol Cell Cardiol, 95*, 42-49. doi:10.1016/j.yjmcc.2015.11.023

Dorsey, E. R., Constantinescu, R., Thompson, J. P., Biglan, K. M., Holloway, R. G., Kieburtz, K., . . . Tanner, C. M. (2007). Projected number of people with Parkinson disease in the most populous nations, 2005 through 2030. *Neurology, 68*(5), 384-386. doi:10.1212/01.wnl.0000247740.47667.03

Durcan, T. M., Tang, M. Y., Perusse, J. R., Dashti, E. A., Aguileta, M. A., McLelland, G. L., . . . Fon, E. A. (2014). USP8 regulates mitophagy by removing K6-linked ubiquitin conjugates from parkin. *EMBO J, 33*(21), 2473-2491. doi:10.15252/embj.201489729

Escobar-Henriques, M. (2014). Mitofusins: ubiquitylation promotes fusion. *Cell Res, 24*(4), 387-388. doi:10.1038/cr.2014.23

Escobar-Henriques, M., & Langer, T. (2014). Dynamic survey of mitochondria by ubiquitin. *EMBO Rep, 15*(3), 231-243. doi:10.1002/embr.201338225

Fiesel, F. C., Ando, M., Hudec, R., Hill, A. R., Castanedes-Casey, M., Caulfield, T. R., . . . Springer, W. (2015). (Patho-)physiological relevance of PINK1-dependent ubiquitin phosphorylation. *EMBO Rep, 16*(9), 1114-1130. doi:10.15252/embr.201540514

Fiesel, F. C., Caulfield, T. R., Moussaud-Lamodiere, E. L., Ogaki, K., Dourado, D. F., Flores, S. C., . . . Springer, W. (2015). Structural and Functional Impact of Parkinson Disease-Associated Mutations in the E3 Ubiquitin Ligase Parkin. *Hum Mutat, 36*(8), 774-786. doi:10.1002/humu.22808

Geisler, S., Holmstrom, K. M., Skujat, D., Fiesel, F. C., Rothfuss, O. C., Kahle, P. J., & Springer, W. (2010). PINK1/Parkin-mediated mitophagy is dependent on VDAC1 and p62/SQSTM1. *Nat Cell Biol, 12*(2), 119-131. doi:10.1038/ncb2012

Geisler, S., Holmstrom, K. M., Treis, A., Skujat, D., Weber, S. S., Fiesel, F. C., . . . Springer, W. (2010). The PINK1/Parkin-mediated mitophagy is compromised by PD-associated mutations. *Autophagy, 6*(7), 871-878. doi:10.4161/auto.6.7.13286

Gibb, W. R., & Lees, A. J. (1988). The relevance of the Lewy body to the pathogenesis of idiopathic Parkinson's disease. *J Neurol Neurosurg Psychiatry, 51*(6), 745-752. doi:10.1136/jnnp.51.6.745

Gottlieb, R. A., & Adachi, S. (2000). Nitrogen cavitation for cell disruption to obtain mitochondria from cultured cells. *Methods Enzymol, 322*, 213-221. doi:10.1016/s0076-6879(00)22022-3

Greene, A. W., Grenier, K., Aguileta, M. A., Muise, S., Farazifard, R., Haque, M. E., . . . Fon, E. A. (2012). Mitochondrial processing peptidase regulates PINK1 processing, import and Parkin recruitment. *EMBO Rep, 13*(4), 378-385. doi:10.1038/embor.2012.14

Greene, J. C., Whitworth, A. J., Kuo, I., Andrews, L. A., Feany, M. B., & Pallanck, L. J. (2003). Mitochondrial pathology and apoptotic muscle degeneration in Drosophila parkin mutants. *Proc Natl Acad Sci U S A, 100*(7), 4078-4083. doi:10.1073/pnas.0737556100

Heikkila, R. E., Nicklas, W. J., Vyas, I., & Duvoisin, R. C. (1985). Dopaminergic toxicity of rotenone and the 1-methyl-4-phenylpyridinium ion after their stereotaxic administration to rats: implication for the mechanism of 1-methyl-4-phenyl-1,2,3,6-tetrahydropyridine toxicity. *Neurosci Lett, 62*(3), 389-394. doi:10.1016/0304-3940(85)90580-4

How Proximity Ligation Assay (PLA) Works. (n.d.). Retrieved from https://www.sigmaaldrich.com/technical-documents/protocols/biology/how-pla-works.html

Husnjak, K., Elsasser, S., Zhang, N., Chen, X., Randles, L., Shi, Y., . . . Dikic, I. (2008). Proteasome subunit Rpn13 is a novel ubiquitin receptor. *Nature, 453*(7194), 481-488. doi:10.1038/nature06926

Kalia, L. V., & Lang, A. E. (2015). Parkinson's disease. *Lancet*, 386(9996), 896-912. doi:10.1016/S0140-6736(14)61393-3

Kane, L. A., Lazarou, M., Fogel, A. I., Li, Y., Yamano, K., Sarraf, S. A., . . . Youle, R. J. (2014). PINK1 phosphorylates ubiquitin to activate Parkin E3 ubiquitin ligase activity. *J Cell Biol, 205*(2), 143-153. doi:10.1083/jcb.201402104

Karbowski, M., Neutzner, A., & Youle, R. J. (2007). The mitochondrial E3 ubiquitin ligase MARCH5 is required for Drp1 dependent mitochondrial division. *J Cell Biol, 178*(1), 71-84. doi:10.1083/jcb.200611064

Katayama, H., Kogure, T., Mizushima, N., Yoshimori, T., & Miyawaki, A. (2011). A sensitive and quantitative technique for detecting autophagic events based on lysosomal delivery. *Chem Biol, 18*(8), 1042-1052. doi:10.1016/j.chembiol.2011.05.013

Khan, N. L., Jain, S., Lynch, J. M., Pavese, N., Abou-Sleiman, P., Holton, J. L., . . . Wood, N. W. (2005). Mutations in the gene LRRK2 encoding dardarin (PARK8) cause familial Parkinson's disease: clinical, pathological, olfactory and functional imaging and genetic data. *Brain, 128*(Pt 12), 2786-2796. doi:10.1093/brain/awh667

Kim, N. C., Tresse, E., Kolaitis, R. M., Molliex, A., Thomas, R. E., Alami, N. H., . . . Taylor, J. P. (2013). VCP is essential for mitochondrial quality control by PINK1/Parkin and this function is impaired by VCP mutations. *Neuron, 78*(1), 65-80. doi:10.1016/j.neuron.2013.02.029

Kitada, T., Asakawa, S., Hattori, N., Matsumine, H., Yamamura, Y., Minoshima, S., . . . Shimizu, N. (1998). Mutations in the parkin gene cause autosomal recessive juvenile parkinsonism. *Nature, 392*(6676), 605-608. doi:10.1038/33416

Knott, A. B., Perkins, G., Schwarzenbacher, R., & Bossy-Wetzel, E. (2008). Mitochondrial fragmentation in neurodegeneration. *Nat Rev Neurosci, 9*(7), 505-518. doi:10.1038/nrn2417

Kondapalli, C., Kazlauskaite, A., Zhang, N., Woodroof, H. I., Campbell, D. G., Gourlay, R., . . . Muqit, M. M. (2012). PINK1 is activated by mitochondrial membrane potential depolarization and stimulates Parkin E3 ligase activity by phosphorylating Serine 65. *Open Biol, 2*(5), 120080. doi:10.1098/rsob.120080

Koshiba, T., Detmer, S. A., Kaiser, J. T., Chen, H., McCaffery, J. M., & Chan, D. C. (2004). Structural basis of mitochondrial tethering by mitofusin complexes. *Science, 305*(5685), 858-862. doi:10.1126/science.1099793

Koyano, F., Okatsu, K., Kosako, H., Tamura, Y., Go, E., Kimura, M., . . . Matsuda, N. (2014). Ubiquitin is phosphorylated by PINK1 to activate parkin. *Nature, 510*(7503), 162-166. doi:10.1038/nature13392

Koyano, F., Yamano, K., Kosako, H., Tanaka, K., & Matsuda, N. (2019). Parkin recruitment to impaired mitochondria for nonselective ubiquitylation is facilitated by MITOL. *J Biol Chem, 294*(26), 10300-10314. doi:10.1074/jbc.RA118.006302

Kucera, A., Bakke, O., & Progida, C. (2016). The multiple roles of Rab9 in the endolysosomal system. *Commun Integr Biol, 9*(4), e1204498. doi:10.1080/19420889.2016.1204498

Kumar, A., Chaugule, V. K., Condos, T. E. C., Barber, K. R., Johnson, C., Toth, R., . . . Walden, H. (2017). Parkin-phosphoubiquitin complex reveals cryptic ubiquitin-binding site required for RBR ligase activity. *Nat Struct Mol Biol, 24*(5), 475-483. doi:10.1038/nsmb.3400

Kumar, A., Tamjar, J., Waddell, A. D., Woodroof, H. I., Raimi, O. G., Shaw, A. M., . . . van Aalten, D. M. (2017). Structure of PINK1 and mechanisms of Parkinson's disease-associated mutations. *Elife, 6*. doi:10.7554/eLife.29985

Langston, J. W., Ballard, P., Tetrud, J. W., & Irwin, I. (1983). Chronic Parkinsonism in humans due to a product of meperidine-analog synthesis. *Science, 219*(4587), 979-980. doi:10.1126/science.6823561

Langston, J. W., & Ballard, P. A., Jr. (1983). Parkinson's disease in a chemist working with 1-methyl-4-phenyl-1,2,5,6-tetrahydropyridine. *N Engl J Med, 309*(5), 310. doi:10.1056/nejm198308043090511

Lazarou, M., Jin, S. M., Kane, L. A., & Youle, R. J. (2012). Role of PINK1 binding to the TOM complex and alternate intracellular membranes in recruitment and activation of the E3 ligase Parkin. *Dev Cell, 22*(2), 320-333. doi:10.1016/j.devcel.2011.12.014

Lazarou, M., Sliter, D. A., Kane, L. A., Sarraf, S. A., Wang, C., Burman, J. L., . . . Youle, R. J. (2015). The ubiquitin kinase PINK1 recruits autophagy receptors to induce mitophagy. *Nature, 524*(7565), 309-314. doi:10.1038/nature14893

Leboucher, G. P., Tsai, Y. C., Yang, M., Shaw, K. C., Zhou, M., Veenstra, T. D., . . . Weissman, A. M. (2012). Stress-induced phosphorylation and proteasomal degradation of mitofusin 2 facilitates mitochondrial fragmentation and apoptosis. *Mol Cell, 47*(4), 547-557. doi:10.1016/j.molcel.2012.05.041

Lee, M. S., Lee, S. O., Lee, M. K., Yi, G. S., Lee, C. K., Ryu, K. S., & Chi, S. W. (2019). Solution structure of MUL1-RING domain and its interaction with p53 transactivation domain. *Biochem Biophys Res Commun, 516*(2), 533-539. doi:10.1016/j.bbrc.2019.06.101

Liesa, M., & Shirihai, O. S. (2013). Mitochondrial dynamics in the regulation of nutrient utilization and energy expenditure. *Cell Metab, 17*(4), 491-506. doi:10.1016/j.cmet.2013.03.002

Lundmark, R., & Carlsson, S. R. (2009). SNX9 - a prelude to vesicle release. *J Cell Sci, 122*(Pt 1), 5-11. doi:10.1242/jcs.037135

Martin, I., Dawson, V. L., & Dawson, T. M. (2011). Recent advances in the genetics of Parkinson's disease. *Annu Rev Genomics Hum Genet, 12*, 301-325. doi:10.1146/annurev-genom-082410-101440

Maruyama, M., Ikeuchi, T., Saito, M., Ishikawa, A., Yuasa, T., Tanaka, H., . . . Tsuji, S. (2000). Novel mutations, pseudo-dominant inheritance, and possible familial affects in patients with autosomal recessive juvenile parkinsonism. *Ann Neurol, 48*(2), 245-250. Retrieved from https://www.ncbi.nlm.nih.gov/pubmed/10939576

Matheoud, D., Sugiura, A., Bellemare-Pelletier, A., Laplante, A., Rondeau, C., Chemali, M., . . . Desjardins, M. (2016). Parkinson's Disease-Related Proteins PINK1 and Parkin Repress Mitochondrial Antigen Presentation. *Cell, 166*(2), 314-327. doi:10.1016/j.cell.2016.05.039

Matsuda, N., Sato, S., Shiba, K., Okatsu, K., Saisho, K., Gautier, C. A., . . . Tanaka, K. (2010). PINK1 stabilized by mitochondrial depolarization recruits Parkin to damaged mitochondria and activates latent Parkin for mitophagy. *J Cell Biol, 189*(2), 211-221. doi:10.1083/jcb.200910140

McLelland, G. L., & Fon, E. A. (2018). MFN2 retrotranslocation boosts mitophagy by uncoupling mitochondria from the ER. *Autophagy, 14*(9), 1658-1660. doi:10.1080/15548627.2018.1505154

McLelland, G. L., Goiran, T., Yi, W., Dorval, G., Chen, C. X., Lauinger, N. D., . . . Fon, E. A. (2018). Mfn2 ubiquitination by PINK1/parkin gates the p97-dependent release of ER from mitochondria to drive mitophagy. *Elife, 7*. doi:10.7554/eLife.32866

McLelland, G. L., Lee, S. A., McBride, H. M., & Fon, E. A. (2016). Syntaxin-17 delivers PINK1/parkin-dependent mitochondrial vesicles to the endolysosomal system. *J Cell Biol, 214*(3), 275-291. doi:10.1083/jcb.201603105

McLelland, G. L., Soubannier, V., Chen, C. X., McBride, H. M., & Fon, E. A. (2014). Parkin and PINK1 function in a vesicular trafficking pathway regulating mitochondrial quality control. *EMBO J, 33*(4), 282-295. doi:10.1002/embj.201385902

Michel, M. A., Swatek, K. N., Hospenthal, M. K., & Komander, D. (2017). Ubiquitin Linkage-Specific Affimers Reveal Insights into K6-Linked Ubiquitin Signaling. *Mol Cell, 68*(1), 233-246 e235. doi:10.1016/j.molcel.2017.08.020

Nakamura, N., Kimura, Y., Tokuda, M., Honda, S., & Hirose, S. (2006). MARCH-V is a novel mitofusin 2- and Drp1-binding protein able to change mitochondrial morphology. *EMBO Rep, 7*(10), 1019-1022. doi:10.1038/sj.embor.7400790

Narendra, D., Tanaka, A., Suen, D. F., & Youle, R. J. (2008). Parkin is recruited selectively to impaired mitochondria and promotes their autophagy. *J Cell Biol, 183*(5), 795-803. doi:10.1083/jcb.200809125

Narendra, D., Walker, J. E., & Youle, R. (2012). Mitochondrial quality control mediated by PINK1 and Parkin: links to parkinsonism. *Cold Spring Harb Perspect Biol, 4*(11). doi:10.1101/cshperspect.a011338

Narendra, D. P., Jin, S. M., Tanaka, A., Suen, D. F., Gautier, C. A., Shen, J., . . . Youle, R. J. (2010). PINK1 is selectively stabilized on impaired mitochondria to activate Parkin. *PLoS Biol, 8*(1), e1000298. doi:10.1371/journal.pbio.1000298

Neuspiel, M., Schauss, A. C., Braschi, E., Zunino, R., Rippstein, P., Rachubinski, R. A., . . . McBride, H. M. (2008). Cargo-selected transport from the mitochondria to peroxisomes is mediated by vesicular carriers. *Curr Biol, 18*(2), 102-108. doi:10.1016/j.cub.2007.12.038

Nordmann, M., Cabrera, M., Perz, A., Brocker, C., Ostrowicz, C., Engelbrecht-Vandre, S., & Ungermann, C. (2010). The Mon1-Ccz1 complex is the GEF of the late endosomal Rab7 homolog Ypt7. *Curr Biol, 20*(18), 1654-1659. doi:10.1016/j.cub.2010.08.002

Okatsu, K., Kimura, M., Oka, T., Tanaka, K., & Matsuda, N. (2015). Unconventional PINK1 localization to the outer membrane of depolarized mitochondria drives Parkin recruitment. *J Cell Sci, 128*(5), 964-978. doi:10.1242/jcs.161000

Okatsu, K., Oka, T., Iguchi, M., Imamura, K., Kosako, H., Tani, N., . . . Matsuda, N. (2012). PINK1 autophosphorylation upon membrane potential dissipation is essential for Parkin recruitment to damaged mitochondria. *Nat Commun, 3*, 1016. doi:10.1038/ncomms2016

Okatsu, K., Sato, Y., Yamano, K., Matsuda, N., Negishi, L., Takahashi, A., . . . Fukai, S. (2018). Structural insights into ubiquitin phosphorylation by PINK1. *Sci Rep, 8*(1), 10382. doi:10.1038/s41598-018-28656-8

Ordureau, A., Paulo, J. A., Zhang, W., Ahfeldt, T., Zhang, J., Cohn, E. F., . . . Harper, J. W. (2018). Dynamics of PARKIN-Dependent Mitochondrial Ubiquitylation in Induced Neurons and Model Systems Revealed by Digital Snapshot Proteomics. *Mol Cell, 70*(2), 211-227 e218. doi:10.1016/j.molcel.2018.03.012

Ordureau, A., Sarraf, S. A., Duda, D. M., Heo, J. M., Jedrychowski, M. P., Sviderskiy, V. O., . . . Harper, J. W. (2014). Quantitative proteomics reveal a feedforward mechanism for mitochondrial PARKIN translocation and ubiquitin chain synthesis. *Mol Cell, 56*(3), 360-375. doi:10.1016/j.molcel.2014.09.007

Pacelli, C., Giguere, N., Bourque, M. J., Levesque, M., Slack, R. S., & Trudeau, L. E. (2015). Elevated Mitochondrial Bioenergetics and Axonal Arborization Size Are Key Contributors to the Vulnerability of Dopamine Neurons. *Curr Biol, 25*(18), 2349-2360. doi:10.1016/j.cub.2015.07.050

Park, J., Lee, S. B., Lee, S., Kim, Y., Song, S., Kim, S., . . . Chung, J. (2006). Mitochondrial dysfunction in Drosophila PINK1 mutants is complemented by parkin. *Nature, 441*(7097), 1157-1161. doi:10.1038/nature04788

Park, Y. Y., Lee, S., Karbowski, M., Neutzner, A., Youle, R. J., & Cho, H. (2010). Loss of MARCH5 mitochondrial E3 ubiquitin ligase induces cellular senescence through dynamin-related protein 1 and mitofusin 1. *J Cell Sci, 123*(Pt 4), 619-626. doi:10.1242/jcs.061481

Parkinson, J. (2002). An essay on the shaking palsy. 1817. *J Neuropsychiatry Clin Neurosci, 14*(2), 223-236; discussion 222. doi:10.1176/jnp.14.2.223

Parsons, J. L., Tait, P. S., Finch, D., Dianova, II, Edelmann, M. J., Khoronenkova, S. V., . . . Dianov, G. L. (2009). Ubiquitin ligase ARF-BP1/Mule modulates base excision repair. *EMBO J, 28*(20), 3207-3215. doi:10.1038/emboj.2009.243

Phu, L., Rose, C. M., Tea, J. S., Wall, C. E., Verschueren, E., Cheung, T. K., . . . Bingol, B. (2020). Dynamic Regulation of Mitochondrial Import by the Ubiquitin System. *Mol Cell, 77*(5), 1107-1123 e1110. doi:10.1016/j.molcel.2020.02.012

Pickles, S., Vigie, P., & Youle, R. J. (2018). Mitophagy and Quality Control Mechanisms in Mitochondrial Maintenance. *Curr Biol, 28*(4), R170-R185. doi:10.1016/j.cub.2018.01.004

Pickrell, A. M., & Youle, R. J. (2015). The roles of PINK1, parkin, and mitochondrial fidelity in Parkinson's disease. *Neuron, 85*(2), 257-273. doi:10.1016/j.neuron.2014.12.007

Pinton, P. (2018). Mitochondria-associated membranes (MAMs) and pathologies. *Cell Death Dis, 9*(4), 413. doi:10.1038/s41419-018-0424-1

Piquereau, J., Godin, R., Deschenes, S., Bessi, V. L., Mofarrahi, M., Hussain, S. N., & Burelle, Y. (2013). Protective role of PARK2/Parkin in sepsis-induced cardiac contractile and mitochondrial dysfunction. *Autophagy, 9*(11), 1837-1851. doi:10.4161/auto.26502

Pissadaki, E. K., & Bolam, J. P. (2013). The energy cost of action potential propagation in dopamine neurons: clues to susceptibility in Parkinson's disease. *Front Comput Neurosci, 7*, 13. doi:10.3389/fncom.2013.00013

Prudent, J., Zunino, R., Sugiura, A., Mattie, S., Shore, G. C., & McBride, H. M. (2015). MAPL SUMOylation of Drp1 Stabilizes an ER/Mitochondrial Platform Required for Cell Death. *Mol Cell, 59*(6), 941-955. doi:10.1016/j.molcel.2015.08.001

Puri, R., Cheng, X. T., Lin, M. Y., Huang, N., & Sheng, Z. H. (2019). Mul1 restrains Parkin-mediated mitophagy in mature neurons by maintaining ER-mitochondrial contacts. *Nat Commun, 10*(1), 3645. doi:10.1038/s41467-019-11636-5

Puri, R., Cheng, X. T., Lin, M. Y., Huang, N., & Sheng, Z. H. (2020). Defending stressed mitochondria: uncovering the role of MUL1 in suppressing neuronal mitophagy. *Autophagy, 16*(1), 176-178. doi:10.1080/15548627.2019.1687216

Qi, Y., Yan, L., Yu, C., Guo, X., Zhou, X., Hu, X., . . . Hu, J. (2016). Structures of human mitofusin 1 provide insight into mitochondrial tethering. *J Cell Biol, 215*(5), 621-629. doi:10.1083/jcb.201609019

Quiros, P. M., Mottis, A., & Auwerx, J. (2016). Mitonuclear communication in homeostasis and stress. *Nat Rev Mol Cell Biol, 17*(4), 213-226. doi:10.1038/nrm.2016.23

Rakovic, A., Shurkewitsch, K., Seibler, P., Grunewald, A., Zanon, A., Hagenah, J., . . . Klein, C. (2013). Phosphatase and tensin homolog (PTEN)-induced putative kinase 1 (PINK1)-dependent ubiquitination of endogenous Parkin attenuates mitophagy: study in human primary fibroblasts and induced pluripotent stem cell-derived neurons. *J Biol Chem, 288*(4), 2223-2237. doi:10.1074/jbc.M112.391680

Rasool, S., Soya, N., Truong, L., Croteau, N., Lukacs, G. L., & Trempe, J. F. (2018). PINK1 autophosphorylation is required for ubiquitin recognition. *EMBO Rep, 19*(4). doi:10.15252/embr.201744981

Rasool, S., & Trempe, J. F. (2018). New insights into the structure of PINK1 and the mechanism of ubiquitin phosphorylation. *Crit Rev Biochem Mol Biol, 53*(5), 515-534. doi:10.1080/10409238.2018.1491525

Riley, B. E., Lougheed, J. C., Callaway, K., Velasquez, M., Brecht, E., Nguyen, L., . . . Johnston, J. A. (2013). Structure and function of Parkin E3 ubiquitin ligase reveals aspects of RING and HECT ligases. *Nat Commun, 4*, 1982. doi:10.1038/ncomms2982

Rose, C. M., Isasa, M., Ordureau, A., Prado, M. A., Beausoleil, S. A., Jedrychowski, M. P., . . . Gygi, S. P. (2016). Highly Multiplexed Quantitative Mass Spectrometry Analysis of Ubiquitylomes. *Cell Syst, 3*(4), 395-403 e394. doi:10.1016/j.cels.2016.08.009

Sarraf, S. A., Raman, M., Guarani-Pereira, V., Sowa, M. E., Huttlin, E. L., Gygi, S. P., & Harper, J. W. (2013). Landscape of the PARKIN-dependent ubiquitylome in response to mitochondrial depolarization. *Nature, 496*(7445), 372-376. doi:10.1038/nature12043

Sauve, V., Lilov, A., Seirafi, M., Vranas, M., Rasool, S., Kozlov, G., . . . Gehring, K. (2015). A Ubl/ubiquitin switch in the activation of Parkin. *EMBO J, 34*(20), 2492-2505. doi:10.15252/embj.201592237

Sauve, V., Sung, G., Soya, N., Kozlov, G., Blaimschein, N., Miotto, L. S., . . . Gehring, K. (2018). Mechanism of parkin activation by phosphorylation. *Nat Struct Mol Biol, 25*(7), 623-630. doi:10.1038/s41594-018-0088-7

Schapira, A. H., Cooper, J. M., Dexter, D., Jenner, P., Clark, J. B., & Marsden, C. D. (1989). Mitochondrial complex I deficiency in Parkinson's disease. *Lancet, 1*(8649), 1269. doi:10.1016/s0140-6736(89)92366-0

Schubert, A. F., Gladkova, C., Pardon, E., Wagstaff, J. L., Freund, S. M. V., Steyaert, J., . . . Komander, D. (2017). Structure of PINK1 in complex with its substrate ubiquitin. *Nature, 552*(7683), 51-56. doi:10.1038/nature24645

Sekine, S., & Youle, R. J. (2018). PINK1 import regulation; a fine system to convey mitochondrial stress to the cytosol. *BMC Biol, 16*(1), 2. doi:10.1186/s12915-017-0470-7

Senyilmaz, D., Virtue, S., Xu, X., Tan, C. Y., Griffin, J. L., Miller, A. K., . . . Teleman, A. A. (2015). Regulation of mitochondrial morphology and function by stearoylation of TFR1. *Nature, 525*(7567), 124-128. doi:10.1038/nature14601

Shimura, H., Hattori, N., Kubo, S., Mizuno, Y., Asakawa, S., Minoshima, S., . . . Suzuki, T. (2000). Familial Parkinson disease gene product, parkin, is a ubiquitin-protein ligase. *Nat Genet, 25*(3), 302-305. doi:10.1038/77060

Simpson, R. J. (2010). Disruption of cultured cells by nitrogen cavitation. *Cold Spring Harb Protoc, 2010*(11), pdb prot5513. doi:10.1101/pdb.prot5513

Singleton, A. B., Farrer, M., Johnson, J., Singleton, A., Hague, S., Kachergus, J., . . . Gwinn-Hardy, K. (2003). alpha-Synuclein locus triplication causes Parkinson's disease. *Science, 302*(5646), 841. doi:10.1126/science.1090278

Soubannier, V., Rippstein, P., Kaufman, B. A., Shoubridge, E. A., & McBride, H. M. (2012). Reconstitution of mitochondria derived vesicle formation demonstrates selective enrichment of oxidized cargo. *PLoS One, 7*(12), e52830. doi:10.1371/journal.pone.0052830

Stolz, A., Ernst, A., & Dikic, I. (2014). Cargo recognition and trafficking in selective autophagy. *Nat Cell Biol, 16*(6), 495-501. doi:10.1038/ncb2979

Sugiura, A., McLelland, G. L., Fon, E. A., & McBride, H. M. (2014). A new pathway for mitochondrial quality control: mitochondrial-derived vesicles. *EMBO J, 33*(19), 2142-2156. doi:10.15252/embj.201488104

Sugiura, A., Nagashima, S., Tokuyama, T., Amo, T., Matsuki, Y., Ishido, S., . . . Yanagi, S. (2013). MITOL regulates endoplasmic reticulum-mitochondria contacts via Mitofusin2. *Mol Cell, 51*(1), 20-34. doi:10.1016/j.molcel.2013.04.023

Surmeier, D. J., Guzman, J. N., Sanchez-Padilla, J., & Goldberg, J. A. (2010). What causes the death of dopaminergic neurons in Parkinson's disease? *Prog Brain Res, 183*, 59-77. doi:10.1016/S0079-6123(10)83004-3

Tanaka, A., Cleland, M. M., Xu, S., Narendra, D. P., Suen, D. F., Karbowski, M., & Youle, R. J. (2010). Proteasome and p97 mediate mitophagy and degradation of mitofusins induced by Parkin. *J Cell Biol, 191*(7), 1367-1380. doi:10.1083/jcb.201007013

Tang, F. L., Liu, W., Hu, J. X., Erion, J. R., Ye, J., Mei, L., & Xiong, W. C. (2015). VPS35 Deficiency or Mutation Causes Dopaminergic Neuronal Loss by Impairing Mitochondrial Fusion and Function. *Cell Rep, 12*(10), 1631-1643. doi:10.1016/j.celrep.2015.08.001

Tang, M. Y., Vranas, M., Krahn, A. I., Pundlik, S., Trempe, J. F., & Fon, E. A. (2017). Structure-guided mutagenesis reveals a hierarchical mechanism of Parkin activation. *Nat Commun, 8*, 14697. doi:10.1038/ncomms14697

Tanida, I., Ueno, T., & Kominami, E. (2008). LC3 and Autophagy. *Methods Mol Biol, 445*, 77-88. doi:10.1007/978-1-59745-157-4_4

Trempe, J. F., Sauve, V., Grenier, K., Seirafi, M., Tang, M. Y., Menade, M., . . . Gehring, K. (2013). Structure of parkin reveals mechanisms for ubiquitin ligase activation. *Science, 340*(6139), 1451-1455. doi:10.1126/science.1237908

Veeriah, S., Taylor, B. S., Meng, S., Fang, F., Yilmaz, E., Vivanco, I., . . . Chan, T. A. (2010). Somatic mutations of the Parkinson's disease-associated gene PARK2 in glioblastoma and other human malignancies. *Nat Genet, 42*(1), 77-82. doi:10.1038/ng.491

Vincow, E. S., Merrihew, G., Thomas, R. E., Shulman, N. J., Beyer, R. P., MacCoss, M. J., & Pallanck, L. J. (2013). The PINK1-Parkin pathway promotes both mitophagy and selective respiratory chain turnover in vivo. *Proc Natl Acad Sci U S A, 110*(16), 6400-6405. doi:10.1073/pnas.1221132110

Viret, C., Rozieres, A., & Faure, M. (2018). Novel Insights into NDP52 Autophagy Receptor Functioning. *Trends Cell Biol, 28*(4), 255-257. doi:10.1016/j.tcb.2018.01.003

Vogtle, F. N., Wortelkamp, S., Zahedi, R. P., Becker, D., Leidhold, C., Gevaert, K., . . . Meisinger, C. (2009). Global analysis of the mitochondrial N-proteome identifies a processing peptidase critical for protein stability. *Cell, 139*(2), 428-439. doi:10.1016/j.cell.2009.07.045

Wahabi, K., Perwez, A., & Rizvi, M. A. (2018). Parkin in Parkinson's Disease and Cancer: a Double-Edged Sword. *Mol Neurobiol, 55*(8), 6788-6800. doi:10.1007/s12035-018-0879-1

Wang, X., Winter, D., Ashrafi, G., Schlehe, J., Wong, Y. L., Selkoe, D., . . . Schwarz, T. L. (2011). PINK1 and Parkin target Miro for phosphorylation and degradation to arrest mitochondrial motility. *Cell, 147*(4), 893-906. doi:10.1016/j.cell.2011.10.018

Wauer, T., & Komander, D. (2013). Structure of the human Parkin ligase domain in an autoinhibited state. *EMBO J, 32*(15), 2099-2112. doi:10.1038/emboj.2013.125

Wauer, T., Simicek, M., Schubert, A., & Komander, D. (2015). Mechanism of phospho-ubiquitin-induced PARKIN activation. *Nature, 524*(7565), 370-374. doi:10.1038/nature14879

Wenzel, D. M., Lissounov, A., Brzovic, P. S., & Klevit, R. E. (2011). UBCH7 reactivity profile reveals parkin and HHARI to be RING/HECT hybrids. *Nature, 474*(7349), 105-108. doi:10.1038/nature09966

Winklhofer, K. F. (2014). Parkin and mitochondrial quality control: toward assembling the puzzle. *Trends Cell Biol, 24*(6), 332-341. doi:10.1016/j.tcb.2014.01.001

Woodroof, H. I., Pogson, J. H., Begley, M., Cantley, L. C., Deak, M., Campbell, D. G., . . . Muqit, M. M. (2011). Discovery of catalytically active orthologues of the Parkinson's disease kinase PINK1: analysis of substrate specificity and impact of mutations. *Open Biol, 1*(3), 110012. doi:10.1098/rsob.110012

Wu, H., Carvalho, P., & Voeltz, G. K. (2018). Here, there, and everywhere: The importance of ER membrane contact sites. *Science, 361*(6401). doi:10.1126/science.aan5835

Xu, S., Cherok, E., Das, S., Li, S., Roelofs, B. A., Ge, S. X., . . . Karbowski, M. (2016). Mitochondrial E3 ubiquitin ligase MARCH5 controls mitochondrial fission and cell sensitivity to stress-induced apoptosis through regulation of MiD49 protein. *Mol Biol Cell, 27*(2), 349-359. doi:10.1091/mbc.E15-09-0678

Yamano, K., Fogel, A. I., Wang, C., van der Bliek, A. M., & Youle, R. J. (2014). Mitochondrial Rab GAPs govern autophagosome biogenesis during mitophagy. *Elife, 3*, e01612. doi:10.7554/eLife.01612

Yamano, K., & Youle, R. J. (2013). PINK1 is degraded through the N-end rule pathway. *Autophagy, 9*(11), 1758-1769. doi:10.4161/auto.24633

Yang, J. Y., & Yang, W. Y. (2013). Bit-by-bit autophagic removal of parkin-labelled mitochondria. *Nat Commun, 4*, 2428. doi:10.1038/ncomms3428

Yonashiro, R., Ishido, S., Kyo, S., Fukuda, T., Goto, E., Matsuki, Y., . . . Yanagi, S. (2006). A novel mitochondrial ubiquitin ligase plays a critical role in mitochondrial dynamics. *EMBO J, 25*(15), 3618-3626. doi:10.1038/sj.emboj.7601249

Yun, J., Puri, R., Yang, H., Lizzio, M. A., Wu, C., Sheng, Z. H., & Guo, M. (2014). MUL1 acts in parallel to the PINK1/parkin pathway in regulating mitofusin and compensates for loss of PINK1/parkin. *Elife, 3*, e01958. doi:10.7554/eLife.01958

Zhao, F., Wang, W., Wang, C., Siedlak, S. L., Fujioka, H., Tang, B., & Zhu, X. (2017). Mfn2 protects dopaminergic neurons exposed to paraquat both in vitro and in vivo: Implications for idiopathic Parkinson's disease. *Biochim Biophys Acta Mol Basis Dis, 1863*(6), 1359-1370. doi:10.1016/j.bbadis.2017.02.016

Zheng, X., & Hunter, T. (2013). Parkin mitochondrial translocation is achieved through a novel catalytic activity coupled mechanism. *Cell Res, 23*(7), 886-897. doi:10.1038/cr.2013.66

APPENDIX

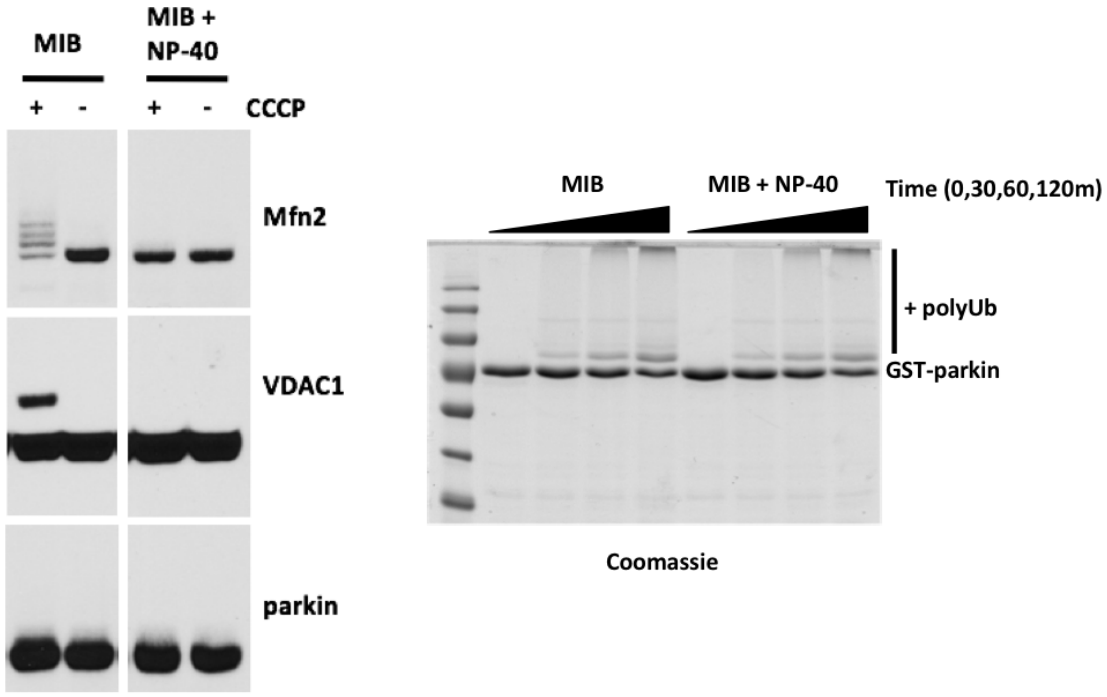

Figure 1: Proximity to pUb dictates Parkin's preference towards Mfn2 (performed by Dr. Jean-François Trempe). *In organello* assay revealed that Mfn2 ubiquitination is abolished upon the addition of the non-ionic detergent NP-40, which solubilizes the cells membranes (left figure), while Parkin autoubiquitination is unaffected (right figure).

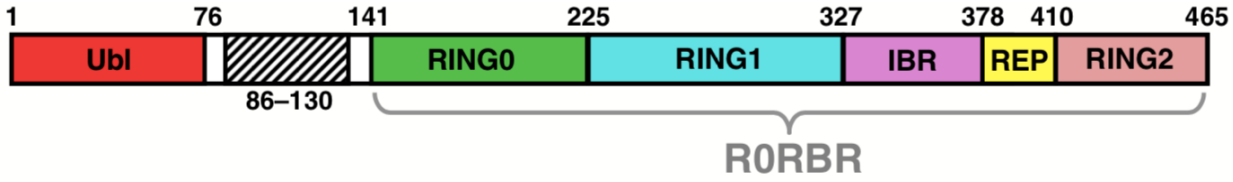

Figure 2: domains of Parkin and representation of R0RBR. Parkin's R0RBR consists of RING0, RING1, IBR, REP and RING2 domains. Figure adapted from Sauvé et al. 2015.

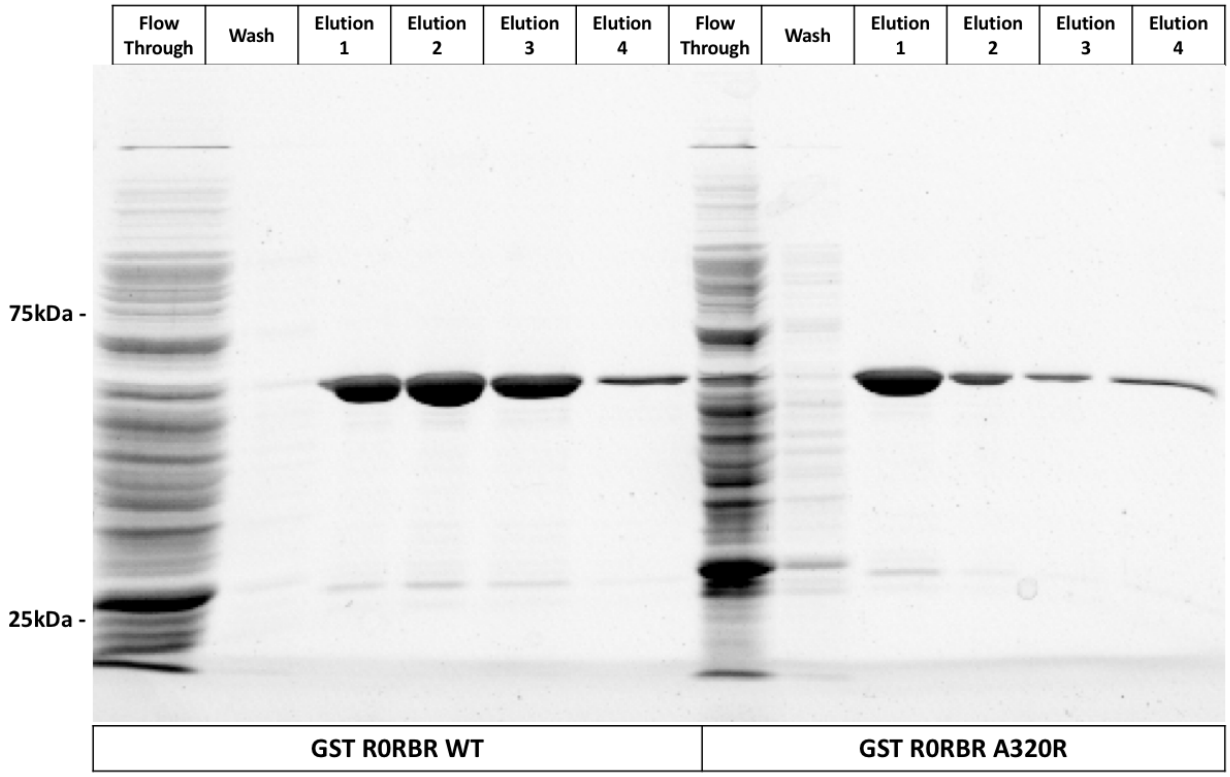

Figure 3: GST-R0RBR WT and A320R were successfully purified. A Coomassie-stained 10% poly-acrylamide gel was used to evaluate the quality of GST-R0RBR gravity column purification. 5 μg of proteins were loaded on each lane. The faint band around 25 kDa corresponds to GST monomer. The expected GST-R0RBR bands are situated at around 60 kDa. The molecular weight in kDa are shown on the left.